DEVELOPMENT OF CHICK CHORIOALLANTOIC MEMBRANE AS A BIOLOGICAL TESTING MEMBRANE

TAY LI MEI, STEPHANIE

B.Sc. (Pharm.) (Hons.), NUS

A THESIS SUBMITTED FOR THE DEGREE OF DOCTOR OF PHILOSOPHY

DEPARTMENT OF PHARMACY

NATIONAL UNIVERSITY OF SINGAPORE

2010

ACKNOWLEDGEMENTS

My deepest gratitude and sincere appreciation to my supervisors, Assoc. Prof. Chan Lai Wah and Assoc. Prof. Paul Heng. Prof Chan has been the epitome of dedication and excellence in her steadfast role as supervisor. Her care and concern was instrumental in driving the project forward. Prof Heng's infallible expertise and ability to think broadly as well as his unselfish help proved to be a formidable pillar of support, especially in 'egg buying'! Thanks also to Dr. Celine Liew for unselfishly sharing knowledge and ideas, her thoughtfulness and enjoyable company.

I am grateful to the National University of Singapore for the research scholarship as well as to Assoc. Prof. Chan Sui Yung, Head of Department, Pharmacy, NUS for the kind support of resources and facilities in the Department.

My thanks also to Ms. Teresa Ang, Ms. Wong Meiyin and Ms. Yong Sock Leng for their technical expertise as well as the kindness they showed with regards to instrument/consumable matters.

The camaraderie at GEANUS has provided much fun, laughter and joy during the postgraduate years. I enjoyed the past seminars, conferences, experiments, lunches and meetings with very pleasant companionship. I am proud to say that some GEANUS-ians have become close friends and I value all past and present GEANUS-ians for their support, advice as well as friendship all these years.

My friends and family deserve a big thank you for supporting me all these years in all sorts of ways. My friends have helped to pushed me toward the finishing line. Last not but least, my parents, to whom I owe a lifetime of debt. They have been selfless in providing everything that they possibly can and instrumental in my acheivements. I would not have come this far without them. This thesis is dedicated to them.

Stephanie
2010

TABLE OF CONTENTS

SUMMARY

The chick choriollantoic membrane (CAM) is a potentially useful model that can be used for *in vivo* as well as *in situ* studies. The use of the CAM does not pose much ethical challenges. In addition, its relatively easy availability and consistency in quality render it a convenient biological model for use in experiments requiring live tissues. Furthermore, the CAM has been used as an alternative to the Draize test for irritancy assessment. The vascularity and easy access to the CAM would allow it to be used in vasoactive studies, whereby the extent of drug absorption can be ascertained via change in blood perfusion as well as the change in diameter of the CAM vessels. To date, the CAM has not been compared with other membranes in terms of permeation profiles. This provided the impetus to conduct permeation studies with the CAM alongside other biological membranes so as to determine which biological membrane the CAM best represents.

This study showed that the partial deshelling method was more suitable then the full deshelling method for preparing the CAM to investigate blood perfusion, vessel diameter and irritancy. The egg should ideally be deshelled at embryonic age 7 days to allow adequate maturation and to avoid damage to the fragile CAM. The CAM was useful for assessing irritancy, which was manifested as hyperamaemia, hemorrhage and clotting. Nicotine, glycerin and high concentrations of propranolol were found to cause irritancy to the CAM. Measurement using the laser Doppler perfusion imager (LDPI) was significantly affected by the amplitude and threshold settings. A software written using Matlab was found to be more efficient than the manual method for determining the changes in vessel diameter. Changes in vessel diameter were more

sensitive and reliable than blood perfusion in response to the test substances. Changes in blood perfusion and vessel diameters with drug concentration were generally complex due to the compensatory mechanisms of the biological system. Nevertheless, glyceryl trinitrate was a potentially useful model drug for assessing the effects of formulation factors on drug absorption through biological membranes. The drug permeation studies revealed that the CAM best mimic the buccal mucosa, compared to skin and retina. This paves the potential of the CAM for use as a "live" *in vivo* model for assessing formulations for buccal delivery. Overall, the development of CAM assays is timely as an alternative "living animal" model to reduce testing using animals.

LIST OF ABBREVIATIONS

CAM	Chorioallantoic membrane
CAMVA	Chorioallantoic membrane vascular assay
CV	Coefficient of variance
EA	Embryo age
GTN	Glyceryl trinitrate
HET-CAM	Hen's egg test – Chorioallantoic membrane
HPLC	High performance liquid chromatography
K_p	Permeability coefficient
LDPI	Laser Doppler perfusion imager
NMP	N-methyl-2-pyrrolidone
PAMPA	Parallel artificial membrane permeation assay
SE	Standard error
UV	Ultraviolet

LIST OF TABLES

LIST OF FIGURES

INTRODUCTION

A. The three Rs in experimentation

The concept of Reduction, Refinement and Replacement was introduced in 1959. In spite of the three Rs initiative, it is of interest to note that the number of animals used for experiments is still on the rise (Festing, 2008). This trend has not abated even though the number of new drug submissions has been falling over these few years (Bhogal, 2009). Laboratory animals continue to play an important role in research, teaching and testing (Balls, 2009). It is crucial to persist in the search for alternative models of biological membranes in order to reduce the need for live whole animals. There are various experimental models, and the next section will discuss some examples that are currently employed in the pharmaceutical area.

B. *In vitro* and *in vivo* models

Numerous *in vitro* and *in vivo* test models are employed in the pharmaceutical industry, especially in the area of drug discovery and development. *In vivo* models are used in the study of pharmacological activity and toxicity, metabolism, pharmacokinetics and mechanism of action. The contention with such *in vivo* models is the ethical consideration surrounding the use of live animals. Some common live animals used as *in vivo* models in experiments include rats, mice and guinea pigs. Increasingly, there is a push towards the use of *in vitro* models in studies in view of the antagonism towards animal testing. In the campaign spearheaded by Russell and Burch in 1959 to adopt alternatives to *in vivo* methods, numerous *in vitro* concepts have been adopted (Straughan et al., 1996). *In vitro* models, such as cell lines derived from human tissues and computional programmes, do not make use of live animals. However, the use of *in vitro* models is fraught with complications. The *in vitro*

process bypasses the biotransformation processes that some drugs undergo *in vivo*. Furthermore, the test compound may be required to undergo modification so as to achieve the desired functionalities during *in vitro* testing, such as aqueous solubility enhancement, which will not be suitable for an *in vivo* situation. As such, the results garnered from such experiments would not be representative of the actions of the drug *in vivo* (Straughan et al., 1996). It is of particular interest to look at other current *in vivo* methods that take absorption, irritancy and permeation into consideration. Knowledge of these characteristics would enable pharmaceutical companies to appropriately tailor and improve on formulations so as to bring safe and effective drug products into the market.

C. Drug absorption

C.1. An overview

Bioavailability of compounds is affected mainly by the absorption and metabolism that occur in the body. The distribution and metabolism processes hinge on the presumption that the drug is able to undergo absorption and enters the circulation of the body. *In vivo* drug absorption is one of the critical parameters used to determine bioavailability of a drug. The rate and extent of absorption of a drug from its dosage form into the systemic circulation is known as bioavailability. Drug absorption is a complex process which is influenced by numerous factors, including the surface area available for absorption, physicochemical drug properties, physiological variables and formulation factors (Pontiroli et al., 1989, Senel and Hincal, 2001, Subramanian et al., 2004). For the oral route of administration, factors such as the constituents of the gastrointestinal fluid, rate of gastric emptying, disease state, drug metabolism and interaction between the drug and gastrointestinal fluid affect drug bioavailability. The

ultimate therapeutic effect of the drug is a function of the plasma drug concentration. Hence, one of the main goals of formulation studies is to enhance drug permeation across biological membranes. In the commonly used method of evaluating drug bioavailability, the drug is administered to an animal and its blood or urine is collected at different time intervals for assay. A plot of drug concentration of drug versus time is constructed and the area under the curve is used to indicate the extent of drug bioavailability. Computational and simulation methods which make use of curve fitting by compartmental analysis have also been employed, such as Wagner-Nelson and the Loo Riegelman methods (Cryan et al., 2007). Permeability and solubility of a drug can be interrelated to obtain an estimation of absorption with the maximum absorbable dose (Burton and Tullett, 1985). A method has to be sensitive and specific enough to accurately detect the change in blood drug level that reflects absorption, whether it is drug concentration in blood/plasma or metabolites in the urine. Hence, the instruments needed are relatively sophisticated and expensive.

C.2. *In vitro* and *in vivo* models to assess drug absorption

In vitro and *in vivo* models that have been used to assess the absorption of drugs include animal intestines, artificial membrane, *caco-2* cells (Dash et al., 2001, Hugger et al., 2002, Mathieu et al., 1999, Walgren and Walle, 1999), cultured epithelial and endothelial cells (Audus et al., 1990), and live animals such as rabbits (Kang and Singh, 2005), monkeys, rats and beagle dogs (Keller et al., 2007, Pu et al., 2004). Cell cultures are prone to contamination by microorganisms, as well as cross-contamination with other cell types. *In vitro* models have the potential for high throughput, but they do not possess biological factors such as enzymes, drug transporters or the cellular pathways through which drugs pass. The parallel artificial

membrane permeability assay (PAMPA) requires a long incubation time, which decreases its suitability for unstable compounds (Hidalgo, 2001). Graphical approaches to estimate human oral bioavailability from absorption, distribution, metabolism and excretion data and a pharmacokinetic approach that integrates with *in vitro* data have also been attempted (Cai et al., 2006, Mandagere et al., 2002). These methods are simple and do not require any biological tissues. The lipid composition of the PAMPA system can also be tailor-made to represent different lipid components present in the gut. However, PAMPA systems are unable to assess transcellular passive diffusion, which is the predominant route by which drugs are absorbed. The *caco*-2 cell lines, although capable of high throughput, are also unable to mimic the transport mechanisms in human tissue fully, and face the problem of inter-laboratory variability (Dressman et al., 2008).

C.3. Advantages and limitations in the use of animal and human tissues

The methods which involve animals are not only expensive but also time consuming. Human tissues are therefore preferred to animals but the availability of human tissues, especially large pieces of tissue, is subject to ethical considerations. This is particularly problematical when considerable quantities are needed. There are also considerable ethical concerns, thus making human tissues not as easily available. In addition, there are risks of diseases transfering to handlers of human tissues (Qvist et al., 2000). Moral issues are also brought into play when the potential donors are deceased, aborted human fetuses or even healthy volunteers. There is a moral obligation to use the human tissue in an appropriate and befitting manner. In the pursuit of alternatives, it would be ideal to have an *in vivo* model that is sensitive, inexpensive and capable of high throughput to handle the large number of samples

associated with formulation and related studies. Hence, the chick chorioallantoic membrane (CAM) is potentially a good candidate for an *in vivo* drug absorption model.

D. The fertilized chicken egg and its chorioallantoic membrane

D.1. An Overview

Chicken eggs (Figure 1) have been used in studies concerning developmental biology since the 19th century AD. An attractive factor is its reasonable price relative to other animal models. However, there are over 400 different breeds of chicken, with the White Leghorn breed being the most commonly used commercially to produce eggs. Upon fertilization, an egg takes about 20 hours from shell formation to when the egg is laid. After the egg is laid, the cooling of its contents causes the inner egg membrane, which is under the outer egg membrane located directly under the shell, to contract away from the shell, resulting in the formation of an air sac. Below the air sac is the inner egg membrane, followed by the chick chorioallantoic membrane (CAM). The CAM, which is found in fertilized egg, is derived from the fusion of 2 extra-embryonic membranes: chorion and allantois. The chorion and allantois start to fuse together to form the CAM at about 4 days after the egg is laid (Romanoff, 1960). The incubation period of the chicken egg is 21 days. The day that the egg is incubated, which may not coincide with the day that it is laid, is known as embryonic age 0 day (EA 0). The second day is embryonic age 1 day (EA 1), followed by embryonic age 2 days (EA 2), and so on.

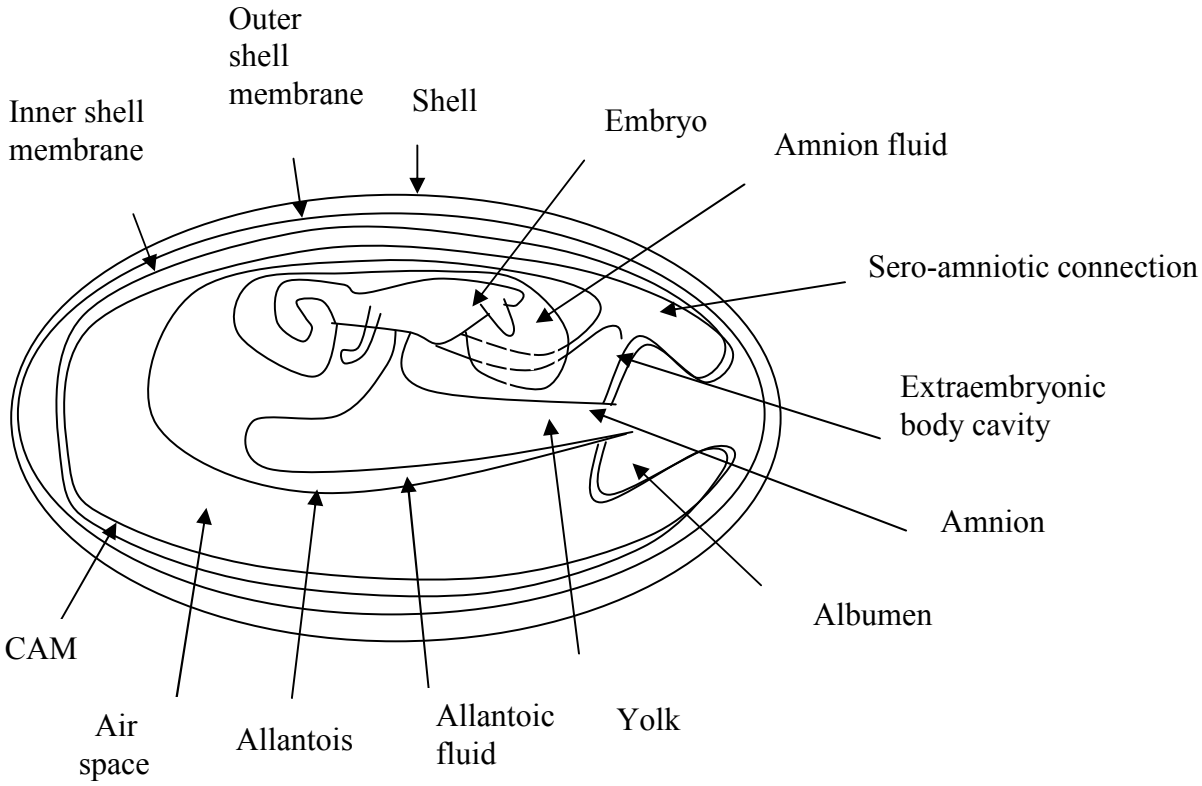

Figure 1. Structure of a fertilized chicken egg

D.2. The CAM

Histologically, the CAM consists of three layers: ectoderm, mesoderm and endoderm (Fuchs and Lindenbaum, 1988). The characteristics of the three germ layers at the 10th day of incubation are as follows. The ectoderm cells are flat and aligned in a single layer, with another one or two layers of cells beneath. The capillaries, which were previously located in the mesoderm are now found in the ectoderm layer. The mesoderm is an embryonic connective tissue with blood vessels passing through it. The respiratory capillaries are located on the outermost part of the mesoderm at this stage. The ectoderm is made up of largely cuboidal cells. Besides being a respiratory and excretory organ, the CAM provides support to the underlying extra-embryonic

blood vessels such as the vitelline vessels found on the surface of the yolk. The CAM is also involved in the transport of sodium and chloride ions from the allantoic sac which is located close to the amnion sac, and calcium from the eggshell to the vasculature. Through dilation of the associated blood vessels (known as chorioallantoic vessels), the embryo is able to avoid overheating for a relatively long time (Valdes et al., 2002, Burggren et al., 2004). The CAM is supplied with blood by the allantoic artery which stems from the chick embryo (Hochel et al., 1998). The CAM capillaries are known as the 1st order vessels. These vessels merge to form 2nd order vessels. Subsequently, 2nd order vessels merge to form 3rd order vessels. The CAM is sensitive to changes in oxygen tension and develops inflammatory responses to a number of irritants (Staton et al., 2009).

D.3. Applications of the CAM

As the CAM is thin and transparent, the highly vascular structures located within can be easily seen. Hence, it was employed in vasoreactivity studies (Dunn et al., 2005). The vascularity of the CAM allows it to be used as a model to assess damage to the vasculature. It was used to assess the damage to vessels induced by phototherapy (Chin et al., 2004, Kelly et al., 2005, Hammer-Wilson et al., 2002, Saw et al., 2005b, Saw et al., 2005c) and neovascularization (Dimitropoulou et al., 1998, Lewis et al., 2006, Patan et al., 1997, Pegaz et al., 2006, Romanoff, 1967). Its immature immune system allows it to be used in irritancy testing. It was used in irritation studies as an alternative to the Draize test (Curren and Harbell, 2002, Daston and McNamee, 2005, Harvell and Maibach, 1998, Lagarto et al., 2006, Vinardell and Garcia, 2000) and also in the evaluation of inflammatory and growth responses to biomaterials, implants, smoke and contaminants (Cobb et al., 2003, Klueh et al., 2003, Melkonian et al.,

2004, Uchil et al., 2004, Valdes et al., 2003). In addition, the immature endothelial cells of the CAM allow the implantation and growth of grafted tissue. Endometriosis lesions (Gigli et al., 2005, Nap et al., 2003, Nap et al., 2004, Nap et al., 2005, Navarro et al., 2003), fungus and virus (Fuller and Kolb, 1968, Gow et al., 2003, Hahon, 1959, McPhee et al., 1984) have been grafted and grown on the CAM. The optimum age of the CAM for use in graft procedures ranges from EA 9 to EA 12 (Ausprunk et al., 1974). The acute and chronic inflammatory responses exhibited by the CAM in response to the presence of biomaterials have also been found to be similar to that of humans (Valdes et al., 2002). The CAM was utilized as a model for heart rate irregularities to assess the effect of drugs on heart rate (Hochel et al., 1998, Yoshiyama and Kanke, 2005a, Yoshiyama and Kanke, 2006, Yoshiyama and Kanke, 2005b, Yoshiyama et al., 2003, Yoshiyama et al., 2004). It was used as a model for wound healing (Ribatti et al., 1999, Zaugg et al., 1999), myeloma (Ribatti et al., 2003), diabetes (Yoshiyama et al., 2005), human skin (Kunzi-Rapp et al., 1999), human eye (Fitzgerald et al., 2002, Schmid et al., 1996) and endocrine system (Cobb et al., 2003). Some researchers had used the CAM as a platform to test compounds for angiogenic and antigiogenic properties (Brand et al., 2006, Forough et al., 2003, Richardson et al., 2005, Tanojo et al., 1999, Zacharakis et al., 2006), anti-inflammatory properties (Brantner et al., 2002) and investigate the efficacy of permeation enhancers in photodynamic therapy (Keller et al., 2007, Saw et al., 2007a, Saw et al., 2007b, Saw et al., 2007c, Saw et al., 2007d). In addition, the CAM was used to investigate the role of growth factors during angiogenesis (Drenkhahn et al., 2004, Gabrielli et al., 2003, Gabrielli et al., 2004, Maeda and Noda, 2003, Nico et al., 2004) and to generate material for gene expression analysis (Gow et al., 2003).

D.4. Advantages and limitations of the fertilized egg and CAM as models

Fertilized eggs are much less expensive and easier to handle than live animals. The egg is first disinfected and an opening made through the shell to expose the CAM for investigation. The CAM can be viewed directly through the opening that is kept sealed by the use of a transparent tape (Valdes et al., 2002). No restrainment of the CAM is necessary in comparison with other live animal models. The use of anesthesia or other pharmacological agents is also not necessary with the CAM (Dunn et al., 2005). The CAM was largely used in studies whereby topical application of the test substance was employed. The accessibility of the CAM allows for numerous applications to be done with relative ease (Staton et al., 2009). Numerous formulations have been tested on the CAM. This provides useful information on formulation characteristics in view of the fact that the CAM can be used as a model for numerous conditions as well as human organs, as previously discussed in Section D.3. The CAM is more sensitive at EA 10 than EA 14. In the United Kingdom, fertilised eggs up to 10 days old can be used without the need for a permit for animal experimentation (Gow et al., 2003). This is line with the British Animal Welfare Act (1986) that considers an embryo as an animal only when it has reached half of its gestational age. In the case of the egg, this translates to the fact that eggs up to EA 10 can be used for experimentation without restrictions. In Germany, eggs up to EA 10 are classified as foodstuffs, which allow them to be used as a non-animal entity. In addition, ethics committee approval for the use of chicken eggs is not required in countries such as USA and Switzerland. The use of the CAM concurs with the initiative of the European Partnership which seeks alternative approaches to animal testing. The European Center for the Validation of Alternative Methods, as well as the European Partnership for Alternatives to Animal Testing, have accepted the use of the

CAM model as an alternative to animal testing. This is a step towards reducing experimental animal use. The CAM also possesses advantages over non-animal models, such as *caco-2 cells,* as it represents a whole *in vivo* system, unlike *caco-2 cells* which are ultimately *in vitro* systems or at best, *in situ*.

There are, however, a number of limitations associated with the use of fertilized egg and CAM. The short incubation period of the egg coupled with disturbances associated with the increasing embryo movements at older ages, decreases the period of time during which an egg can be employed for experimentation (Zaman et al., 2009). In angiogenesis assays, the naked eye is used to assess changes in vasculature in response to drug instilled. This method is subjective and not sensitive to minute changes in vasculature dimensions. The use of instruments to measure dimensions and density of vessels expressed as fractional image area and vascular density index is more appropriate for quantification (Strick et al., 1991). The results may be affected by a number of confounding factors. For example, it is crucial to determine the angiogenic response of the CAM at the appropriate time frame. After 24 hours, only vasodilation occurs. Furthermore, the vessel density measured does not distinguish vasodilation from neovascularization. The latter refers to the proliferation of blood vessels in tissue not normally containing them, which can be determined by sequential photography. The CAM does not allow for large volumes of blood to be removed, in view of its small size and capacity. It is also not suitable for long term studies as the partially deshelled egg is prone to contamination and the developing embryo is very fragile (Valdes et al., 2002). Unlike animal models, such as the mouse, rabbit or dog, an egg is not suitable to investigate different routes of administration. Although it was used as an alternative to the human skin, it lacks the keratinized layer. There are a

number of factors that may affect the growth and development of the egg. These factors include the chicken breed used, the stage of development of the egg when it is placed into the incubator, the time lapse after it was laid and before incubation, the temperature of the egg when it is placed in the incubator and the size of the egg (Hamburger and Hamilton, 1992). The effects of these factors were minimized in a study by using the same breed of eggs throughout the experiments, consistently incubating eggs of roughly similar lapse time and standardizing the size of the eggs.

D.5. The CAM as a model for human tissue

Table 1 summarises the features of the CAM in comparison with other biological membranes. The CAM lacks keratin and is not stratified. The CAM does not have cilia or mucus. The CAM, however, is very richly supplied with blood. The CAM does not contain tight junctions. The absence of tight junctions signify little barrier to drug permeation (McCormick et al., 1984). In view of these characteristics, the CAM would be structurally similar to the retina, buccal mucosa, lungs, placenta and blood brain barrier tissues as compared to other human tissues. The buccal route is of considerable interest due to the high permeability of buccal tissue that allows for the rapid attainment of therapeutic concentrations in the blood. Therefore, if successful as a buccal model, the CAM could be used to evaluate the biological absorption of vasoactive drugs by measuring blood perfusion. The highly vascularised nature of the CAM allows for the assessment of changes in blood perfusion. Hence, it may be possible to measure blood perfusion of the CAM using a laser Doppler perfusion imager (LDPI). Furthermore, the transparent matrix of the CAM does not significantly absorb nor scatter any incident visible radiation (Hammer-Wilson et al., 2002). The application of a vasoactive drug on the CAM was postulated to modify its

blood perfusion in accordance with the mechanism of drug action. In addition, blood perfusion could be quantified by the laser Doppler perfusion imaging (LDPI) method to indicate the rate and amount of drug absorption. Another approach of assessing absorption involves the evaluation of the permeation profile of the drug through the CAM.

Table 1. Comparison of composition between the CAM and human tissues

Tissue	**Keratin**	**Stratum corneum**	**Stratification**	**Blood supply**	**Mucus layer**	**Cilia**	**Enzymes**
CAM	X	X	X	√	X	X	Unknown
Skin	√	√	√	√	X	X	√
Buccal mucosa	X	X	X	√	√	X	√
Intestine	X	X	X	√	√	√	√
Lung	X	X	X	√	√	√	X
Retina	X	X	X	√	X	X	X
Nasal mucosa	X	X	Pseudo	√	√	√	√
Placenta	X	X	X	√	X	√	√
Blood brain barrier	X	X	X	√	√	X	√

X refers to absence of the characteristic whilst √ refers to the presence of the characteristic. Pseudo refers to the presence of pseudo stratification, which are cells that appear to be in layers. The term unknown indicates that the presence of enzymes in the CAM has not been established.

E. The laser Doppler perfusion imager (LDPI)

E.1. Principle of Operation

The laser Doppler principle involves the use of a helium-neon laser light beam directed on a tissue sample with vasculature. The moving red blood cells in the vessels reflect the photons of light back at an altered frequency, i.e. the Doppler effect. Back-scattered light is collected and converted into signals that can be used to interpret the perfusion pattern of the tissue sample (Bircher, 1995) (Figure 2). The light source emitting the laser as well as the mirrors used to direct the laser beam unto the test sample is encased in the Doppler head and cannot be seen. The detector which converts the signals into perfusion units is likewise concealed within the Doppler head. Only the laser beam emitted from the Doppler head can be visually captured. In a nutshell, the method uses two-dimensional horizontal scanning of the tissue of interest, with a depth of up to a few hundred micrometers, resulting in the visualization of spatial variation (Miyai et al., 2005).

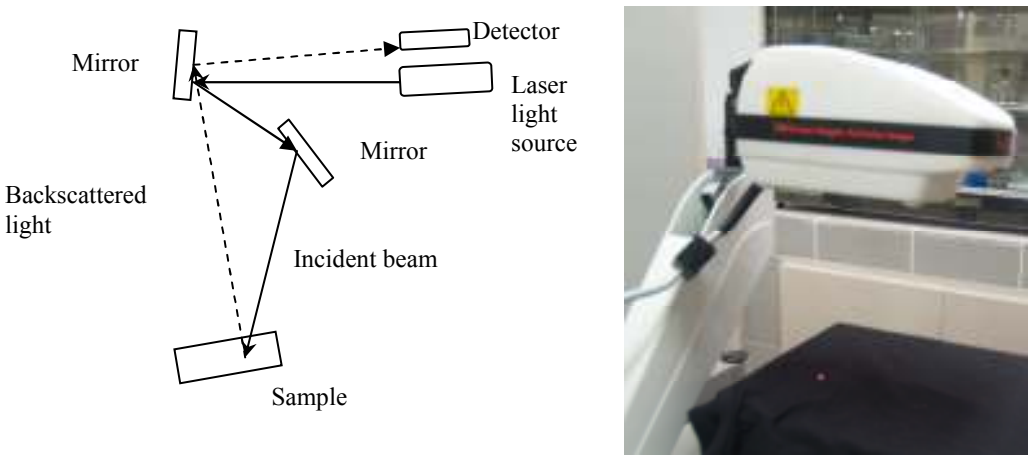

Figure 2. Schematic diagram of the LDPI measurement

The laser Doppler perfusion imager (LDPI) measures a parameter termed as *perfusion*. Perfusion is expressed as the average velocity of blood cells (V) multiplied by the concentration of blood cells (Equation 1). Perfusion is calculated automatically and expressed in arbitrary units of Volts.

$$P = V \times C \qquad \text{Equation 1}$$

where P = Perfusion in Volts

The readings obtained are affected by ambient temperature and light as well as the physiological condition of the test sample. The readings are depicted as an image and a photo. The photo shows the test area, whilst the image depicts the test area with its corresponding perfusion values. The resolution of the photo obtained can be adjusted to requirement with no additional information required except extended waiting time for higher resolution photos. The resultant image is colour coded according to the magnitude of perfusion (Figure 3). The scale moves from black and dark blue, representing the lowest value of perfusion, to red representing the highest value of perfusion as detected in each particular perfusion measurement. This allows for easy identification of areas with high or low perfusion when viewing the perfusion image.

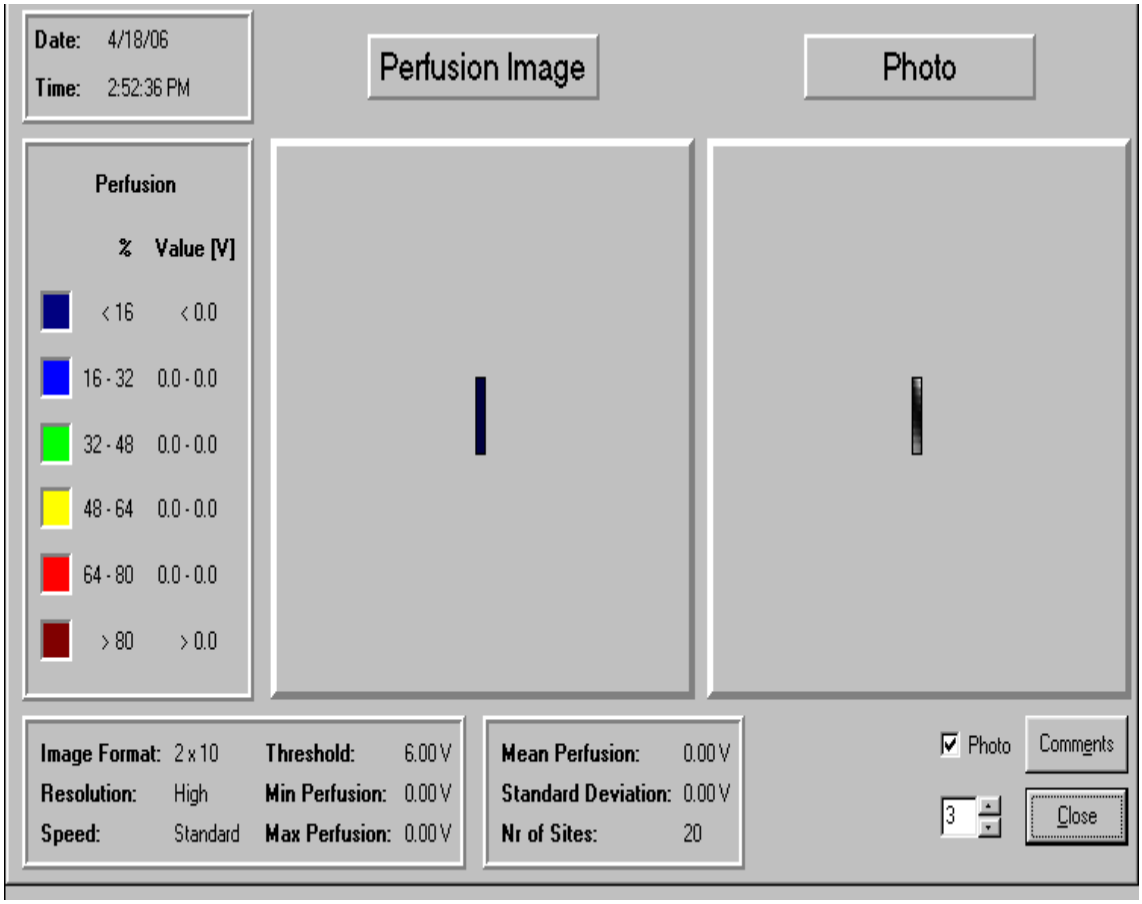

Figure 3. A representative set of readings obtained in the LDPI measurement

Besides the LDPI, other equipment used directly or indirectly to evaluate perfusion employ techniques such as fluorescence microscopy, intravital microscopy, isotope washout methods, capillaroscopy, optical coherence tomography, magnetic resonance imaging, laser Doppler flowmetry, near infrared spectroscopy, thermography and photoplethysmography (Mori et al., 2005, Wright et al., 2006).

E.2. Applications of the LDPI

The ease of use of the LDPI, as well as its non-invasive property, has resulted in its extensive use in various studies. The LDPI is a sensitive tool that is able to provide rapid assessment of changes in blood perfusion (Hoff et al., 2009). Characterization of

the forearm skin circulation (Fullerton et al., 2002b, Lantsberg and Goldman, 1990, Zhong et al., 1998, Wardell et al., 1994), cerebral blood flow (Nakase et al., 2002), basal skin blood flow during the menstrual cycle (Mayrovitz et al., 2007), retinal blood flow (Avila et al., 1998, Yoshida et al., 2003), colonic blood flow (Sakaguchi et al., 1990), skin microcirculation (Berardesca et al., 1995, Johannes Frank et al., 2001, Svedman et al., 1998) and even microvascular blood flow in animal muscles (Handley et al., 1990, Fuchs and Lindenbaum, 1988, Lam and Ferrell, 1993, Miyajima et al., 2005, Monnet et al., 2006) have been conducted using the LDPI. The LDPI was used in a predictive study that computed tissue metabolic activity from evaluation of oxygen saturation based on tissue hemoglobin saturation and blood cell velocity (Binzoni et al., 2003). The LDPI was proven useful in numerous studies that investigated medical conditions and treatments that are associated with changes in blood perfusion. Such studies include the investigation of change in perfusion with epicondykitis (Ferrell et al., 2000), postherpectic neuralgia (Stucker et al., 1997), rheumatic disease (Ferrell et al., 2000, Murray et al., 2004), reflex sympathetic dystrophy (Sorensen et al., 1996) and peripheral arterial obstructive disease (Morales et al., 2005). Last but not least, treatments that induce change in blood perfusion have been investigated. Some of these studies revolve around treatments such as smoking cessation (Fulcher et al., 1998), capsaicin treatment (Andrews et al., 1999, Krogstad et al., 1999, Van der Schueren et al., 2008), corticosteroid therapy (Hoffmann et al., 1998, Jacobi et al., 2006, Noon et al., 1996, Sommer et al., 1998), analgesia (Andrews et al., 1999, Arildsson et al., 2000a, Arildsson et al., 2000b, Li Kam Wa et al., 1990) or irritation induced by various drugs (Andrews et al., 1999, Arildsson et al., 2000a, Arildsson et al., 2000b, Bjarnason et al., 1999, Fullerton et al., 2002a, Goon et al., 2004, Li Kam Wa et al., 1990, Sutinen et al., 2000, Wigger-Alberti W. et al., 2001),

penetration of methyl nicotinate (Issachar et al., 1998), permeation enhancer studies (Tanojo et al., 1999), gingival blood flow in the treatment of peridontitis (Donos et al., 2005), peripheral vascular responses to temperature (Freccero et al., 2003, Miyai et al., 2005), blood flow analysis during hemodialysis (Davis and Johns, 1990, Niwayama and Sanaka, 2005) and change in perfusion during burns (Bray et al., 2003, Droog et al., 2001).

E.3. Advantages and limitations of the LDPI

Laser Doppler perfusion imaging is a non-invasive procedure that can be automated. It is simple to use, sensitive and produces fast, objective and accurate results. A large specific test area can be monitored continuously without compromising resolution. Measurement does not involve direct contact with the test site. This is advantageous as physical contact may elicit certain responses, such as change in blood flow rate of the tissue. Studies have shown that blood perfusion measurements obtained with the LDPI were reproducible and that the technique was selective in measuring the perfusion of the object in question (Stucker et al., 1995). The LDF employs the same principle of operation as the LDPI but involves the use of a probe that has to be in contact with the test object in order for blood perfusion measurements to be registered. Physical contact with the CAM should be avoided as a LDF study conducted on chick yolk sac membrane detected a drop in blood flow when the probe was in contact with the yolk sac membrane (Gush et al., 1990). Movement of the LDF probe can also potentially cause a shift in baseline blood flow measurement (Goode and Klein, 2002). The LDPI can decrease the incidence of movement artifacts and also achieve more reproducible results with a larger area of measurement in contrast to the results obtained with the LDF. Differences between malignant and normal

tissues can also be investigated with the LDPI but not the LDF as the LDPI has the ability to measure perfusion differences on adjacent sites (Bornmyr et al., 2001, Humeau et al., 2007). In addition to improvement in sensitivity, the LDPI also gives an average perfusion map of the measured area after scanning it. Validated blood flow measurement methods such as hydrogen clearance, flow through glass capillaries and radioactive microsphere methods were conducted (Tanaka et al., 1974). The findings from these methods were found to be correlated with LDF measurements, indicating that the LDF could provide quantitative determination of blood flow. A comparison of the LDPI with the LDF and dynamic thermographic imaging had shown good correlations (Harrison et al., 1993, Zhong et al., 1998). This indicates that LDPI measurements correlated well with the validated blood flow measurement methods. In one such study, blood was diluted in saline to obtain various concentrations of red blood cells, which was then run through using an infusion pump. Separate perfusion measurements with the LDPI were taken and compared to the estimated flow parameter values. The estimated flow parameter values were calculated by multiplying the product of the velocities of the red blood cells and their various concentrations aided by a mechanical flow stimulator. The perfusion readings showed a correlation coefficient of 0.996 between the perfusion through a mechanical flow stimulator and the estimated flow parameter (Wardell et al., 1993). The LDPI is also a cheaper method as compared to the use of other techniques involving various equipment and methodologies. Examples of alternate blood flow monitoring systems include diffuse correlation spectroscopy, dynamic contrast enhanced data and model independent convolution analysis to monitor tumor blood flow or the use of dynamic susceptibility contrast enhanced magnetic resonance imaging to obtain an autoregressive moving average model that is also in need of correlation and validation

(Murase and Miyazaki, 2007, Murase et al., 2003, Yu et al., 2005). Furthermore, constant improvements are being made to the LDPI, with the possibility of real time perfusion imaging with high speed camera function.

At higher concentrations of red blood cells, the perfusion values obtained may underestimate the true perfusion values, as the red blood cells will cause multiple scattering and produce successive Doppler shifts (Wardell et al., 1993). Other limitations include the possibility of artifacts when the Doppler head is shifted. Artifacts can thus be avoided by maintaining a constant setup of the LDPI throughout the experiments. Increasing advances in technology have narrowed down the depth of measurement to a few hundred μm. In the case of the CAM, this depth penetration is sufficient as the thickness of the CAM generally does not go beyond 200 μm. In addition, calibration standards may not be sufficient to simulate the actual physiological conditions that may affect blood perfusion. However, motility standards based on flow models have been derived that are able to provide a suitable gauge for the calibration of the LDPI (Rajan et al., 2008).

E.4. Assessment of drug absorption on the CAM

The use of the LDPI to measure perfusion of the CAM has not been reported. On the other hand, two methods involving LDF had been employed (Broekhuizen et al., 1995, Nakazawa et al., 1986). One of these involved optical Doppler tomography, which is a hybrid of the LDF and optical coherence tomography. Optical Doppler tomography presents the results in the form of a structural image. The image depicts the diameter of the vessels and its dimensions, and the image is colour coded to represent the velocity within the test areas. It was employed to study the change in

blood perfusion following pharmacological and photodynamic therapies and the topical application of glyceryl trinitrate. Using this method, the normal perfusion of blood in the CAM was found to be pulsatile (Chen et al., 1998, Zhongping Chen et al., 1997). The other method, which is based on Fourier domain optical Doppler tomography, is more sensitive. Fourier domain optical Doppler tomography was used on the CAM as an imaging tool to demonstrate *in vivo* blood perfusion (Zhang and Chen, 2005). However, this is an expensive method that has not yet been extensively studied. Screening of vasodilators was attempted with cellular biosensing approach. An example of which includes the monitoring of changes in the artery of the bovine myocardium (Haruyama, 2006), but it is an *in vitro* assay. There are several other methods to measure blood flow (Chernyavsky et al., 2010, Li et al., 2010, Lin et al., 2009, Qian et al., 2009). The term blood flow refers to the speed or velocity of blood cells movement, whereas perfusion includes the added dimension of blood concentration in a specific volume. The basic concepts of blood flow and blood perfusion are comparable, with the assumption that the space through which blood cells pass through does not change dramatically.

Laser Doppler perfusion imaging is generally regarded as an improved technique over most blood perfusion measurement methods and its application on CAM has not been well investigated. Since the CAM is a potentially useful model for assessment of drug absorption, there is an impetus to develop the CAM-LDPI method as an alternative to animal studies.

Vasoactive drugs are known to be capable of enhancing the effects of other drugs (Hadgraft, 1999). Vasoconstrictors restrict blood perfusion and allow the drug to

remain in the area of application for an extended period to exert a prolonged effect locally. Vasodilators enhance blood perfusion and can potentially facilitate the transport of accompanying bioactive drug into the systemic circulation to exert its effect at other parts of the body. The clearance of a small molecule during maximal vasodilation in skin was found to increase by 4 folds (Clough and Gush, 2009). The CAM is thus potentially useful for screening additives that can be added to drug formulations to enhance either local or systemic effects through the above mentioned mechanisms.

F. Imaging

F.1. An overview

Digitized images have been used in numerous scientific applications. The use of imaging allows for clear visualization of the process being studied and the analysis of the obtained images provides for more comprehensive data of the mechanisms involved or sequential changes that took place. Applications that employ digitized images include gamma scintigraphy, single photon emission computed tomography, nuclear imaging and positron emission tomography among others. These methods have been used to monitor particles through the lungs to determine the pathways of drug absorption (Cryan et al., 2007). Information on the microvascular density in tumour tissue was obtained after staining and measuring the fluorescent area with an image analysis system (Pendleton et al., 1998). Diagnosis of oral premalignant and malignant lesions can also be achieved with digitized endoscopic imaging (Qian et al., 2009). Image analysis was used in the scoring of cytotoxicity studies on cell cultures (Tillmann et al., 1989). Scanned images were able to assess ischemic damage, with ischemic areas presented in a different colour from normal unaffected areas (Wexler

et al., 2002). Pharmaceutical processes also make use of video imaging processes to monitor the movement of particles, such as those in a pan coater (Pandey and Turton, 2005). For the purpose of focused discussion in relation to the CAM, imaging related to irritancy and toxicity screening, and measurement of vessel diameters will be discussed in greater detail.

F.2. Pertinent applications, advantages and limitations

Non-invasive *in vivo* magnetic resonance imaging was used to determine the diameters of the carotid arteries (Manka et al., 2000). Imaging processes provided speckle maps which were used to determine artery diameters by counting the number of pixels (Forough et al., 2005). In addition, visualization of surface microvessels can be obtained with optical microscopy (Wright et al., 2006). Digital image analysis was used to measure the size of retinal vessels (Remky et al., 1996). Graphical programmes, such as LabView, are other examples that have been used to measure the external diameters of vessels in retinal tissue (Yu et al., 2003).

F.3. Imaging studies conducted on the CAM

Numerous imaging processes have been used to measure vascularity parameters of the CAM, in a bid to characterize the CAM vessels. Measurement of vessel diameter was executed by casting the CAM in resin, followed by observation under a light microscope for details of its vascular structure (Dimitropoulou et al., 1998, Reizis et al., 2005). Although these studies are highly informative and provide detailed information of the vascular structure of the CAM, such experimental procedures would result in sacrificing the egg, without the possibility for subsequent experiments. Microscopy of the CAM can also be achieved to obtain black and white images of the

vasculature (DeFouw et al., 1989). Modeling of the CAM vessels can be further conducted with the discrete vasculature (DIVA) thermal model, which was successfully applied to the vessels in the eye (Flyckt et al., 2006). Vasodilation can also be assessed with high resolution ultrsonography, but this is an invasive method (Moens et al., 2005). The use of image analysis also enabled angiogenesis to be quantified with the use of fractal dimension, vascular density as well as change in length and number of vessel branches obtained from images taken with a photomicroscope or computer assisted morphometry (Ribatti et al., 2000, Thompson and Brown, 1987). Wall differentiation and minute details of the capillary had been elucidated with the use of electron microscopy analysis studies (Mysliveckova and Rychter, 1975). Measurements of blood perfusion through the CAM cardiovascular circulation and vessel diameters have been investigated using a Doppler spectral optical coherence tomography microscope system (Davis and Johns, 1990). In addition to the high cost of equipment, optical coherence tomography is unable to resolve blood flow profiles, thereby resulting in a reduction of optical contrast of blood. A 'shadow' is typically seen below the blood vessel, which adds to the noise in the Doppler measurement and thus, inaccuracies in the blood flow measurements. Nonetheless, the use of such digitized images without sacrificing the egg has its advantages and serves two purposes. Firstly, this accentuates the 'refinement' of the experimentation process, a step toward alternative methods to animal testing. Secondly, the imaging process is non-destructive and thus allows further experiments to be conducted on the same egg, allowing for more intensive use of the egg, before ultimately sacrificing the egg at the end of the experiment. Besides reducing cost, biological variation can also be reduced. The CAM can be used repeatedly on the condition that it has not been subject to toxic effects that would consequently affect its

response to further testing. A computer software may be required for rapid and automated measurements of the diameters of vessels in the CAM. Quail CAM had been characterized, as a test bed for the modeling of retinal vessels, as the smaller size of the egg allowed for easier manipulation and handling (Vickerman et al., 2009). However, this translates to a smaller surface area of CAM to perform experiments or to assess for vascular changes. Chicken CAM is normally preferred by most researchers in experimental studies due to their larger size as well as their ready availability when compared to other types of eggs.

G. Irritancy

G.1. An overview

Toxicity refers to a broad term that can be classified into different categories. Some examples include acute toxicity, subacute and subchronic toxicity, irritation and sensitization, phototoxicity and mutagenesis. Currently, toxicity is assessed from the determination of lethal dose with cell lines, such as neuronal, muscle and myocardium cells or animals (Allen et al., 2008). The use of cell lines is hampered by problems relating to cell stability, viability and contamination (Allen et al., 2005). Tests performed to determine irritancy include cell proliferation assays, cell membrane integrity tests and basal cytotoxicity tests. The CAM has been extensively used as an alternative to the Draize test in the assessment of ocular irritation.

G.2. Irritancy assessment using the CAM

The 2 main assays that employ the CAM to test for irritancy are HET - CAM (hen's egg test - chorioallanoic membrane) and CAMVA (choriallantoic membrane vascular assay) test methods. These 2 tests differ in the age of CAM used and criteria for

assessing irritancy. In the HET – CAM test, the CAM at either EA 9 or EA 10 is employed. In contrast, more mature CAM at EA 10 or EA 14 is employed in the CAMVA test (Spielmann et al., 1997). The test substance is placed on the surface of the exposed CAM and vascular changes in the CAM are then examined with the naked eye. Irritancy of the test substance is scored appropriately, in conjunction with the various vascular changes seen and in the time frame that it occurs. This would be explored in greater detail in Section B.2. in the Methods section.

The HET – CAM test takes into consideration the time lapsed before the manifestation of respective irritancy effects. The CAMVA test determines the concentration of the test material that causes an irritancy effect in 50% of the eggs. The irritation index calculated from the HET – CAM test takes into account the appearance of haemorrhage, vessel lysis and coagulation that may have occurred after the introduction of the test substance. For the CAMVA test, the endpoint is generally regarded as the emergence of bleeding and/or ghost vessels. Ghost vessels refer to vessels that are devoid of blood and appear transparent. Many variations of these methods to assess irritancy with modifications in the interpretation of the results have since evolved and adopted. CAMVA test is currently used as a screening tool by the cosmetic industries in the United States of America. On the other hand, the HET-CAM is one of the four *in vitro* methods recognized by the regulatory authorities in Europe, with regard to the assessment and classification of severe eye irritants. The HET-CAM test is also used for safety testing of cosmetics (Liebsch and Spielmann, 2002). The Organisation for Economic Co-operation and Development implemented a stepwise approach to the evaluation of dermal and eye irritancy and the HET-CAM test is one of the methods adopted (Mancebo et al., 2008). In general, the easy

accessibility of the CAM allows for fast assessment of responses to test substances and information on the irritancy of the test substances. The manifestation of irritancy in the CAM with severe irritants can sometimes be seen as early as within 10 s upon application of the irritant.

H. Permeation studies

Permeation studies predominantly make use of a diffusion cell to assess the amount and rate of drug that passes through membranes such as the skin. This will be discussed in the following section. Permeation assays can also be conducted with the use of *caco-2* cells. Monolayers of these cultivated intestinal epithelial cells are used to assess the mechanism of transport, as well as the quantification of the permeated amount of the test substance (Alsenz and Haenel, 2003). *Caco*-2 cell culture models can be used to obtain an apparent permeability index. This apparent permeability index is only valid under strictly linear conditions, where the transfer rate of the test substance across the membrane of *caco-2* cells is proportional to the amount of test substance placed on the membrane. Ultimately, an *in vivo* condition cannot be fully reproduced (Ingels and Augustijns, 2003). Other methods of assessing permeation involve the use of computational approaches that may involve one or more of the following: calculation of log of the oil-water partition coefficient, partial least squares method, neural networks, the Abraham descriptors which consists of datasets developed by the Abraham group, polar surface area, 3D molecular field models that relate to physiochemical properties, quantum chemical approaches and prediction of biological permeation with electrotopological state indices that make use of the topological and electronic environment of each atom in a molecule (Malkia et al., 2004). On-line visualization of the diffusion of a dye through skin using confoccal

laser scanning microscopy has also been employed. However, the fluorescence gradient for the dermis part of the skin is only limited to the first few micrometers, preventing the investigation into permeation beyond the limit of detection (Grams et al., 2004).

H.1. Franz transdermal diffusion cell

The drug solution is added to the donor compartment which is separated from the receptor compartment by a membrane. A constant area through which the permeation of the drug occurs is maintained throughout the experiment. The solution in the receptor compartment is constantly stirred with the aid of a magnetic stirring bar to ensure that no concentration gradient of the drug builds up. The receptor compartment possesses a side arm where samples are withdrawn for assay. Sampling occurs at pre-set intervals and the amount of drug present in each sample determined. The cumulative amount indicates the total amount of drug that has permeated through the membrane and the time taken for the permeation process is used to calculate the rate of drug permeation. In the study of transdermal drug delivery, the whole setup is maintained at a constant temperature of 33°C to mimic the physiological condition of the skin. Although the Franz cell is predominantly used for transdermal studies, it has also been used to assess the permeation of drugs through other biological membranes.

H.2. Principle of operation

Diffusion cells consist of 2 basic models, one-chambered and two-chambered cells. The one-chambered cell is most commonly used to assess transdermal permeation. The membrane being studied is placed across the receptor compartment. The test substance is placed on the membrane and its diffusion through the membrane to the

receptor compartment is monitored. The test substance is used at a sufficiently high concentration to maintain a concentration gradient for diffusion to occur and for accurate analysis. The two-chambered cell consists of a donor compartment and a receptor compartment separated by a membrane. The donor compartment is filled with a solution of the test substance. The permeation of the test substance from the donor compartment into the receptor compartment through the membrane is monitored.

H.3. Applications

The Franz cell is an example of a one-chambered diffusion cell. It however has a cell top above the membrane, which can be employed as a donor chamber. The Franz cell was used extensively in studies to evaluate the permeation of substances across human skin. It can also be used in conjunction with confocal microscopy (Yu et al., 2005). Some examples of permeation studies performed with the Franz cell include the investigation on the effects of glycol ethers (Venier et al., 2004), clobetasol propionate (Borges et al., 2003), permeation enhancers (Kikwai et al., 2005, Zwadlo-Klarwasser et al., 2001) and new drug delivery systems on drug permeation through biological membranes (Dayal et al., 2005). In addition, the effect of synthetic membranes on permeation (Dias et al., 1999) and the effect of formulation development have also been studied (Pawar and Majumdar, 2006).

H.4. Advantages and limitations

Results obtained using the Franz cell with the same compound on different days were found to be similar, indicating the reproducibility of the Franz cell method (Akomeah et al., 2007). The Franz cell setup may be programmed to automatically replace any

sample volume withdrawn with an identical volume of fresh medium into the receptor compartment. However, some diffusion cells are not designed to perform this operation. As such, the volume of the receptor medium would be gradually reduced and unless this is taken into consideration, the results may not be accurate. Franz cells are fragile as they are made of transparent glass and transparency allows the user to note any presence of air bubbles developing for necessary corrective actions to remove them. In systems made from Teflon ®, the opacity of the Teflon ® does not allow for easy detection and removal of air bubbles. The presence of air bubbles may result in an incorrect sample volume and thus affect concentration analysis (Rapedius and Blanchard, 2001).

The Franz cell uses membranes in its assessment of drug permeation. The use of biological membranes as opposed to *in vitro* cell cultures to measure permeability has its advantages. The permeability of water through buccal mucosa was evaluated using a TR146 cell culture model that was designed to mimic buccal epithelium (Nielsen and Rassing, 2000). It was found that the porcine buccal mucosa, a frequently used model to represent human buccal mucosa, formed a tighter barrier than the cell culture. The use of membranes in the assessment of permeation is more realistic than the use of cell cultures. Furthermore, the Franz cell is capable of giving a good approximation of the permeation rates of different substances through different types of membranes (Zorin et al., 1999). As such, the Franz cell can be used to assess drug permeation through the CAM as well as other biological membranes to allow for comparison of the results.

H.5. Assessment of drug permeation using the CAM

Membrane transport studies with the use of the CAM have been attempted. The test substance is applied on the CAM and washed away after an appropriate time interval, to determine the amount of test substance unabsorbed (Saw et al., 2005b, Saw et al., 2005c, Saw et al., 2007d). However, no permeation studies were carried out with the CAM on the Franz cell. Based on its structural characteristics, the CAM has been postulated to mimic certain biological membranes, such as the buccal, retina or human skin. However, comparisons of the CAM and other biological membranes had not been made nor were these studies carried out to determine the drug permeation profiles using the CAM as an *in situ* biological barrier. As such, this study will attempt to determine the type of biological membrane that the CAM would best represent.

HYPOTHESES AND OBJECTIVES

In the design and development of dosage forms, it is of interest to know how various formulation additives affect absorption. The CAM is an inexpensive and easily available biological model that may be employed to assess drug absorption as a function of blood perfusion and vessel dimension changes. It is a transparent matrix, highly vascularised and does not possess much ethical restriction with regards to its use. Hence, it has been used in numerous studies to evaluate irritancy effects of test substances, as a model for various types of organs and conditions, and in the evaluation of angiogenesis. The LDPI is a fast and rapid tool to determine blood perfusion, and has been extensively used to characterize blood perfusion of various organs, assess blood perfusion in disease states as well as evaluate changes in blood perfusion on drug treatment. However, the application of the LDPI has not yet been used to assess blood perfusion of the CAM. In addition, the change of vessel diameter with the CAM in conjunction with changes in blood perfusion has not been evaluated. Furthermore, the CAM has yet to be compared with other biological membranes in terms of permeation properties.

It is important to identify a model vasoactive drug that can be used on the CAM to evaluate the influence of pharmaceutical ingredients on drug absorption. The model drug should ideally exert a definable dose response relationship on the CAM. Using the same amount of model drug, the ingredient that increases drug absorption will elicit a greater change in blood perfusion or change in vessel dimension. The extent of influence on drug absorption can be determined by assessing the degree of change of blood perfusion and vessel diameter. In this project, the primary aim is to study the feasibility of the CAM model to evaluate drug absorption based on changes in blood perfusion and vessel diameter.

A. Hypotheses

1. The CAM, in conjunction with LDPI and video digital imaging, is a useful *in vivo* model that provides a rapid and sensitive method to assess the absorption of vasoactive drugs.

   The response of the CAM to a vasoactive drug can be determined by the changes in blood perfusion and vessel diameters of the CAM.

   The reactivity of the CAM can also be used to screen and assess test substances for irritancy effects.

2. The isolated CAM can be employed as an *in vitro* model with the Franz cell to assess drug permeation through certain biological membranes.

B. Objectives

1. Optimize conditions of the CAM and LDPI to carry out blood perfusion measurements for assessing absorption of vasoactive drugs.
2. Employ the CAM as a screening tool for irritation effects
3. Screen for suitable drugs to be used in blood perfusion measurements
4. Study response of vessel morphology to drugs by imaging
5. Compare the permeation profiles of the CAM and other biological membranes to determine which biological membrane it best represents

MATERIALS AND METHODS

A. Materials

A.1. CAM

Freshly laid fertilized specific pathogen-free (SPF) chicken eggs of the *White Leghorns* species were purchased from Agri-Food and Veterinary Authority of Singapore (AVA), Singapore. The *White Leghorns* species is the most commonly used chicken species for experiments. It is also the most popular commercial species of egg laying chicken used because of its superior egg laying capabilities. The white egg shell of this egg variety allows for greater ease of candling when checking the viability of the eggs (Leighton et al., 1985).

A.2. Blood perfusion and imaging studies

Two forms of glyceryl trinitrate, GTN 0.5 mg per tablet, (Angised™, GlaxoSmithKline) and GTN 1 mg/mL (Merck, Germany) were used as a model drug (Table 2). Other model drugs used included propranolol (Zuellig Pharma, China), theophylline hydrate BP (Janson Chemicals, Singapore) and caffeine BP (Luen Wah Medical Company, Singapore). Sodium chloride (Merck, Germany), glucose monohydrate (Merck, Germany) and deionized water were used in the preparation of solvents.

Other solvents and test substances employed were liquid paraffin (Merck, Germany), glycerin (BDH, England) and 70% ethanol (Far East Distillers, Singapore), N-methyl-2-pyrrolidone (NMP, International Specialty Products, USA), L-nicotine (>99%, Acros Organics, USA) and glucagon (Novo Nordisk, USA). Purified agar, Sabouraud dextrose agar (Acumedia Manufacturing, USA) and tryptone soya broth (Oxoid,

Table 2. Properties of model drugs used

Drug	Mechanism of action in humans	Log partition coefficient (octanol – water)	Molecular weight	Solubility in water at 25°C (mg/L)	Dose used
Propranolol	Antagonism of beta – adrenergic receptors	3.48	295.8	61.7	1, 2, 5, 7.5, 15 and 30 mg/kg; 50, 100, 150, 200 and 250 ng/mL
Theophylline	Antagonism of adenosine receptors	-0.02	198.2	7360	1.5, 2, 2.5, 3, 3.5, 20, 30, 40, 50 and 60 mg/kg
Caffeine	Increase in cAMP levels, inhibition of Ca^{2+} influx, inhibition of PDEs and antagonism of adenosine receptors	-0.07	194.2	0.0216	2, 4, 6, 8 and 10 mg/kg
Glyceryl trinitrate	Release of nitric oxide which stimulates guanylate cyclase	1.62	227.1	1380	Tablet: 0.0125, 0.025, 0.05, 0.1, 0.15 and 0.2 mg/kg Injection: 0.01, 0.03, 0.05, 0.1, 0.15, 0.2 and 0.5mg/kg
Glucagon	Possibly affects cAMP levels	Not available	3485	Low	0.1% w/v
Menthol	Not available	3.38	156.3	420	2% w/v

cAMP: cyclic adenosine monophosphate, PDE: 3',5'-cyclic-nucleotide phosphodiesterase

USA) were employed for sterility testing of the cleansphere. The cleansphere provides an isolated and clean environment for experimental procedures.

A.3. Franz cell diffusion studies

L-Nicotine (Acros Organics, USA) and glyceryl trinitrate, 1 mg/mL (Merck, Germany) were used as model drugs. Shed King Cobra skin from *Ophiophagus hannah* was a gift from Khon Kaen University, Thailand. Pig abdominal skin, buccal mucosa as well as retina tissue were obtained from 4-month old Yorkshire-Duroc mix breed female pigs (Animal Holding Unit, National University of Singapore). Disodium hydrogen orthophosphate dodecahydrate (BDH Chemicals, England), sodium dihydrogenphosphate dehydrate (Nacalai Tesque, Japan) and sodium chloride (Merck Germany) were used to prepare isotonic phosphate buffer.

A.3.1. HPLC studies

Sodium acetate (Sigma-Aldrich, USA), triethylamine (Sigma Aldrich, USA), glacial acetic acid (Merck, Germany), deionized water and methanol (Fisher Scientific, USA) were used to prepare the mobile phases for analysis of nicotine and GTN.

B. Methods

B.1. Preparation of the CAM

Two methods were employed to prepare the CAM for experimentation. Both procedures were performed aseptically in a clean environment provided by the Cleansphere (CA100, Safetech Limited, USA). The eggs were deshelled entirely or partially and returned to the incubator (Brinsea, England). The surface of the CAM was examined at different time intervals with the naked eye.

B.1.i. Full deshelling method

The entire exterior of the egg (EA 3 and EA 4) was swabbed with 2 types of disinfectants, 70 % ethanol and 10 % povidone iodine, prior to manipulation. The egg was then cracked into a petri dish to expose the CAM completely for examination (Figure 4a). The petri dish was then covered with a lid and placed in the incubator. The condition of the sample was examined and its blood perfusion measured at daily intervals.

B.1.ii. Partial deshelling method

The entire exterior of the egg (EA 7) was disinfected as described in Section B.1.i. A hole of about 2 cm in diameter was made at the blunt end of the egg (Figure 4b). The two outermost egg membranes were then removed to reveal the CAM for examination. The hole was then covered with parafilm previously sprayed with 70 % ethanol. The egg was then placed in the incubator and the condition of the CAM was examined daily by observing its blood perfusion rate and the diameters of blood vessels.

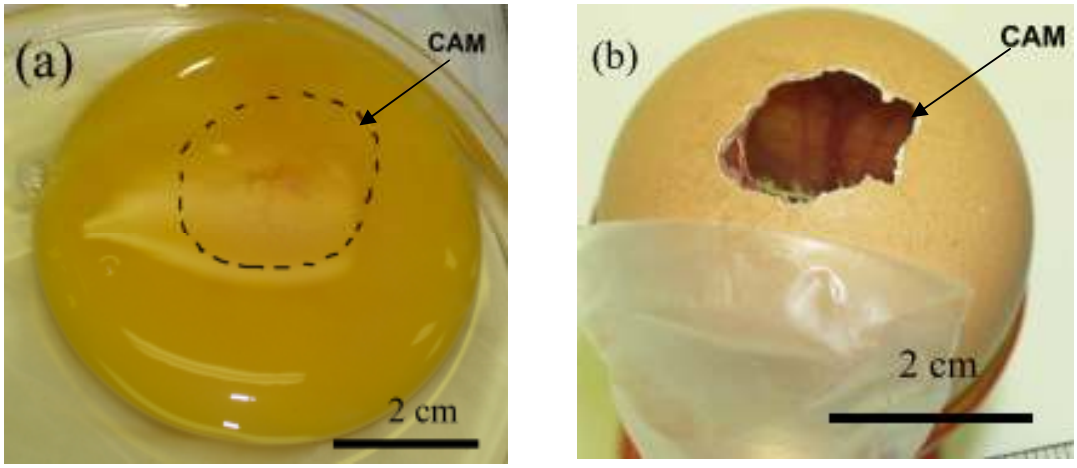

Figure 4. Deshelling methods: (a) Complete exposure of CAM by full deshelling method and (b) Partial exposure of CAM by partial deshelling method

B.1.iii. Assessment of egg weight during incubation

The weights of 10 eggs were individually measured daily for the duration of the incubation period. The change in weight over time was used to indicate the growth rate of the embryo. This method was used to determine if the growth of the eggs is normal under the incubation conditions. If embryo development is normal, a linear relationship between incubation time and loss in egg weight will be observed. The weight loss can be attributed to the loss of water from the egg as the embryo develops.

B.1.iv. Measurement of CAM thickness

The thickness of the CAM was measured with the use of a micrometer (Mitutoyo, Japan). Measurements were taken at 3 different sites of the CAM and the average readings reported.

B.2. Assessment of vessel morphology & irritancy

The CAM from fertilized egg (EA 7) was prepared by the partial deshelling method. Visual assessment of the vessels and surface of the CAM with the naked eye was performed after the application of each test substance. Assessment of irritation effects such as hyperaemia, hemorrhage and clotting were performed. Hyperaemia is indicated by an increased amount of blood, resulting in congestion. Hemorrhage refers to bleeding on the surface of the CAM while clotting refers to coagulation whereby blood forms clumps. Time dependent scores for each irritation effect were then assigned in accordance with the grading system developed in the Luepke Method as shown below (Table 3). Photographs of the CAM were obtained using a stereomicroscope (SZ61, Olympus, Japan) connected to a colour video camera (DP71,

Table 3. Grading system for irritation

Time taken for manifestation of irritation effect	**Score**		
	Hyperaemia	Haemorrhage	Clotting
≤ 0.5 min	5	7	9
> 0.5 to 2 min	3	5	7
> 2 to 5 min	1	3	5

Cumulative score	**Irritation potential**
< 1.0	Negligible
1.0 to 4.9	Slight
5.0 to 8.9	Moderate
9.0 to 21.0	Strong

Olympus, Japan) and computer with an image managing software (DP Controller, Olympus, Japan).

B.3. Investigation of egg parameters affecting blood perfusion

B.3.i. Embryo Age

Eggs of different embryonic age were used to examine the influence of CAM maturity on consistency of blood perfusion readings. CAMs of EA 8 – 18 were investigated in this study.

B.3.ii. Consistency of egg temperature

The method to measure blood perfusion in the CAM was improved by the inclusion of a heated egg cup to maintain a constant egg temperature. A temperature-controlled egg cup, that was connected to a water bath (Grant Instruments, England), was fabricated to hold the egg after it was removed from the incubator for blood perfusion

measurement (Figure 5). The egg cup was warmed by a heated water jacket in an attempt to keep the temperature of the egg constant during blood perfusion measurements. Measurement was made with and without the use of the temperature-controlled egg cup.

The relationship between the temperature of the heated water jacket and the resultant temperature of the egg cup was first established by setting the temperature of the heated water jacket from 40 to 50 ºC at increments of 1 ºC each time. The corresponding temperature of the egg cup was measured with an infrared thermometer (Fluke, Netherlands). The initial setup was allowed to equilibrate for 2 h, following which, subsequent change in temperature required 30 min of equilibration time to achieve a constant temperature. From the results, the temperature of the egg cup was adjusted to about 37 $^{\circ}$C and reproducibility in blood perfusion measurement over time was determined and compared with that determined without the use of the temperature-controlled egg cup.

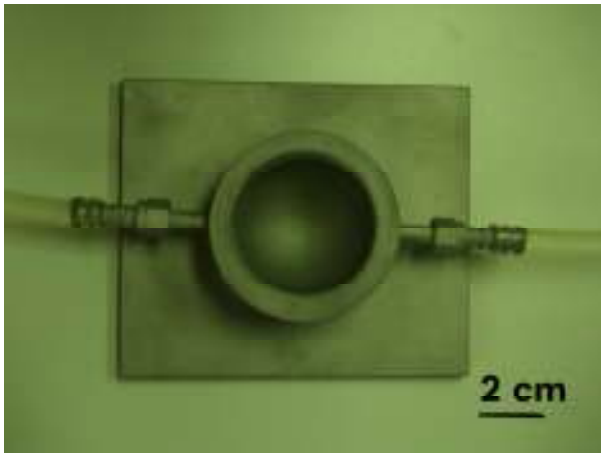

Figure 5. Photograph of the water-jacketed egg cup connected to a circulating heated water bath.

B.4. Investigation of influence of LDPI parameters on blood perfusion measurement

The laser beam was switched on for 15 min prior to perfusion measurements to allow the beam to equilibrate to room temperature with normal ambient light. The test sample was placed on a black cloth to minimize the extent of extraneous back-scattered light from the background. Perfusion readings were made at the same location on the CAM for meaningful comparison. All measurements were carried out at least in triplicates.

An orthogonal array design of L25 (5^4), 4 variables (distance, area, amplitude and threshold) at 5 levels each was conducted (Table 4 and 5). The sum of the readings for each variable at each level was denoted by the K value while the impact of the variable was denoted by the R_k value. The R_k value was determined by obtaining the difference between the highest and lowest K values for each variable. The variable with the greatest influence was indicated by the highest R_k value.

A partial factorial study was further conducted on the 4 variables at 5 levels each to determine the optimal setting to be used for each parameter. The effects of scan speed and resolution setting on the readings were also determined, following optimization of the abovementioned LDPI parameters.

The variables were further investigated with univariate analysis to confirm the results obtained from the partial factorial and orthogonal array design (Table 6).

Table 4. LDPI parameters studied using the orthogonal array and partial factorial design

LDPI Parameters	**Level**				
	Level 1	Level 2	Level 3	Level 4	Level 5
Amplitude	0	3	5	7	10
Threshold	0	3	5	7	10
Measurment area (mm^2)	2 x 5	2 x 8	2 x 10	2 x 12	2 x 15
Distance between Doppler head and CAM (cm)	10	13	15	17	20

B.4.i. Amplitude

The blood perfusion value measured by the LDPI was amplified by the software. Amplitude refers to the enhancement of the blood perfusion value by a certain multiplication value. The minimum amplitude value is 0 and the maximum level is 10.

B.4.ii. Threshold

Threshold refers to the discrimination level between the background and the object of measurement. When the total amount of back-scattered light from the measurement site was lower than the threshold level set, no Doppler signal was recorded. A perfusion measurement was obtained only when the total amount of back-scattered light from the measurement site was higher than the threshold set. The minimum threshold value was 0 and the maximum level was 10.

Table 5. The L25 (5^4) Taguchi design matrix

Trial Number	**Variable at different levels**			
	Amplitude	Threshold	Measurement area	Distance between Doppler head and CAM
1	1	1	1	1
2	1	2	2	2
3	1	3	3	3
4	1	4	4	4
5	1	5	5	5
6	2	1	2	3
7	2	2	3	4
8	2	3	4	5
9	2	4	5	1
10	2	5	1	2
11	3	1	3	5
12	3	2	4	1
13	3	3	5	2
14	3	4	1	3
15	3	5	2	4
16	4	1	4	2
17	4	2	5	3
18	4	3	1	4
19	4	4	2	5
20	4	5	3	1
21	5	1	5	4
22	5	2	1	5
23	5	3	2	1
24	5	4	3	2
25	5	5	4	3

Table 6. LDPI parameters studied with CAM in the univariate analysis

LDPI Parameters	Level										
	Level 1	Level 2	Level 3	Level 4	Level 5	Level 6	Level 7	Level 8	Level 9	Level 10	Level 11
Amplitude	1	2	3	4	5	6	7	8	9	10	11
Threshold	1	2	3	4	5	6	7	8	9	10	11
Measurement area (mm^2)	2 x 5	2 x 6	2 x 7	2 x 8	2 x 9	2 x 10	2 x 11	2 x 12	2 x 13	2 x 14	2 x 15
Distance between Doppler head and CAM (cm)	10	11	12	13	14	15	16	17	18	19	20

B.4.iii. Area of measurement

In a study carried out by Gush et al. (1990), it was observed that the yolk of the egg contributed to the perfusion values, due to the particles present in the yolk undergoing Brownian motion. Hence, in this study, the measurement site was confined to the area of interest, i.e. the CAM vessels, as much as possible. Measurement sites of different sizes were evaluated to determine the measurement area required to capture the blood perfusion level of the CAM vessels accurately. The smallest measurement width needed by the LDPI was 2 mm, thus, all measurement areas investigated were with dimensions of 4 mm^2 or larger.

B.4.iv. Distance of sample from laser head

The distance between sample and laser beam aperture located in the Doppler head, was varied and the resultant perfusion readings were obtained.

B.4.v. Scanning speed and resolution

Scanning speed refers to the time delay between two consecutive perfusion values from adjacent measuring sites and thus, the total time required to capture an entire image. Resolution refers to the geometrical distance between two consecutive measurement sites. These parameters were independently investigated from the partial factorial study once the optimal parameters were determined.

B.4. Drug studies

The blood perfusion of the CAM was first monitored and the drug administered only when blood perfusion values of the CAM were found to be constant. An equilibration period of 15 min was generally necessary to allow the blood perfusion of the CAM to

stabilise. Thirty μL of each drug at various concentrations were applied topically to the CAM surface and the changes in blood perfusion investigated. Propranolol, theophylline and caffeine solutions were prepared with normal saline. Two forms of GTN were used. Sublingual GTN tablets were dissolved in an appropriate amount of normal saline to give the required concentration. The injection form of GTN was diluted to the required concentration with 5 % w/v glucose monohydrate solution. The pH and osmolality of some of the test substances were determined with a pH meter (Hanna Instruments, USA) and a vapour pressure osmometer (Wescor, USA) respectively. In addition, some control substances were also tested to assess their effects on blood perfusion. These substances include glycerin, ethanol, N-methyl-pyrrolidone and glucagon.

B.5. Imaging studies

B.5.i. Imaging of CAM surface

The egg was held in an egg holder that was placed underneath a stereomicroscope (SZ61, Olympus, Japan) connected to a colour video camera (DP71, Olympus, Japan) and computer with an image managing software (DP Controller, Olympus, Japan). This study was performed in a laboratory with constant ambient temperature of 23°C. An equilibration period of 15 min was allowed before images of the CAM were taken at 1 min intervals prior to the administration of the test substance at the 15th min time point. The time interval between image capture was further reduced so as to capture immediate and small changes in vessel diameter that might have occurred after the application of the test substance.

B.5.ii. Image processing

The diameter of the vessel was measured from its digitized image using a software written with Matlab R2007b (Figure 6a). The software employs a canny filter to extract a black and white binary image from a colour image in order to facilitate image processing. In the case of the CAM, the vessels would show up as white pixels against a background of black pixels. Each pixel in the binary image is assigned a value (Figure 6b). A white pixel was assigned a value of 1 and a black pixel was assigned a value of 0. The white pixels were detected by the software methodically and the diameters of the vessels determined.

B.5.iii. Measurement of vessel diameter

The pixel units were calibrated into physical units of measurement such as μm with the aid of a micrometer image included in the same folder as the CAM photos. The various segments composed of white pixels were assigned a cumulative value and the diameters of these segments were subsequently computed in microns. Drugs that were previously found to be vasoactive were employed in this study.

B.6. Permeation studies with the Franz diffusion cell

B.6.i. Sample preparation

Different biological membranes were investigated. They included fresh and frozen CAM, king cobra snake skin, pig skin, pig buccal mucosa and pig retina tissue. The test biological membrane, together with a synthetic membrane, was then fixed on a Teflon disc and mounted on the Franz diffusion cell.

(a)

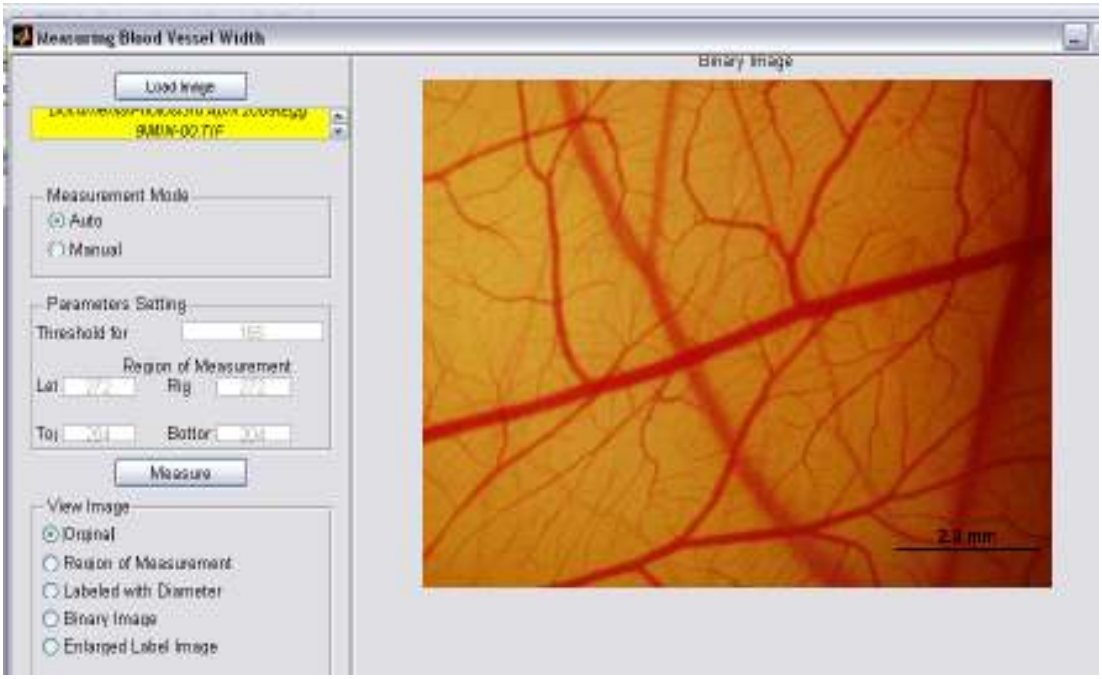

(b)

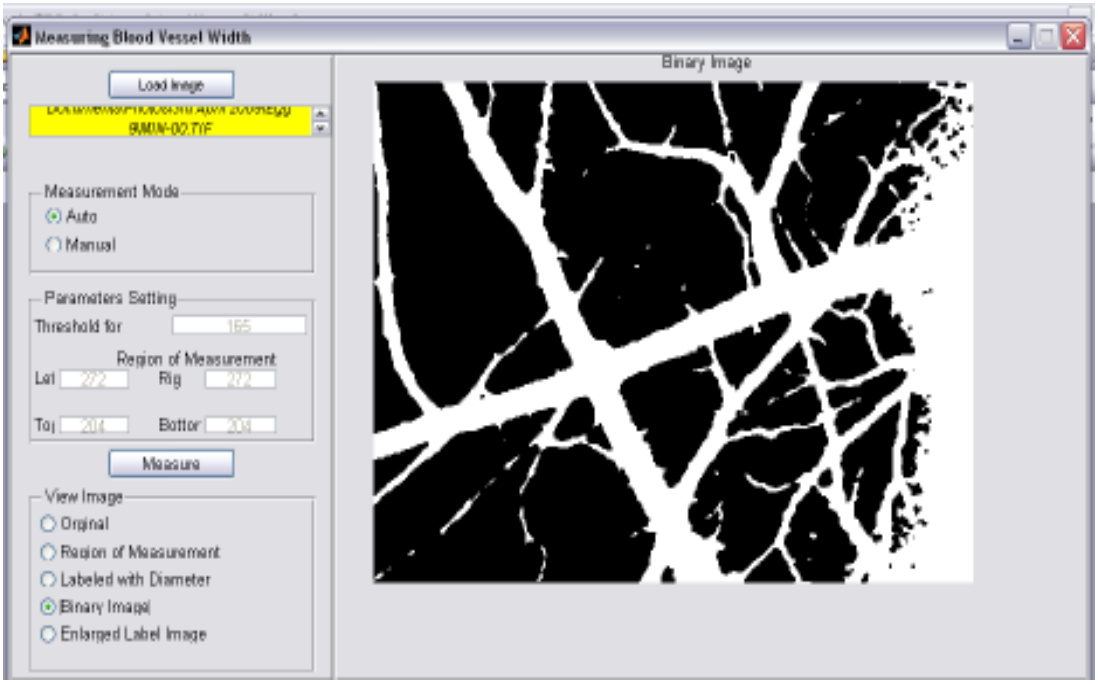

Figure 6. (a) Software interface (b) Binary image of vessel for determination of vessel diameter

B.6.ii. Synthetic membrane

A synthetic membrane composed of regenerated cellulose (Sartorius Stedim Biotech, France) was used to support the test biological membrane in the Franz diffusion cell. The synthetic membrane with a pore size of 0.45 μm was cut into a circular disc to fit the top of the receptor compartment. The test biological membrane was placed on top of the synthetic membrane.

B.6.iii. CAM

The eggs were incubated for different periods of time to obtain CAM of different embryonic age. The CAM was harvested by first making a hole at the blunt end of the egg with a sharp pair of forceps. The eggshell was then cut into half along its length and the contents of the egg emptied, leaving the CAM adhered to the underside of the shell underneath the inner shell membrane. Normal saline was used to wash the surface of the CAM following which the CAM was carefully removed from the inner shell membrane with a pair of forceps. The CAM was rinsed in normal saline again and immediately used in the permeation study or frozen for use at a later date. The thickness of the CAM was also measured with a micrometer at three different locations.

B.6.iv. King cobra skin

The shed king cobra skin was washed and dried at room temperature before being cut into discs and stored at room temperature. The skin disc was hydrated by soaking in isotonic phosphate buffer in a covered petri dish for 30 min prior to use.

B.6.v. Pig skin

Freshly harvested pig skin was frozen at -30^{o}C and thawed prior to preparation. The hair on the specimen was trimmed with a pair of scissors and the harvested skin cut into appropriate sizes. The skin was then rinsed with normal saline and soaked in isotonic phosphate buffer for 30 min prior to use.

B.6.vi. Pig buccal mucosa

The sample supplied consisted of the buccal mucosa with the underlying fat and muscle tissue. Hence, the specimen was first treated by soaking in hot water at 60ºC for 2 min to facilitate the removal of the mucosa layer from the base material tissue with a pair of forceps. The buccal mucosa was then washed with normal saline and soaked in isotonic phosphate buffer for 30 min prior to use.

B.6.vii. Pig retina tissue

The retina tissue was carefully removed from the back of the pig eyeball using a pair of forceps. The retina tissue was then washed with normal saline and soaked in isotonic phosphate buffer for 30 min prior to use.

B.6.viii. Assembly of the Franz diffusion cell

Permeation studies were carried out with the use of the Hanson Microette® apparatus (Hansons Research. USA). The apparatus consisted of six Franz diffusion cells in a vertical arrangement (Figure 7 and Figure 8). Each diffusion cell consisted of a lower receptor compartment and an upper cell top that could serve as the donor compartment. The test substance was placed into the donor compartment. The donor compartment was connected with the receptor compartment by a central orifice of

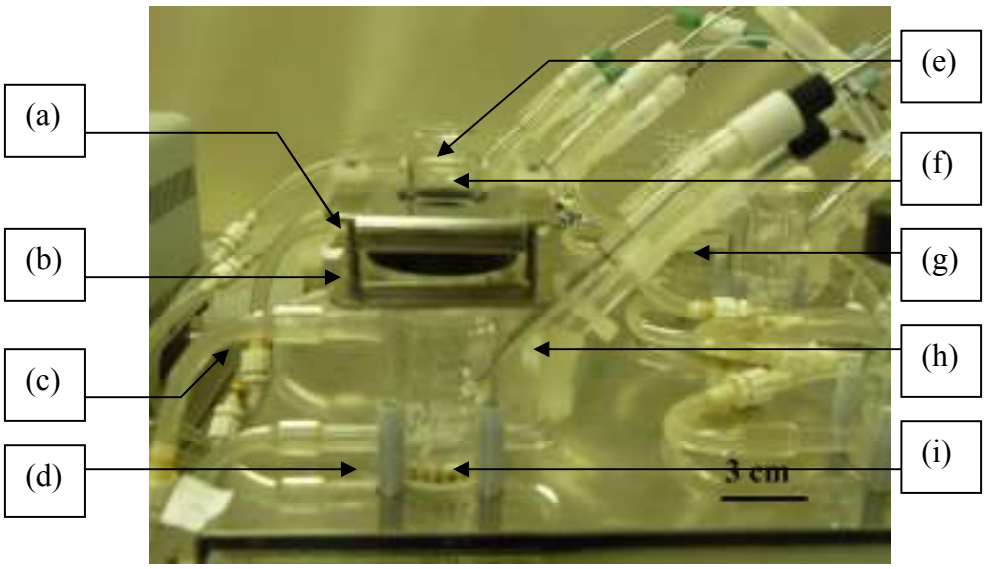

Figure 7. Photograph of the Franz cell used: (a) Clamp to hold setup in place (b) Site for membrane placement (c) Thermostated jacket (d) Receptor Compartment (e) Hole for introduction of test substance (f) Donor compartment (g) Side arm for introduction of fresh medium (h) Side arm from which samples are withdrawn (i) Magnetic stirrer

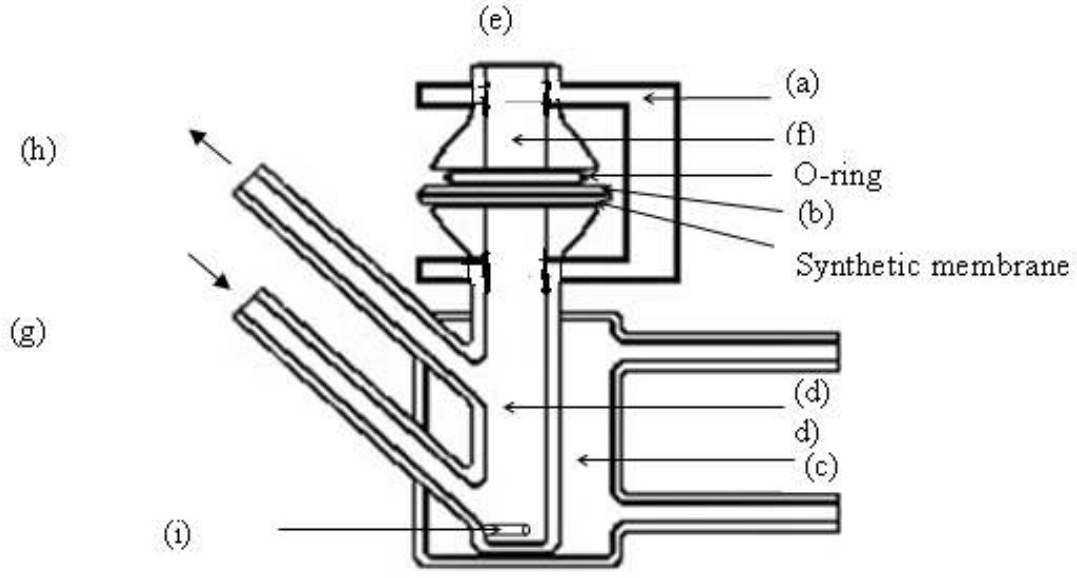

Figure 8. Diagram of the cross section of the Franz cell setup: (a) Clamp to hold setup in place (b) Site for membrane placement (c) Thermostated jacket (d) Receptor Compartment (e) Hole for introduction of test substance (f) Donor compartment (g) Side arm for introduction of fresh medium (h) Side arm from which samples are withdrawn (i) Magnetic stirrer

diameter 15 mm. The test membrane, with an underlying synthetic membrane, was placed on a Teflon disk with a central orifice of diameter 8 mm or 15 mm. A synthetic membrane was used to provide additional structural support. The fixture was then fastened between the donor and receptor compartments with the use of a clamp. The donor compartment was filled with 1 mL of drug solution. The receptor compartment was filled to its capacity with 7 mL of isotonic phosphate buffer. The membrane was allowed to equilibrate in the Franz diffusion cell for 1 h prior to sampling using a system of six syringes connected to a vacuum-controlled autosampler. Sampling was conducted over pre-determined time intervals. Sink conditions were maintained with the continuous use of a helix stirrer set at 600 rpm, as well as with the continuous top up of fresh isotonic phosphate buffer in the receptor compartment following the withdrawal of a sample from the receptor compartment at specific time intervals. The setup was maintained at a constant temperature of 37 ^{o}C. The constant temperature was provided by a water jacket controlled by a circulator water bath (Hanson Instruments, USA). The samples collected were analysed by HPLC according to the procedure described in Section B.6.ix.

B.6.ix. HPLC analysis

B.6.ix.a. Nicotine

The quantification of nicotine was performed with reversed-phase HPLC using a C-18 column (Hypersil, 5 μm, 4.6 mm x 200 mm). The mobile phase consisted of 0.05M sodium acetate and methanol in the proportion of 88:12 v/v, with 0.5 % triethylamine. The pH of the mobile phase was then adjusted with glacial acetic acid to pH 4.2. Flow rate was set at 1 ml/min with sample injection volume of 20 μL and nicotine assayed

spectrophotometrically at 259 nm. The retention time obtained was between 6.5 to 7.5 minutes, as reported in the literature (Pongjanyakul et al., 2002, Berner et al., 1992). Under these conditions, the calibration plot for nicotine between 0.0005 % and 0.2 % v/v demonstrated good linearity and reproducibility ($r^2 > 0.99$).

B.6.ix.b. GTN

The quantification of GTN was performed with reversed-phase HPLC using a C18 column (Hypersil, 5µm, 4.6 mm x 200 mm). The mobile phase consisted of HPLC grade methanol and deionized water in the proportion of 73:37 v/v. Flow rate was set at 0.9 mL/min with sample injection volume of 20 µL and GTN assayed spectrophotometrically at 210 nm. The retention time obtained was between 3.5 to 3.6 min. Under these conditions, the calibration plot for GTN between 0.0032 % and 0.045 % v/v was obtained.

B.6.ix.c. Data analysis

Sink conditions were maintained in the receptor compartment by the maintenence of a constant amount of medium in the receptor compartment, as supplied by the addition of fresh medium after the withdrawal of sample. As such, the amount of drug that permeated through the membrane can be described by Equation 2 (Baker et al., 1990).

$$M_T[n] = V_r \cdot C[n] + V_s \cdot \sum_{i=1}^{i=n-1} \{C[n-1]\} \qquad \text{Equation 2}$$

where $M_T[n]$ = Cumulative amount of drug transported across the membrane at time t, C[n] = Concentration of the drug in the receptor medium, V_r = Volume of the receptor medium, V_s = Volume of sample removed for analysis at each sampling point and $\sum\{C[n-1]\}$ = Summation of the previously measured concentrations.

Steady state flux, an indicator of absorption, can then be established by Fick's first law of diffusion that is descriptive of the steady state diffusion through a membrane (Equation 3).

$$J = \frac{dQ}{dt}\ \frac{1}{A} = K_p C_D \qquad \text{Equation 3}$$

Where J = Steady state flux, Q = Amount of drug that permeated through the membrane, t = Exposure time, A = Area of application, K_p = Permeability coefficient and C_D = Concentration applied to area of application

The cumulative amount of drug that permeated through the membrane per unit area $^{Q}/_{A}$ can be calculated and plotted as a function of time, *t*. Steady state flux, *J* can be obtained via linear regression analysis of the initial linear portion of the plot. Further comparison can be made with permeability coefficient, K_p values. The K_p value was obtained by dividing the steady state flux value by the concentration of drug applied. A total of 3 determinations were obtained for each permeation study.

B.7. Statistical Analysis

The normality of the data was assessed with the Kolmogorov-Smirnov test. Statistical analysis of the data obtained was performed using one-way ANOVA. Assessment of the influence of LDPI parameters on blood perfusion measurements were conducted with a orthogonal array design using Minitab (Version 14, Minitab Inc, USA) with significance level set at 0.05. Linear correlation of data was tested with the Pearson correlation test. Statistical analysis of the changes in blood perfusion values and vessel diameters were performed using the paired samples T-test for individual eggs. The tests were performed using the statistical software SPSS for Windows (Version 11, Lead Technologies, USA), with significance level set at 0.05.

RESULTS AND DISCUSSION

A. Preparation of the CAM

A.1. Full deshelling method

It should be pointed out that various methods involving complete deshelling of the egg have been employed since the 1970s. In the earlier studies, the egg was de-shelled and its contents placed in a container under saturated humidity conditions with either 1 – 2 % carbon dioxide throughout the whole incubation period or in 5 – 6 % carbon dioxide after 10 days of incubation (Bartholomew and Crawley, 1980, Dunn et al., 2005). Other methods described the use of containers in the form of polyethylene film across a ring stand (Tuan, 1980) and petri dishes with or without a polyethylene film to hold the contents of the egg (Lugassy. et al., 2006, Tufan. et al., 2004). The latter method was employed in this study and termed as full de-shelling method. If the CAM were present, it might be injured when the egg was cracked into halves and the content transferred into the sterile petri dish. Hence, eggs at EA 3 and EA 4, when the CAM has not completely formed, were used.

The survival rate of the embryos using the full deshelling method was generally low. The cracking caused the yolk of some of the eggs to leak (Figure 9a). Yolk leakage is usually an indication of injury leading to poor survival rates (Richardson and Singh, 2003). Only 32 % of the eggs survived beyond a day after cracking the shell. When an embryo died, the CAM blood vessels were gradually devoid of blood because of the failure of the circulatory system and the CAM appeared translucent (Figure 9b). For those that survived more than a day, the histological development of the embryos as well as their blood vessels was generally delayed and abnormal when compared to the normal unshelled egg embryo development process. Fully deshelled embryos did not proceed to form distinct organs and limbs such as the feet and wings that were

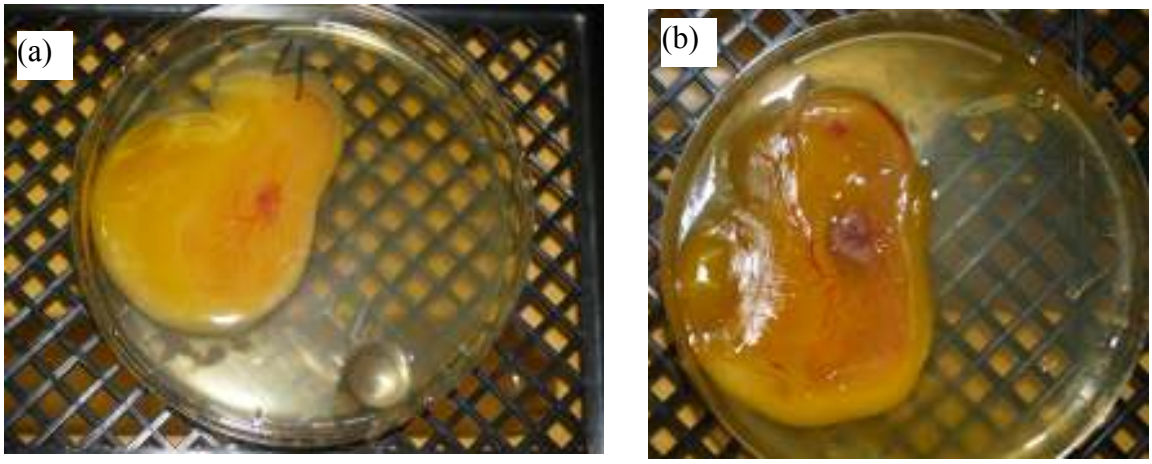

Figure 9. (a) Viable embryo (b) Dead embryo

expected at that embryonic age (Hamburger and Hamilton, 1992). This retardation of growth with the full deshelling method was previously reported (Tuan, 1980) and damage to the CAM was also documented (Samkoe and Cramb, 2003). Such a drastic technique also increases the risk of suffocation as the porous egg shell, which allows gas and water to permeate through the pores, is removed and replaced by a petri dish (Vogelaar and Boogert, 1925). Water is not able to permeate through the petri dish and water condensation occurred on the cover of the petri dish. The content of the egg being transferred into a petri dish allowed for a greater degree of expansion and freedom of movement than was provided for in the shell, thus the membrane had a possibility of being stretched considerably. As such, any measurements gleamed from the CAM was not as consistent nor accurate as the CAM was not in its natural state and its properties may have been altered in light of being in an unconfined space. Such an *ex ova* system was also hampered by the exposure of the chick embryo to the environment as opposed to the sheltered and controlled environment provided by the egg shell. The survival rates of the embryos in the earlier studies were not reported. In

the present study, it was clearly demonstrated by the poor survival rate that the complete deshelling method was harmful to the embryo. Hence, the complete deshelling method did not appear to be a viable method for preparing the CAM for experimental studies. Another point in favour of the use of the partial deshelling method is the availability of a cup-like cavity with measurable exposed CAM area. This allows for a fixed area for drug diffusion when experiments to determine pharmacokinetic parameters are carried out.

A.2. Partial deshelling method

Other more technically challenging methods that have been described in the literature are the dropped membrane and Zwillig techniques. The dropped membrane method involves the formation of a window in the blunt end of the egg with the use of a drill. Negative pressure, provided from the sucking mechanism of a rubber bulb, is introduced prior to the removal of the inner shell membrane from the egg (McCormick et al., 1984). In the Zwillig method, a hole is drilled through the CAM to remove the albumen so as to create a false air sac where the CAM will continue to grow without being attached to the inner shell membrane (Zwilling, 1959). Improper coverage of the hole can affect oxygen tension. This should be avoided as it was found that changes in oxygen tension can lead to changes in CAM vascularity (Strick et al., 1991). The partial deshelling method was adapted from the dropped membrane technique. In the partial deshelling method, older eggs with a higher chance of survival as compared to the eggs used in the full deshelling method were employed. The basic structure of the CAM would have already been formed in these embryonically older eggs.

Preliminary investigations were carried out to determine the optimal embryo age for partial de-shelling to prepare the CAM. As the CAM had not developed fully before EA 4, partially egg deshelling can only be carried out after this age. Deshelling eggs from EA 4 to EA 6 proved to be a very delicate task as the CAMs were still very fragile. After EA 7, the CAM was found to adhere too strongly to the egg membrane, making it more challenging and precarious to separate the CAM from the 2 outermost membranes, often resulting in bleeding after the deshelling procedure. The CAM was found to adhere strongly to the inner shell membrane at EA 8 and beyond (Dimitropoulou et al., 1998), hence making deshelling increasingly non viable.

After preliminary investigations, it was decided that the eggs for CAM measurements would be partially deshelled at EA 7 and placed in the incubator to stabilize and mature till EA 9, the desired EA for experimentation on the CAM. This allowed the CAM sufficient time after the partial deshelling process to recover before experimentation. This also helped to eliminate problematical eggs that would succumb to the trauma of partial deshelling during the interim period. The CAM was visually assessed before experimentation, to ascertain that the CAM appeared healthy. Healthy CAMs should possess vessels that are free of bleeding or shrinkage, yolk bright yellow in colour and the embryo showing signs of activity.

The partial deshelling method was found to be more successful when compared to the full deshelling method as the average egg survival rate was around 50 % and often markedly higher. For the full deshelling method, measurements of the vessel diameters and assessment of a suitable embryonic age at which to prepare the CAM

was not carried out. Hence, only partial deshelling method was adopted for subsequent experiments.

A.3. Egg weight with incubation time

The decrease in egg weight over time exhibited a linear trend as shown in Figure 10. The trend is consistent with that reported for water loss in chicken embryos (Snyder and Birchard, 1982). Water was lost at a constant rate during the incubation period as the permeable egg shell presented a constant surface area for water loss. This finding indicates that the handling and incubation conditions used were appriopriate and unlikely to affect the normal development of the egg. These findings also showed that the conditions in the incubator were relatively consistent and well controlled.

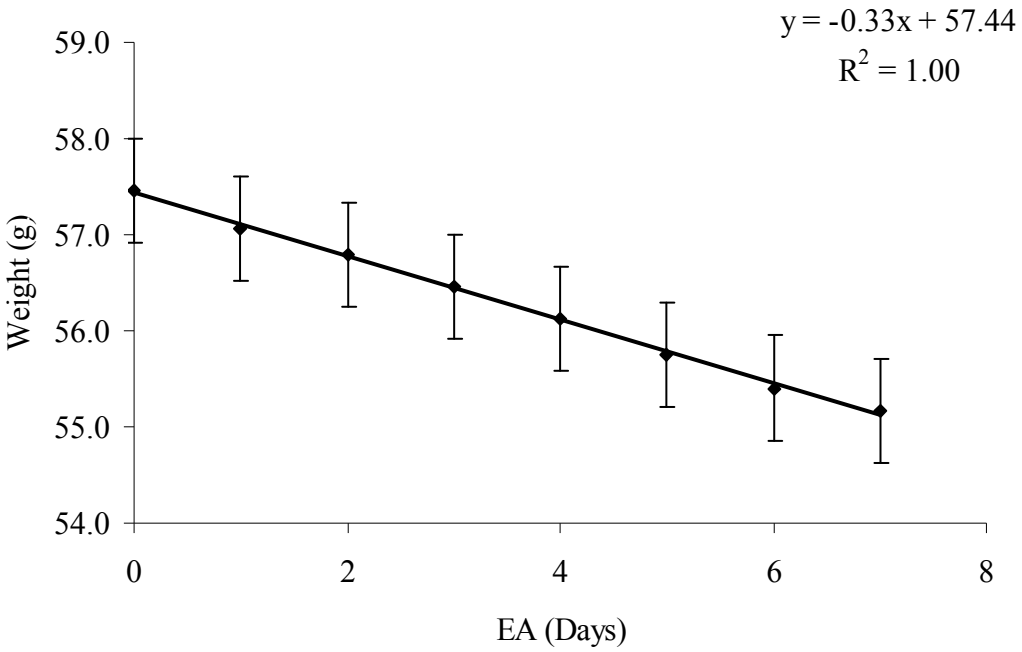

Figure 10. Decrease in egg weight over time (n = 10)

A.4. CAM thickness

The thickness of the CAM was reported to differ depending on the site of measurement. The thickness of the CAM under the air sac was found to be thinner than other parts of the egg. The average thickness of the CAM at EA 9 was 60.6 μm, with a coefficient variance of 22 %. The value obtained from this study was comparable to that reported (Reizis et al., 2005).

B. Influence of CAM on blood perfusion measurement

B.1. Embryo age

Blood perfusion of the CAM was found to follow a normal distribution pattern ($p > 0.05$) according to the Kolmogorov-Smirnov test for normality of data. This shows that the data from the CAM was normal, and hence can be subjected to statistical tests for normal data. The blood perfusion values showed less variation from EA 8 to EA 14, beyond which, blood perfusion increased sharply and then decreased beyond EA 16 (Figure 11). Measurements were not made at EA 7, which was the day deshelling was performed, to avoid any possible influences of the trauma of deshelling on the perfusion readings. The standard error of the readings generally increased with the embryo age. This could be due to the movement of the embryo as it aged and grew bigger. The diameters of vessels in the CAM generally ranged from 160 to 300 μm, with the diameters of some vessels reaching 500 μm, depending on the age of the embryo and the order and branch of vessel measured.

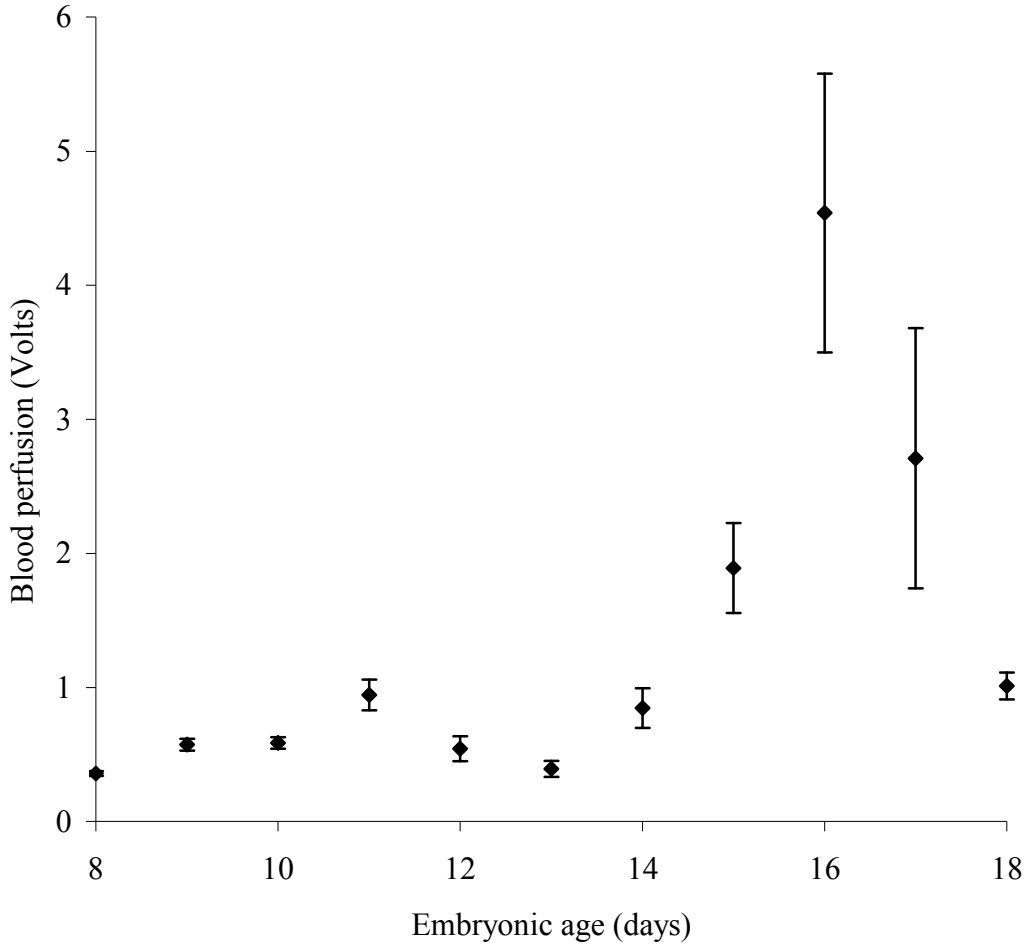

Figure 11**.** Baseline blood perfusion in CAM at different EA. The bars represent the standard error of the measurements. (n = 3 for each data point)

Embryonic age of 14 -18 days is classified as the late stage of embryo development during which the microvasculature of the CAM is fully matured (Shumko et al., 1988). This could have accounted for the sharp increase in blood perfusion of the CAM after EA 14. The subsequent decline was probably due to the degradation of the mesoderm in the CAM where the CAM vessels were located (Shumko et al., 1988). The choice of embryo age for experimentation was based on several factors. The chosen embryo age should give consistent blood perfusion readings with low standard error. This was to ascertain that any changes in blood perfusion were due largely to

the effects of the test substance and not because of natural fluctuations in baseline blood perfusion. From the preliminary perfusion readings made, the window for measurements was narrowed down to an EA range of 8 to 14 days. As mentioned previously, the CAM should be allowed time to recover from the trauma of deshelling at EA 7. Furthermore, the experiments were recommended to be performed 3 days after deshelling in view of the potential of immune or inflammatory responses (Staton et al., 2009). Taking the 2 abovementioned factors into consideration, EA 8 was deemed too early for experimentation. The embryo at EA 13 had been reported to move considerably and hindered blood vessel measurements (Hammer-Wilson et al., 2002). This eliminated EA 13 as being a suitable choice to perform blood perfusion measurements. The embryo was better developed at EA 10 than EA 9. This would increase the potential of embryo movement at EA 10, which would affect the blood perfusion readings obtained. It should be recalled that the fertilized egg at EA below 10 is not considered as a "living" whole animal as yet and thus exempted from ethical considerations. It is also of interest to note that a previous study concerning an investigation into the hyperemic reaction of the CAM by epoxyeicosatrienoic acids found that only CAMs of EA 9 and no other age, gave 100 % positive responses to epoxyeicosatrienoic acids at a dose that was known to be angiogenic (Dunn et al., 2005). This suggests that EA 9 was a sensitive age suitable for experimentation with regards to the suitability of the CAM vessels. Hence, EA 9 was chosen as the optimal embryo age to perform the subsequent perfusion experiments.

B.2. Egg temperature

Short term temperature fluctuations were found to affect the consistency of the blood perfusion readings significantly (p value > 0.05) (Figure 12). Cooling was reported to decrease the rate of blood perfusion (Bornmyr et al., 2001). Further investigation therefore was carried out to improve measurement reproducibility by controlling the measurement temperature using an experimental setup that maintained the temperature of the egg during measurements. The egg was placed in a jacketted egg cup that was kept at a constant temperature by circulation of water from a temperature-controlled water bath. The temperature of the water bath was varied and the corresponding temperature of the egg cup was determined. The results showed a linear relationship which enabled control of the egg cup temperature by adjusting the temperature of the water bath (Figure 13). The temperature of the water bath had to be adjusted to 44°C and the setup allowed to equilibrate for 2 h to obtain an egg cup temperature of 36 – 37°C. An egg for experimentation was then removed from the incubator and placed immediately in the egg cup and allowed to equilibrate for 15 min before commencement of blood perfusion measurements. The normalized perfusion readings were found to be relatively constant with time (p value > 0.05), indicating that the constant temperature provided to the egg had enabled more consistent perfusion readings (Figure 12). Clearly, the specially fabricated egg cup was important for consistent perfusion measurement of the CAM using the LDPI equipment.

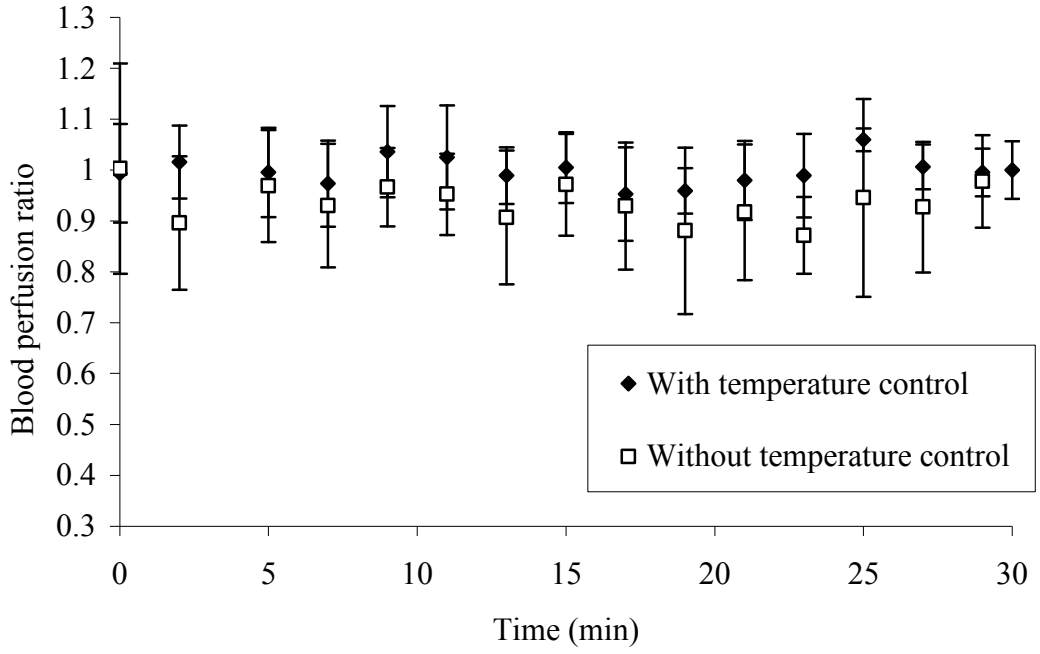

Figure 12. Blood perfusion readings of CAM (EA 9) over time with temperature control of 36 – 37 ^{0}C and without the use of temperature control (ambient, 26 – 30 ^{0}C) (n = 3)

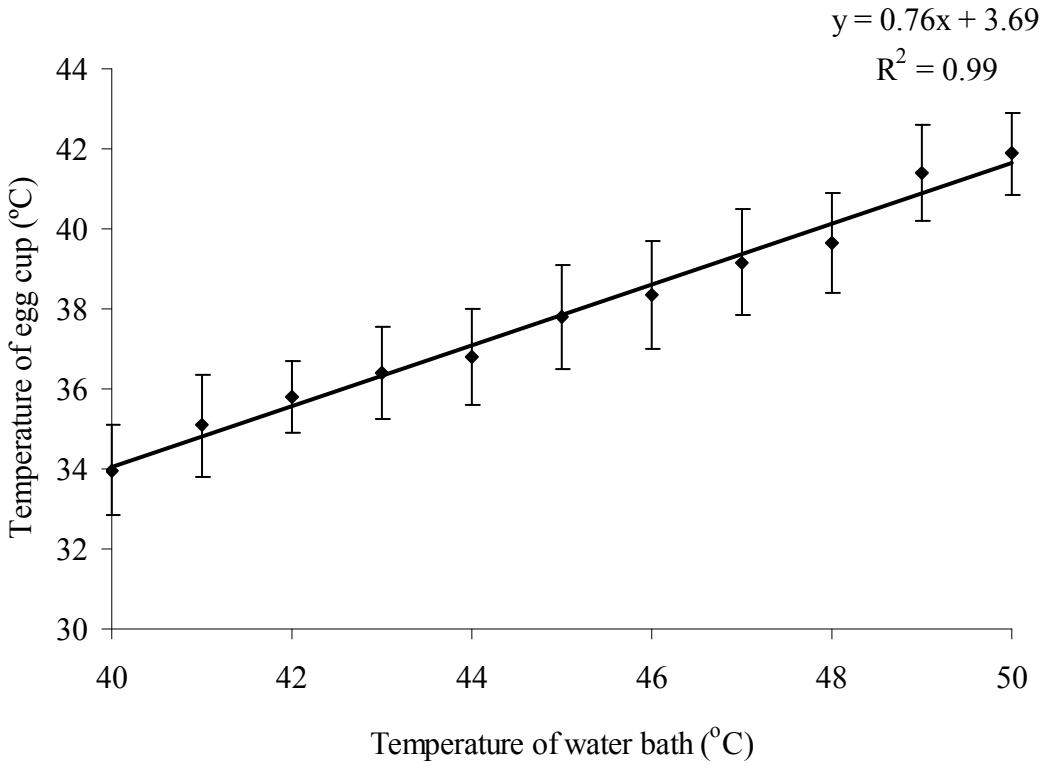

Figure 13. The relationship between the temperature of the water bath and the temperature of the egg cup (n = 3)

C. Investigation of LDPI parameters on blood perfusion measurements using orthogonal array and partial factorial design

The settings of the laser Doppler for CAM blood perfusion measuements were examined experimentally by statistical design studies. An orthogonal design study was carried out and amplitude was ranked as the variable of greatest influence (Tables 7 and 8). The second most influential variable was found to be threshold, followed by distance and area of measurement. A second partial factorial study conducted found amplitude and threshold to be significant contributors to the perfusion measurements (p values < 0.05). However, no significant differences were observed for the different measurement and different distances between Doppler head and sample tested. Whilst the orthogonal array design and partial factorial studies were able to ascertain the more influential LDPI parameters, these studies were not able to determine the appropriate settings of each significant parameter for accurate measurement of blood perfusion.

C.1. Univariate analysis

A more detailed study was performed with different amplitude and threshold values to assess the extent of contribution of these variables to blood perfusion. Each of the LDPI parameters was evaluated one at a time by varying a specific parameter while keeping the other parameters constant. Area of measurement and distance of the sample from the Doppler head were also included in this analysis to confirm their non-significance. Perfusion measurements were made at the same location on the CAM for meaningful comparison and eggs of EA 9 were used.

Table 7. The L25 (54) Taguchi design matrix for influence of LDPI parameters on blood perfusion

Expt	**Variables**				**Outcome**	
	Distance	Area	Amplitude	Threshold	Blood perfusion (v)	Standard error
1	0.00	0.00	0.00	0.00	0.00	0.00
2	0.00	3.00	3.00	3.00	3.82	0.32
3	0.00	5.00	5.00	5.00	6.81	0.59
4	0.00	7.00	7.00	7.00	6.73	1.70
5	0.00	10.00	10.00	10.00	0.00	0.00
6	3.00	0.00	3.00	5.00	3.66	0.14
7	3.00	3.00	5.00	7.00	4.19	1.75
8	3.00	5.00	7.00	10.00	0.00	0.00
9	3.00	7.00	10.00	3.00	9.93	0.03
10	3.00	10.00	0.00	3.00	0.00	0.00
11	5.00	0.00	5.00	10.00	0.00	0.00
12	5.00	3.00	7.00	0.00	9.76	0.15
13	5.00	5.00	10.00	3.00	9.99	0.01
14	5.00	7.00	0.00	5.00	0.00	0.00
15	5.00	10.00	3.00	7.00	7.10	1.81
16	7.00	0.00	7.00	3.00	9.15	0.34
17	7.00	3.00	10.00	5.00	9.80	0.11
18	7.00	5.00	0.00	7.00	0.00	0.00
19	7.00	7.00	3.00	10.00	0.00	0.00
20	7.00	10.00	5.00	0.00	7.66	0.35
21	10.00	0.00	10.00	7.00	2.00	2.00
22	10.00	3.00	0.00	10.00	0.00	0.00
23	10.00	5.00	3.00	0.00	5.02	0.62
24	10.00	7.00	5.00	3.00	7.14	0.32
25	10.00	10.00	7.00	5.00	9.42	0.12

Table 8. Influence of LDPI parameters investigated in accordance with an orthogonal array design

	Blood perfusion (V)			
	Distance	Area	Amplitude	Threshold
K_1	3.471	2.961	0.000	6.474
K_2	3.555	5.513	3.918	6.018
K_3	5.368	4.362	5.158	5.937
K_4	5.322	4.759	7.011	4.002
K_5	4.715	4.836	6.344	0.000
R_K	1.898	2.552	7.011	6.474

K_1, K_2, K_3, K_4 and K_5 refer to the average reading for each variable at levels 1, 2, 3, 4 and 5 respectively. R_k refers to the range of K values for each variable, i.e. K_{max} - K_{min}

C.2. Area of measurement

Equivalent perfusion readings with comparable standard errors (Figure 14) were obtained for the 6 different measurement areas investigated. Statistical analysis of the data showed no significant differences ($p > 0.05$) among the readings, showing that the perfusion reading was not markedly affected by the size of the measurement area in the range chosen. Thus, an intermediate measurement area with the smallest width and medium length, 2 mm X 10 mm was chosen.

C.3. Distance between sample and Doppler head

The distance between sample and laser beam aperture located in the Doppler head was varied and it was found that a variation from 10 cm to 20 cm had insignificant effect on the perfusion readings ($p < 0.05$). A study reported in the literature also

suggested that the distance between the test object and the Doppler head was best kept constant to eliminate variation of total quantity of reflected light which may contribute to random errors (Pemp et al., 2009). The amount of backscattered light, which is used to calculate the perfusion measurement may decrease with an increase in the distance from the sample to the Doppler head (Kernick and Shore, 2000). Hence, the Doppler head was kept at a constant distance of 11 cm away from the sample (Figure 15).

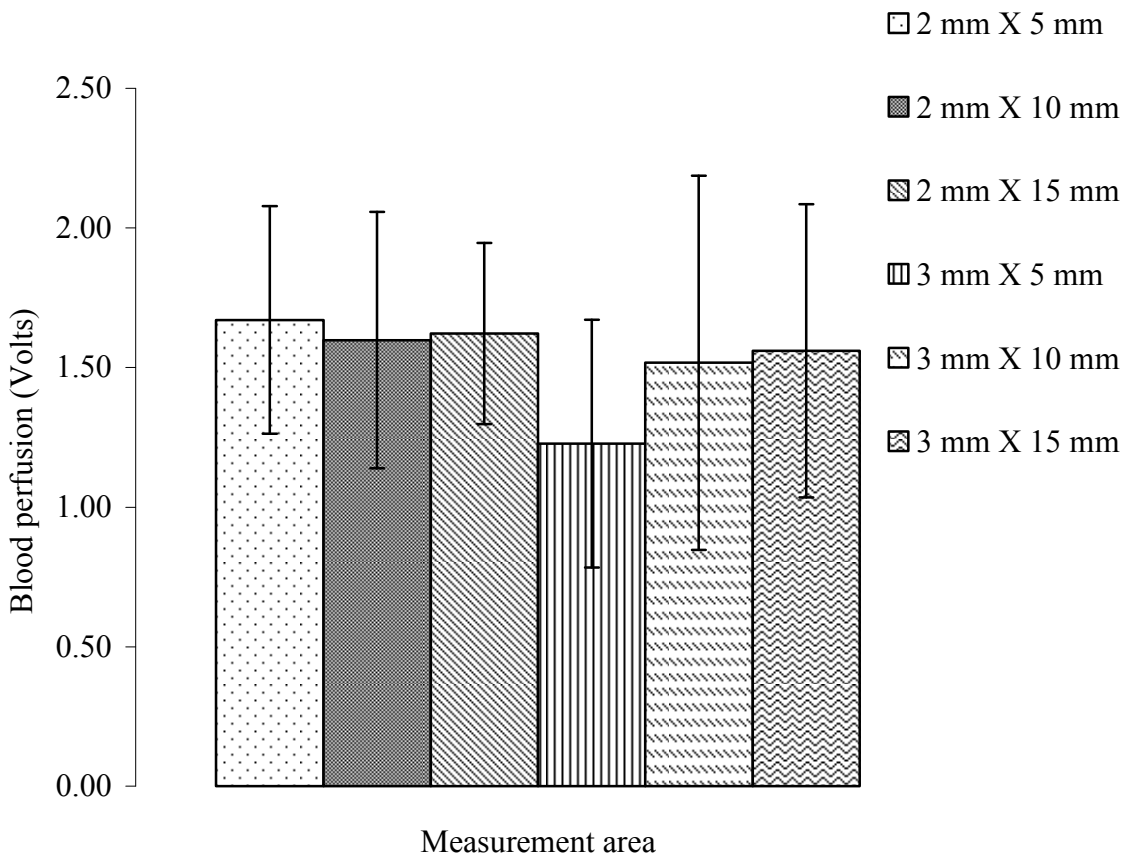

Figure 14. Blood perfusion readings using different measurement areas (n = 3)

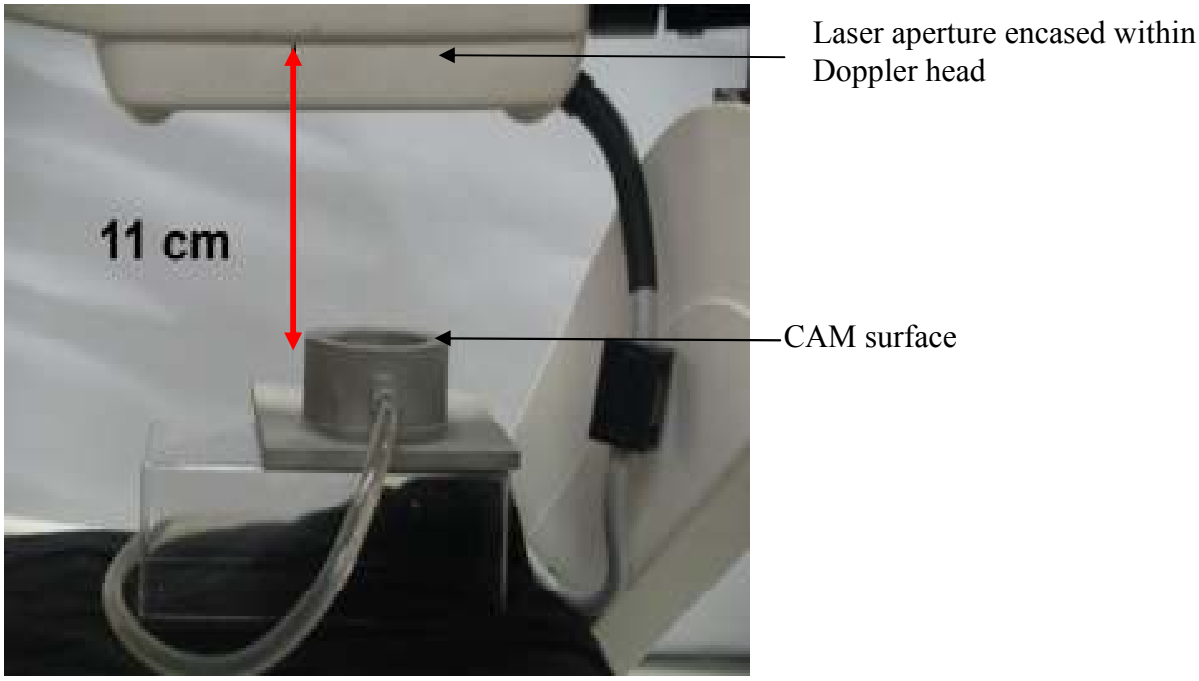

Figure 15. Diagram of LDPI and egg cup illustrating distance between the Doppler head and sample.

C.4. Amplitude

Blood perfusion readings were found to increase linearly with the amplitude over the range of 0 to 10 (R^2, 0.99). However, the standard error also increased proportionally. The same trend was observed for standard errors of the readings, indicating greater variation of blood perfusion with increased amplitude values. Thus, an amplitude of 1 was chosen as the most reliable as it enabled a sensitive measurement with the lowest standard error value (Figure 16). The choice of amplitude setting coincided with the recommendation of the equipment manufacturer.

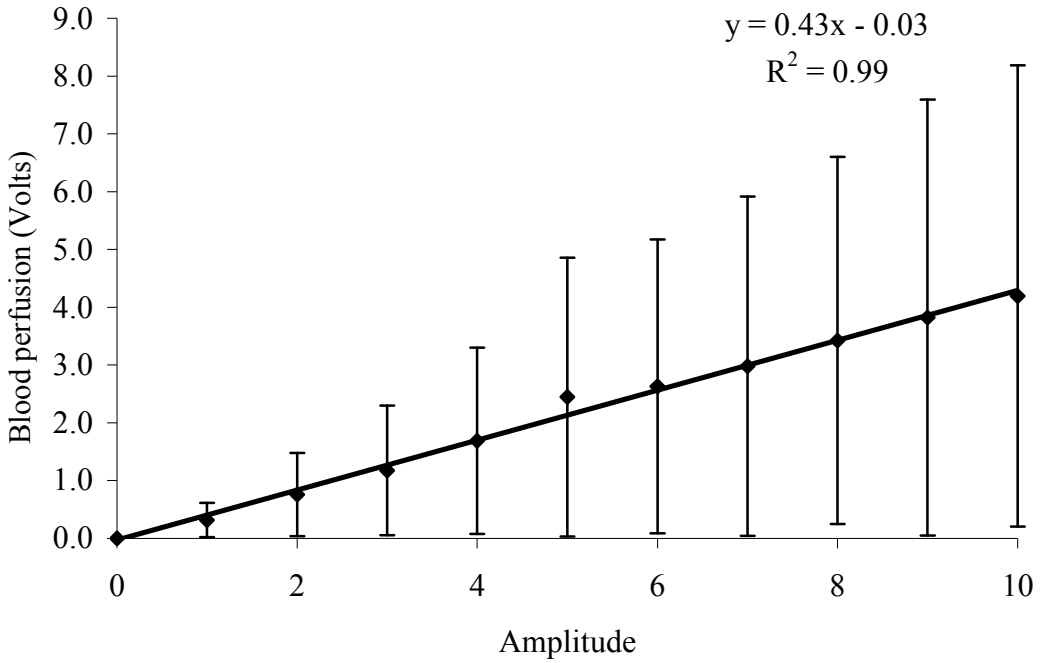

Figure 16. Relationship between amplitude and blood perfusion of CAM (EA 9) (n = 3)

C.5. Threshold

Beyond threshold 7, the blood perfusion readings decreased markedly, and decreased to almost zero (Figure 17). Hence, threshold beyond 7 was deemed unsuitable for blood perfusion measurements. For a measurement, a high threshold was expected to be more sensitive and therefore a reasonably high threshold value of 6 was chosen for subsequent experiments. These optimization experiments were conducted using the CAM without the application of any test substance. A higher threshold would serve to adequately capture blood perfusion readings that may be increased or decreased on the addition of the test substance.

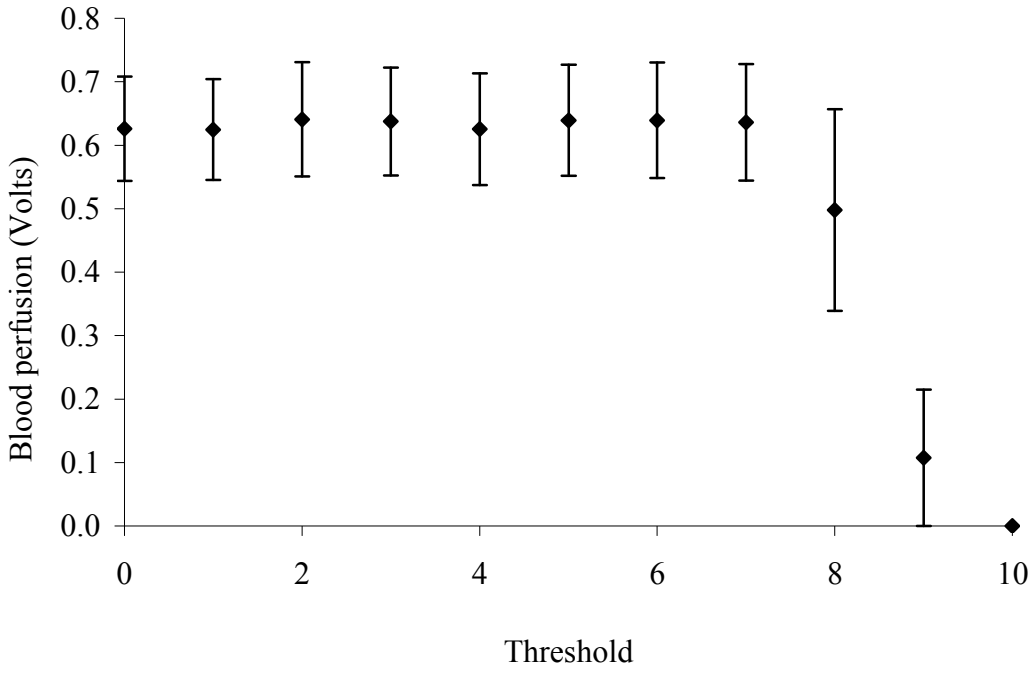

Figure 17. Relationship between threshold and blood perfusion of CAM (EA 9) (n = 3)

C.6. Scanning speed and resolution

The effects of scan speed and resolution were also studied in an attempt to elicit the sharpest image for measurement over the shortest possible scan time as a higher scan speed reduced the measurement time. The influence of scan speed and resolution on the resultant image data is depicted in Figure 18. A larger area of 16 mm x 16 mm using a human hand was employed to provide a clearer illustration of the effect of these two parameters on the resultant images and data. The use of high scan speed compromised the quality of the image obtained, leading to less reliable results(Figure 18c). Thus, a low scan speed of 17 mm^2 per second was selected. The measurement area covered when the resolution was set to low was greater than the area covered with a high resolution setting. However, a high resolution setting was necessary to produce sharp images of the test sample (Figure 18d – f).

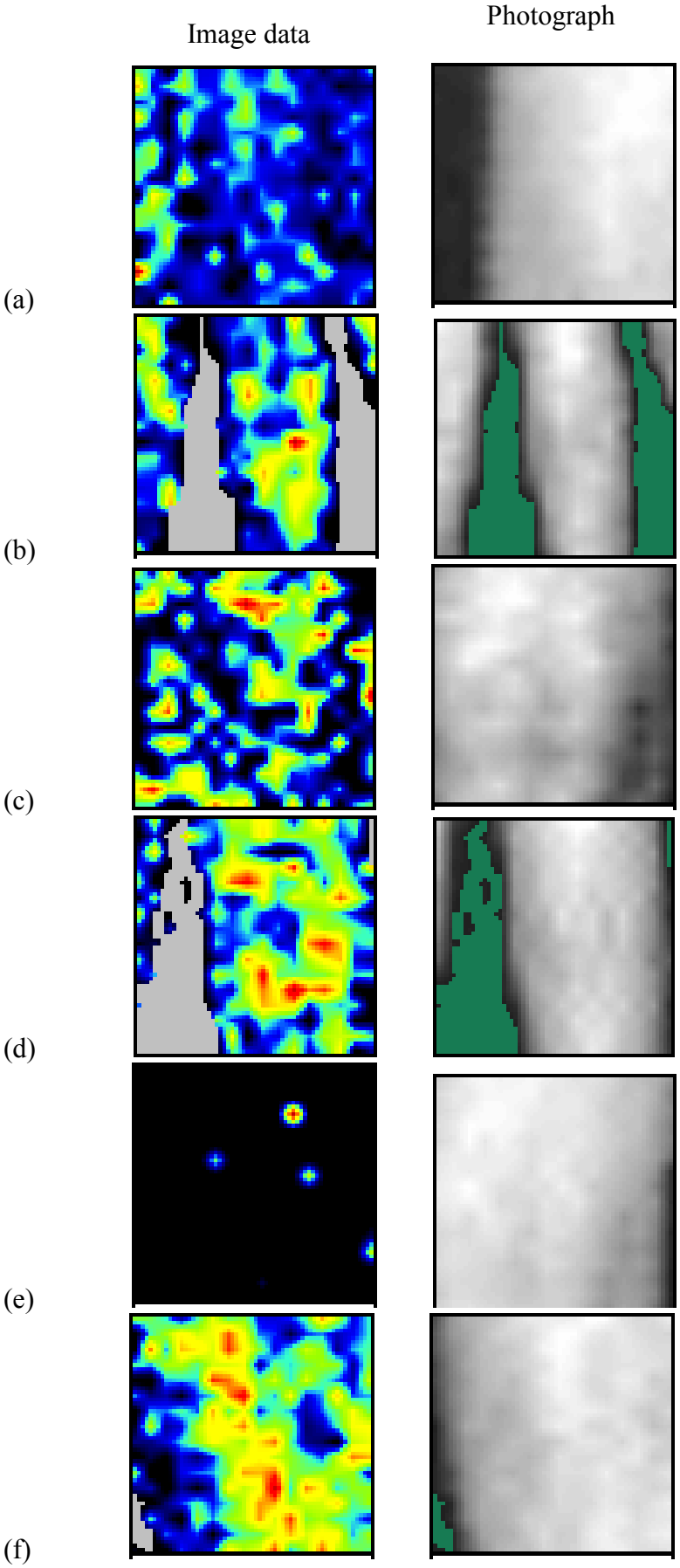

Figure 18. Image data and corresponding photographs obtained with (a) low scan speed, (b) medium scan speed, (c) high scan speed, (d) low resolution, (e) medium resolution and (f) high resolution

From the different investigations carried out, it can be concluded that the partial deshelling method is more suitable than the full deshelling method for preparing the CAM for experimentation. The blood perfusion in the CAM can be measured by the LDPI method. Reliable measurements are possible with the use of fertilized eggs of appropriate age, proper control of egg temperature and LDPI parameter settings.

D. Effects of test substances on tissue morphology & irritancy

D.1. The CAM as a model for irritancy assessment

The effects of photodynamic therapy on the CAM has been investigated (Gottfried et al., 1995). Damage to the CAM was quantified by the extent of haemostasis, clotting and haemorrhage. Clotting and haemorrhage have been previously defined (Methods - Section B.2). Haemostasis refers to the cessation of blood flow. The presence of haemostasis and clotting rendered the CAM as having undergone moderate damage, while extensive damage was depicted by the presence of widespread occlusion and haemorrhage. This method of assessment only focuses on the irritation effect but does not consider the time taken for the effect to be manifested. Since the latter is an important aspect of irritation potential, the aforementioned method may not be ideal.

Irritancy assessment with the aid of the CAM was employed as a replacement to the Draize eye test in the late 1980s and early 1990s (Hjortsjo et al., 2009). In 1985, a time-dependent grading system was proposed for assessing irritancy using the CAM. In the measurement, the test substance was applied to the CAM surface, which was then examined for various effects, such as hyperemia, haemorrhage and clotting. A score was assigned to each effect. The score was time-dependent as it took into account the manifestation time of the effect. A test compound may cause more than

one irritation effect and its irriation potential was indicated by the cumulative score. The reaction of the CAM to irritants was compared to that of mucous membranes and found to be similar (Luepke, 1985). A contact period of 5 min after the instillation of the test substance had been proposed as being sufficient to reveal the irritation or toxic effects on the CAM (Tavaszi and Budai, 2007). The short reaction time needed allows for rapid assessment of irritancy.

In this study, the CAM was employed to determine the irritation potential of various solvents and drugs. The findings would provide useful information for the selection of test substances and media for the subsequent perfusion studies (Table 9). No visible irritancy or changes in morphology were seen with deionized water, normal saline as well as 5% glucose monohydrate solution. The solvents selected are commonly used and not known to exert any adverse effect on the human body. The results of the irritancy assessment concurs with the above. No obvious signs of irritancy and/or toxicity were seen with propranolol at low concentrations, and theophylline, caffeine and GTN at all the concentrations tested. The above solvents and drugs were deemed as safe to use on the CAM at the tested concentrations. A more detailed discussion on some of the test substances will be given in the following section.

Table 9. Irritation potential of various solvents and drugs

Test substance	Concentration of test substance	Effects observed									Cumulative score
		Hyperamia			Haemorrhage			Clotting			
		A	B	C	A	B	C	A	B	C	
Deionized water	-										0
Normal saline	0.9 % w/v										0
5 % w/v glucose monohydrate	5 % w/v										0
Glycerin	-			√							1*
Propranolol (at doses less than 7.5 mg/kg)[#]	0.83 mcg/ml – 10 mg/ml										0
Propranolol (Doses: 7.5, 15, 30 mg/kg)[#]	15 mg/ml – 60 mg/ml			√			√			√	9
Caffeine (2,4,6,8, 10 mg/kg)[#]	4 – 20 mg/ml										0
GTN	1 mg/ml										0
1 % v/v NMP	1% v/v										0
10 % v/v NMP	10% v/v					√					5
70 % v/v Ethanol	70% v/v			√							1
Glucagon	1 mg/ml										0
Theophylline	0.17 – 7 mg/ml										0
Nicotine	0.013 & 0.023 mg/ml			√			√			√	9

A: Manifestation time ≤ 0.5 min
B: Manifestation time > 0.5 to 2 min
C: Manifestation time > 2 to 5 min
***** Grading does not take into account embryotoxicity caused by glycerin
[#] Average weight of the egg was found to be 60g and the amount of drug used was dosed according to the average weight of the egg

D.2. Propranolol

At higher concentrations of propranolol applied, the tissue displayed evidences of clotting, hemorrhage and/or the presence of ghost vessels. Examples of haemorrhage and embryotoxicity are shown in Figure 19. Ghost vessels refer to vessels which were identifiable but devoid of blood flowing through them. The CAM also underwent hemostasis (Figure 20). The propranolol concentration that caused vessel stasis was found to be close to the LD_{50} values reported for rats. LD50 refers to the medial lethal dose or lethal dose 50 %, which indicates the dose that kills 50 % of the animals tested. This suggests that the response of the CAM to toxicity could be akin to that of the rats, which are commonly employed as animal model in irritancy studies.

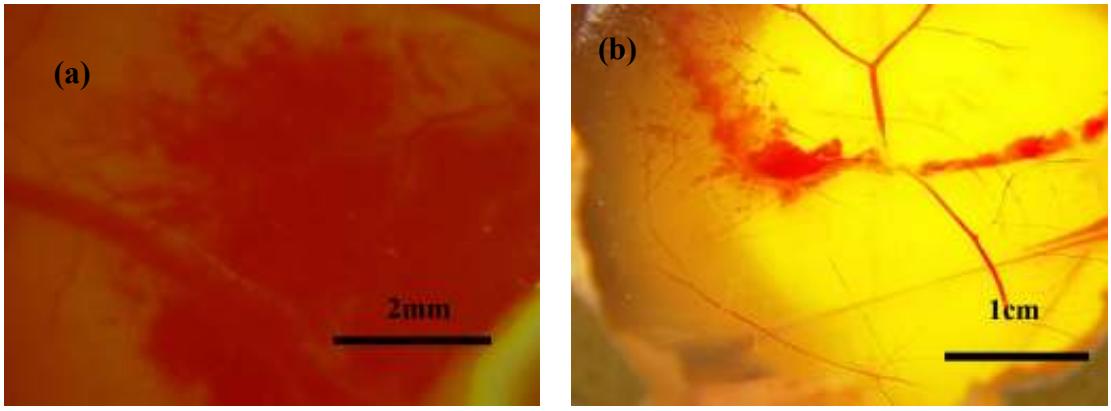

Figure 19. Example of (a) haemorrhage and (b) embryotoxicity

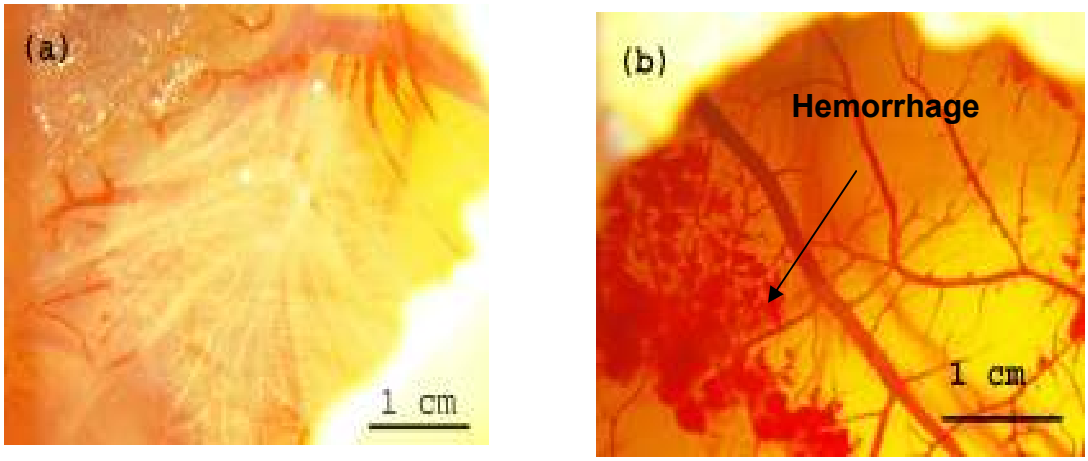

Ghosts vessels are seen. Clotting and haemorrhage of vessels occurred

Figure 20. Appearance of CAM (a) after the application of 30 mg/kg of propranolol and (b) after application of 7.5 mg/kg of propranolol.

D.3. 70% v/v Ethanol

Minimal irritation effects in the form of very slight bleeding occurred on the CAM surface on application of the 70 % v/v ethanol. The bleeding response was not immediate and seen only after at least 15 minutes. This response was rather slow despite the use of a fairly high concentration of ethanol. Thus, ethanol was classified as having slight irriation potential according to the time-dependent scoring system. In the method used to prepare the CAM for experimentation, the surface of the egg was first disinfected with 70% ethanol. There is a possibility of ethanol permeation through the egg shell and it is reassuring to find that 70% ethanol has only slight irritation potential. The use of 70% ethanol as a solvent for perfusion studies may be considered acceptable.

D.4. Glycerin

The CAM showed vessel stasis over time with pure glycerin and the embryo was dead by the end of the hour. This finding indicated the embryotoxicity of glycerin. Glycerin was reported to cause blockage of the small vessels in the CAM. At concentration of 90 % v/v, the main vessels of the CAM were damaged by blockage or coagulation (Forough et al., 2005). Glycerin was reported to cause embryotoxicity (Romanoff, 1960). This could also account for the drop in blood perfusion seen after instillation of glycerin. The application of high concentrations of glycerin to the CAM should be avoided. Therefore, glycerin was found to be an unsuitable solvent for perfusion studies.

D.5. Nicotine

Nicotine displayed signs of clotting, hyperaemia and vessel stasis at concentrations used in transdermal nicotine patches (Figure 21). Hyperemia was reported to occur in response to a reduction in blood flow to the tissue (Thorfinn et al., 2006). It was likely to be triggered by ischaemic stress due to reduced oxygen supply. The toxic effects of nicotine are known to occur mainly on the endothelium of the vascular system of humans (Czernin and Waldherr, 2003). Vessel stasis as a result of nicotine application has also been reported (Galanzha et al., 2007). According to the score obtained in this study, nicotine has strong irritation potential and is thus likely to affect the blood perfusion of the CAM.

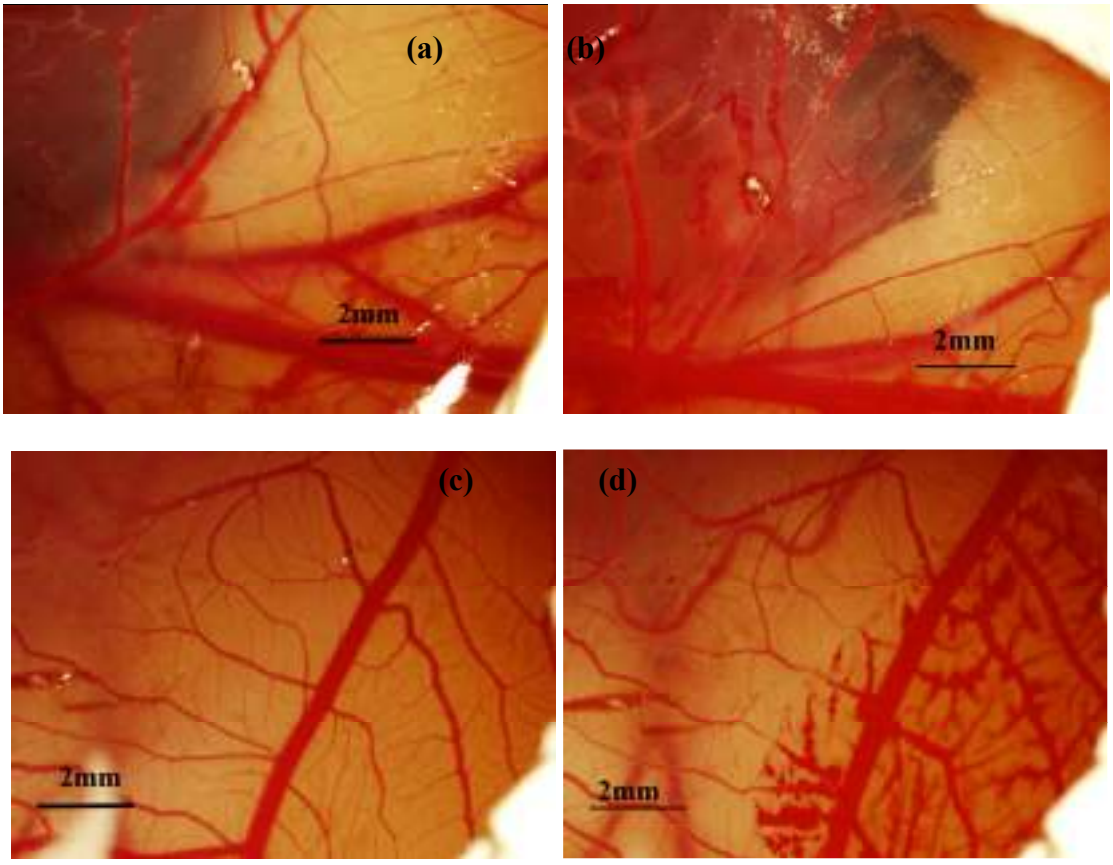

Figure 21. Appearance of CAM (a) before the application of 4 µg of nicotine per egg, (b) after the application of 4µg of nicotine per egg, Vessel stasis was present. (c) before the application of 7 µg of nicotine per egg and (d) after application of 7 µg of nicotine per egg. Slight clotting and hyperaemia of the vessels occurred.

D.6. NMP

Irritancy to the CAM vasculature as evidenced by the signs of hemorrhage were displayed with 10 % v/v NMP but 1 % v/v NMP was relatively non-toxic. While NMP was known to enhance drug permeation, use of high concentrations of NMP was not recommended. These findings were supported by another study that found evidence of embryotoxicity of NMP in rat embryos from concentrations corresponding to greater than 4 % v/v NMP (Flick et al., 2009). Hence, the use of NMP should be minimised to concentrations lower than 10 % v/v when used as a solvent in conjunction with blood perfusion studies of the CAM.

D.7. Effects of pH and osmolality of drug solutions on irritation of the CAM

Osmotic agents have been reported to increase blood flow while extreme pH is known to be harmful to human and microbial cells (Ernest, 1980). It is not clear if pH and osmolality of the drug solution would cause any irritation to the CAM. Hence, the osmolality and pH of the different concentrations of propranolol, theophylline and caffeine solutions were determined (Table 10).

An increase in drug concentration resulted in little change in pH but a significant increase in osmolality for both propranolol and theophylline. Since osmolality is a colligative property, an increase in concentration is expected to increase the osmolality of the solution. The pH values of the different drug concentrations lie within the slightly acidic range of 5.2 to 6.2. A mouse skin test to determine the irritant action of buffer solutions of different pH found that for isomolal conditions, skin irritation was seen with pH values less than 3 or more than 11 (Leighton et al., 1985). Hence, the pH of the propranolol, theophylline and caffeine solutions are most

Table 10. pH and osmolality values of various drugs

Drug	Dose	Concentration of test solution	pH	Osmolality (mmol/kg)
Propranolol	50 ng/ml	0.83 mcg/ml	6.1	318
	100 ng/ml	1.67 mcg/ml	6.1	316
	150 ng/ml	2.50 mcg/ml	6.1	319
	200 ng/ml	3.33 mcg/ml	6.2	322
	250 ng/ml	4.17 mcg/ml	6.2	321
	1 mg/kg	2 mg/ml	6.2	327
	2 mg/kg	4 mg/ml	6.0	343
	5 mg/kg	10 mg/ml	5.8	378
	7.5 mg/kg	15 mg/ml	5.7	406
	10 mg/kg	20 mg/ml	5.3	496
	15 mg/kg	30 mg/ml	5.5	448
	30 mg/kg	60 mg/ml	5.8	426
Theophylline	10 mcg/ml	0.17 mg/ml	5.8	313
	20 mcg/ml	0.33 mg/ml	5.9	319
	30 mcg/ml	0.50 mg/ml	5.9	322
	40 mcg/ml	0.67 mg/ml	5.9	326
	50 mcg/ml	0.83 mg/ml	5.8	329
	60 mcg/ml	1 mg/ml	5.8	331
	1.5 mg/kg	3 mg/ml	5.5	334
	2 mg/kg	6 mg/ml	5.5	338
	2.5 mg/kg	5 mg/ml	5.3	339
	3 mg/kg	6 mg/ml	5.3	340
	3.5 mg/kg	7 mg/ml	5.2	348
Caffeine	2 mg/kg	4 mg/ml	5.6	335
	4 mg/kg	8 mg/ml	5.6	346
	6 mg/kg	12 mg/ml	5.7	360
	8 mg/kg	16 mg/ml	5.6	376
	10 mg/kg	20 mg/ml	5.6	391

30 µL of the respective concentrations was applied to the CAM to give the corresponding dose

unlikely to cause any irritation to the CAM. Another study investigated the effect of osmolality on irritancy using the HET-CAM method. The study reported that the cumulative irritancy score did not correlate with the osmolality values of the test substance, in the range of 195 to 2096 mmol/kg (Debbasch et al., 2005). Therefore, any irritation effects of the drug on the CAM was more likely to be attributed to the pharmacological action of the drug rather than the osmolality of its solution.

E. Blood perfusion studies

From the earlier findings, perfusion studies were conducted using the following LDPI parameter settings for robust and accurate perfusion measurements: amplitude 1, threshold 6, scan area of 2 mm X 10 mm, distance between the Doppler head and CAM of 11 cm, low scanning speed of 17 mm s^{-1} and high resolution. The egg (EA 9) was allowed to equilibrate for 15 min in the temperature-controlled egg holder (37ºC) prior to subsequent study.

Following the development of the CAM model, different types of drugs were employed to study the influence of drug concentration on blood perfusion (Table 2). These drugs were chosen as they were reported to exert vasodilation through different mechanisms of action. The types of receptors located in the CAM vessels are not well defined. Therefore, drugs with different mechanisms of action were evaluated to determine which would affect blood perfusion of the CAM. These drugs were also previously found to be safe to the CAM at the concentrations employed. Control experiments were also performed using normal saline, deionized water and 5 % w/v glucose monohydrate solution. These solvents were employed to dissolve the drugs. Glycerin and 70 % v/v ethanol which were previously found to have similar irritation

potential, and NMP were also studied. The latter is known to be an effective permeation enhancer. No appreciable changes in CAM blood perfusion in response to the application of normal saline, deionised water and 5 % w/v glucose monohydrate were found. Hence, these are suitable solvents that can be used in blood perfusion studies with the CAM.

The magnitude of change in blood perfusion in response to the drug solution can be attributed to the absorption of the drug.

E.1. Indicators of vasoactivity

The vasoactive effects of the test substance were sometimes difficult to compare based on their actual measurements due to variations in baseline values. Hence, a ratio was calculated which provided a more meaningful comparison.

E.1.i. Perfusion ratio

Perfusion ratio was obtained by dividing the blood perfusion value of the test substance with the baseline blood perfusion value. Theoretically, a ratio greater than 1 would indicate an increase in blood perfusion whilst a ratio lower than 1 would indicate a decrease in blood perfusion. The perfusion ratios obtained for the different concentrations of test substance are shown in Table 11.

In general, changes in blood perfusion occurred 15 to 25 minutes after the application of the test substance and the change in blood perfusion lasted for about 10 min. Comparison of the change in blood perfusion was carried out by using the mean of the baseline perfusion values prior to the application of the test

Table 11. Perfusion ratio of test substances

Test substance	Concentration of test substance	Perfusion ratio	Standard error	Coefficient of variance
Control (without test substance)	-	0.99	0.03	3.17
Glucose monohydrate	5 % w/v	0.98	0.04	3.30
Deionised water	-	1.04	0.04	3.38
Normal saline	0.9 % w/v	0.96	0.02	2.44
Caffeine	4 mg/ml	1.00	0.04	3.97
	8 mg/ml	0.95	0.02	2.44
	12 mg/ml	0.92	0.02	1.74
	16 mg/ml	0.99	0.03	2.67
	20 mg/ml	0.96	9.95	5.03
GTN	0.016 mg/ml	0.76	0.03	3.42
	0.02 mg/ml	0.99	0.05	4.80
	0.04 mg/ml	0.84	0.03	3.71
	0.06 mg/ml	1.00	0.02	2.41
	0.1 mg/ml	0.94	0.02	2.59
	0.2 mg/ml	1.02	0.06	6.25
	0.3 mg/ml	0.93	0.04	4.81
	0.4 mg/ml	0.99	0.02	2.12
	1 mg/ml	0.95	0.03	3.60
Propranolol	1 mg/kg	1.03	0.11	11.04
	2mg/kg	1.12	0.14	13.73
	5 mg/kg	1.89	0.27	14.29
	10 mg/kg	1.40	0.33	23.93
	15 mg/kg	1.41	0.39	27.82
NMP	1 % v/v	1.00	0.06	6.34
Ethanol	70 % v/v	0.99	0.05	5.36
Glucagon	0.1 % w/v	0.99	0.06	6.61

substance and comparing that with the mean of the perfusion values after the application of the test substance.

The perfusion ratios of the controls were all very close to 1. However, blood perfusion in any biological system will be prone to fluctuations and biological variation, which explains some slight deviations. As such, the SE of the control was used to calculate a range of blood perfusion ratio values, i.e. mean of perfusion ratios for control ± 2SE. The range encompassed by 2SE shows the 95% confidence interval. Any test substance with blood perfusion ratio that occurred outside this range would be deemed to be able to cause a change in blood perfusion. Using this approach, the influence of normal biological fluctuation on blood perfusion changes was eliminated. No distinct relationship between the perfusion ratio and concentration of caffeine or GTN was observed. Most of the perfusion ratio values obtained are close to 1. The sensitivity of the perfusion ratio was rather low. This could be due to the degree of change of blood perfusion being small and thus, not resulting in any large appreciable changes.

E.1.ii. Diameter ratio

Diameter ratio was obtained by dividing the vessel diameter value with the baseline vessel diameter value. Changes in vessel diameter were seen almost instantaneously or 5 – 10 min after the application of drug. The diameter ratios are shown in Table 12. The vasoconstriction seen with ethanol was reflected in its distinctly lower diameter ratio. The vasodilation effect exerted by caffeine and GTN was indicated by diameter ratio values that were greater than 1. Comparison of change in vessel diameter was done by obtaining the mean of the baseline vessel diameter values prior to the

Table 12. Diameter ratio of test substances

Test substance	Concentration of test substance	Diameter ratio	Standard error	Coefficient of variance
Control (without test substance)	-	0.99	0.02	2.34
Glucose monohydrate	5 % w/v	1.02	0.03	2.54
Deionised water	-	0.96	0.01	0.81
Normal saline	0.9 % w/v	1.00	0.01	0.64
Caffeine	4 mg/ml	1.10	0.07	6.48
	8 mg/ml	1.14	0.07	6.44
	12 mg/ml	1.18	0.06	4.63
	16 mg/ml	1.18	0.08	7.02
	20 mg/ml	1.42	0.21	14.99
GTN	0.016 mg/ml	1.06	0.02	1.51
	0.02 mg/ml	1.06	0.05	4.77
	0.04 mg/ml	1.08	0.03	2.97
	0.06 mg/ml	1.05	0.07	7.08
	0.1 mg/ml	1.25	0.11	8.99
	0.2 mg/ml	1.03	0.04	4.14
	0.3 mg/ml	1.01	0.08	8.36
	0.4 mg/ml	1.01	0.09	8.45
	1 mg/ml	1.11	0.09	7.86
NMP	1 % v/v	0.96	0.03	3.14
Ethanol	70 % v/v	0.77	0.11	14.81
Glucagon	0.1 % w/v	1.04	0.12	11.93

application of the test substance and comparing that with the mean of the vessel diameter values that showed a change after the application of the test substance.

Similarly, a range of diameter ratio values, i.e. mean of diameter ratio for control ± 2SE was calculated and used as a benchmark to assess if the test substances caused any change to the vessel size. Any test substance with diameter ratio outside this range would be deemed to be able to cause a change in the vessel diameter. The perfusion ratio and the diameter ratio of different concentrations of the same test compound were compared. The spread of the diameter ratio was much larger than that of perfusion ratio for caffeine but comparable for GTN. This suggests that diameter ratio is a more sensitive indicator of vasoactivity than perfusion ratio.

A more detailed discussion on the the effects of the various test substances is given below. For ease of comparison, the baseline mean ratio and ± 2SE values are included with all the relevant graphs. The former is indicated by a continuous line while the latter by 2 parallel dotted lines.

E.2. Controls

Blood perfusion studies were first conducted on the CAM without the application of any substance, drug or solvent, to assess the baseline blood perfusion pattern of the CAM. Blood perfusion was found to remain relatively constant without any marked fluctuations over time. Consistent blood perfusion values were also seen after instillation of the solvent used to prepare the drug solution for test. The solutions used were water, normal saline and 5 % w/v glucose monohydrate in water. The above observation for normal saline concurs with the absence of irritation to the CAM by

normal saline, as reported by other researchers (Hjortsjo et al., 2009). A typical plot of the blood perfusion ratio over time for the aforementioned solvents is shown in Figure 22. The blood perfusion profile showed a very slight sinusoidal pattern which is similar to that of the baseline blood perfusion without any solvent or drug. Thus, it could be deduced that the solvents did not cause any significant change to the blood perfusion and the effects shown by the drug solutions were largely attributed to the drug.

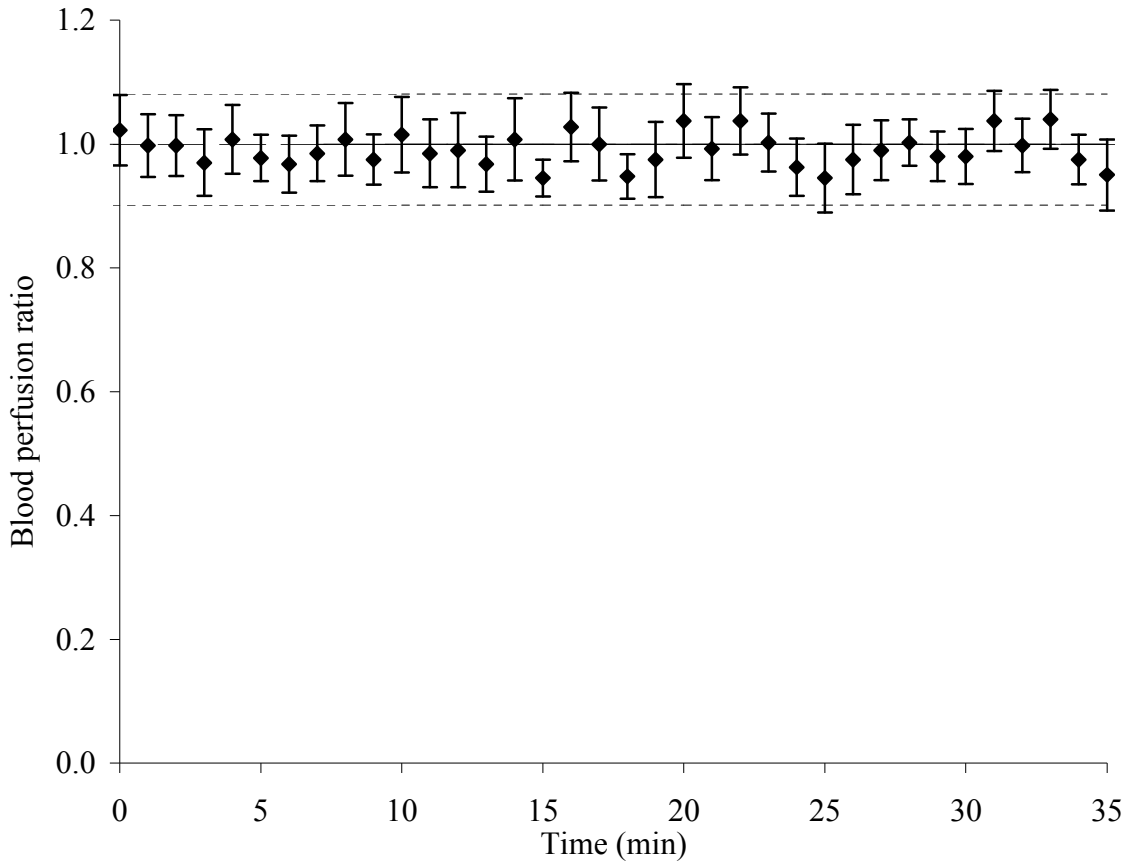

Figure 22. Change in blood perfusion ratio with time following the addition of 5 % glucose monohydrate solution at 0 min (n = 5)

E.3. Glycerin

The blood perfusion profile showed a significant drop in blood perfusion rate immediately after the addition of glycerin, followed by fluctuation within the baseline blood perfusion range and then a significant drop after about 11 min (Figure 23). Glycerin required an incubation period of at least 10 min for its vasoactive property to manifest. The depression in blood perfusion lasted for at least 20 min after the onset of change in blood perfusion, without recovery to baseline level within the duration of the study.

High concentrations of glycerin was reported to cause a reduction in blood flow of the CAM (Forough et al., 2005). The results in this study further show that glycerin exerted a prolonged vasoactive effect on the CAM vasculature and the CAM was unable to re-establish the baseline blood perfusion level within 30 min. It should be recalled that glycerin was previously found to be harmful to the CAM in the irritancy assessment. The embryo died by the end of the hour after the administration of glycerin. Blood perfusion rate had clearly shown deviation from the baseline blood perfusion value. Therefore, glycerin is harmful and has the potential to reduce blood perfusion of the CAM and it would not be a suitable to be used in the evaluation of drug vasoactivity.

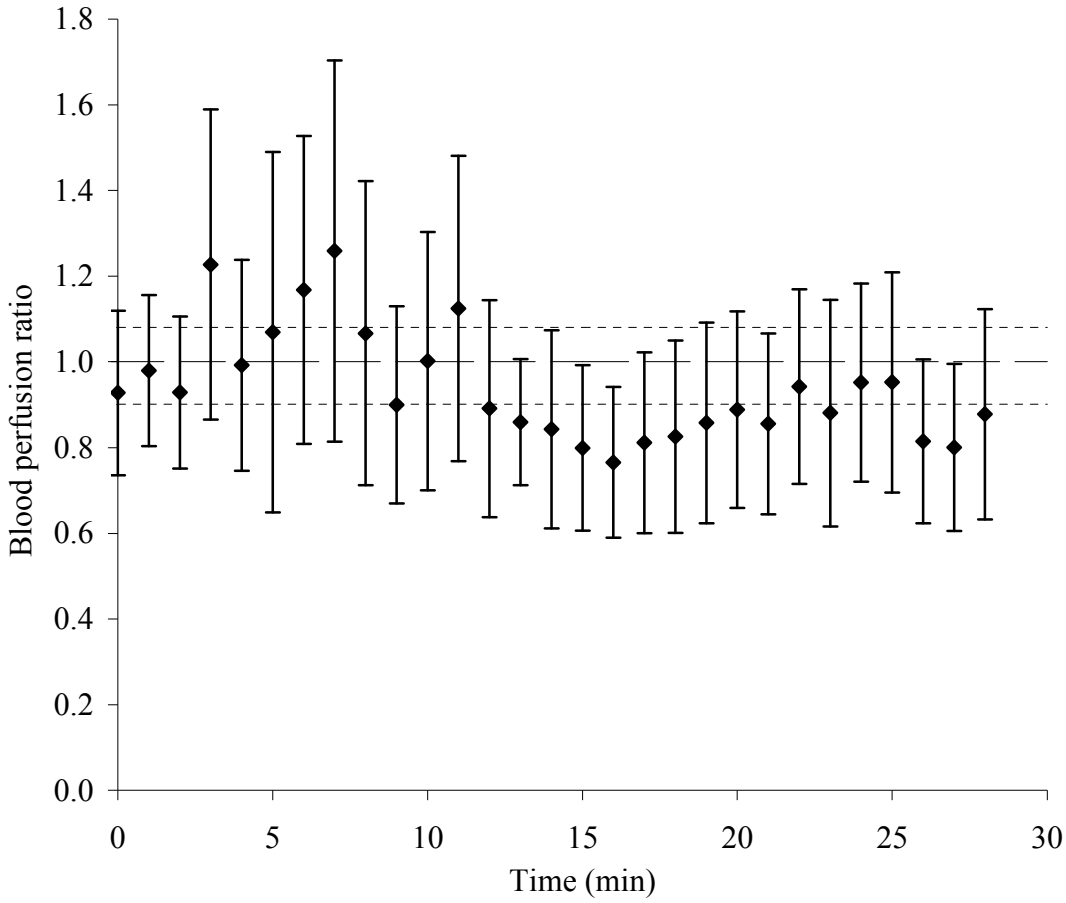

Figure 23. Relationship of blood perfusion ratio with time with 100% glycerin solution added at 0 min (n = 5)

E.4. Glucagon and Menthol

The solubility of menthol in water is extremely poor. Application of heat to increase the aqueous solubility of menthol is not recommended as menthol is volatile. Hence, liquid paraffin was used as a vehicle to dissolve menthol. Instillation of liquid paraffin was previously found to have no appreciable effect on blood perfusion. The effects of 0.1 % w/v glucagon and 2 % w/v menthol on blood perfusion of the CAM were evaluated (Figures 24 and 25). These concentrations are reflective of doses used in many pharmaceutical external medicaments. The application of these two test substances did not result in any clear evidence of a change in blood perfusion. A

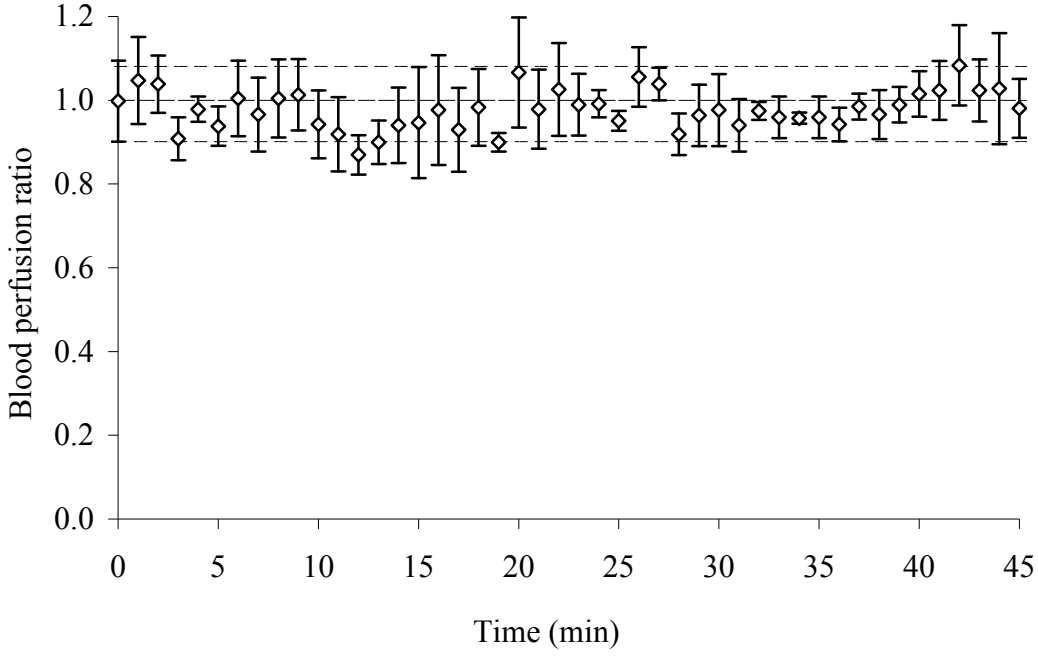

Figure 24. Effect of 2 % w/v menthol on blood perfusion of the CAM (n = 5)

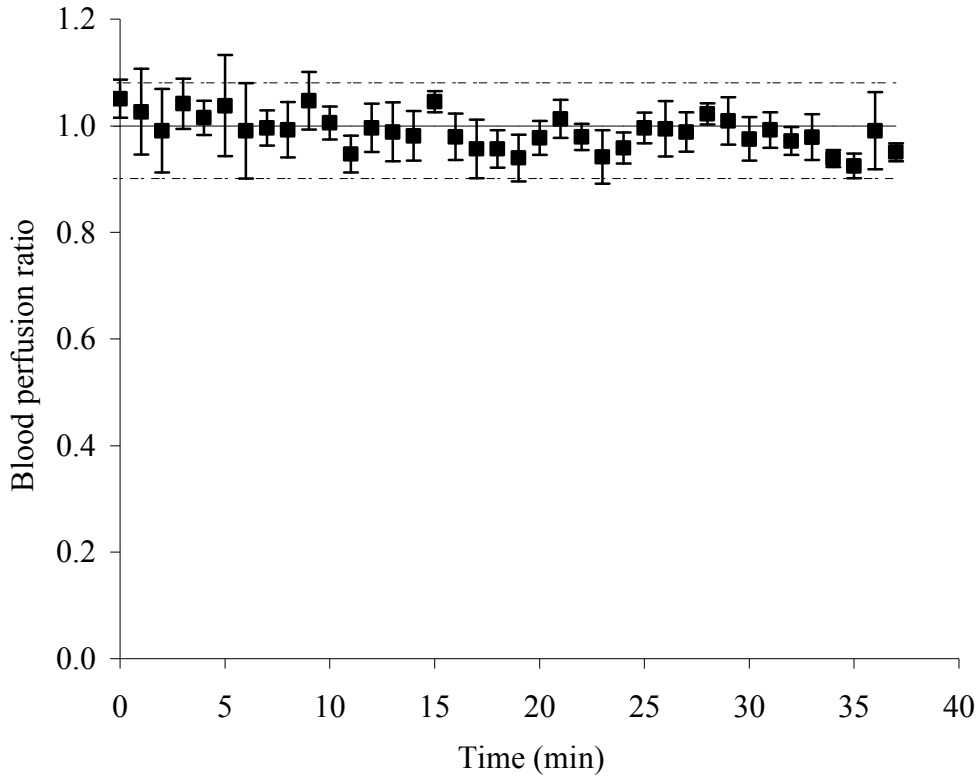

Figure 25. Effect of 0.1 % w/v glucagon solution on blood perfusion of the CAM (n = 5)

slight sinusoidal blood perfusion pattern, similar to that of the baseline blood perfusion was seen. The sinusoidal pattern appeared slightly more exaggerated with menthol. This could be attributed to the physical sensation of coolness often associated with menthol. Both glucagon and menthol have been reported to exert vasodilative effect and increase blood flow (Brain et al., 2006, Farah, 1983). However, no effect on CAM blood perfusion was seen, possibly indicating the absence of the receptors associated with glucagon and menthol. Information on the menthol and glucagon receptors responsible for vasodilation is not readily available, however, it has been postulated that the glucagon receptors affect cAMP levels to induce vasodilation (Farah, 1983). Another possible reason for the limited effect of

glucagon and menthol may be their high affinity for liquid paraffin, and very small amounts of either test substances were available to act on the CAM.

E.5. Ethanol

Ethanol has been reported to be capable of causing both vasoconstriction and vasodilation (Nicoletti et al., 2008, Yogi et al., 2010). Its effect on blood perfusion of the CAM has not been reported. The investigation on the effect of 70 % v/v ethanol served two purposes in this study. Firstly, the influence of 70 % v/v ethanol on the vasculature when it was used as a solvent can be taken into account during data analysis. Secondly, in the disinfection of the eggs before experimentation, 70 % v/v ethanol was applied to the eggs' surface. The egg shell is proprosed to possess pores which allow the loss of water as well as gaseous exchange (Rahn et al., 1987). Clearly, the disinfection process may potentially result in 70 % v/v ethanol being absorbed through the shell. It is important to know if this would affect the perfusion study of drug substances. In this study, ethanol at a concentration of 70 % v/v in water was instilled on the surface of the CAM. The effect of 70 % v/v ethanol on the CAM is shown in Figure 26. Close examination of the blood perfusion profile shows an interesting pattern. Immediately after the application of 70 % v/v ethanol, blood perfusion increased. Fluctuation in blood perfusion was observed but it remained above the baseline. After 12 min, blood perfusion decreased to a level below the baseline. About 20 min after the application of 70 % v/v alcohol, the blood perfusion returned to its baseline value. Overall, the values of the blood perfusion generally lie within the baseline range, indicating that 70 % v/v ethanol exerted little and short-lived effect on the blood perfusion. The use of 70 % v/v ethanol to disinfect the eggs is therefore unlikely to affect the perfusion studies.

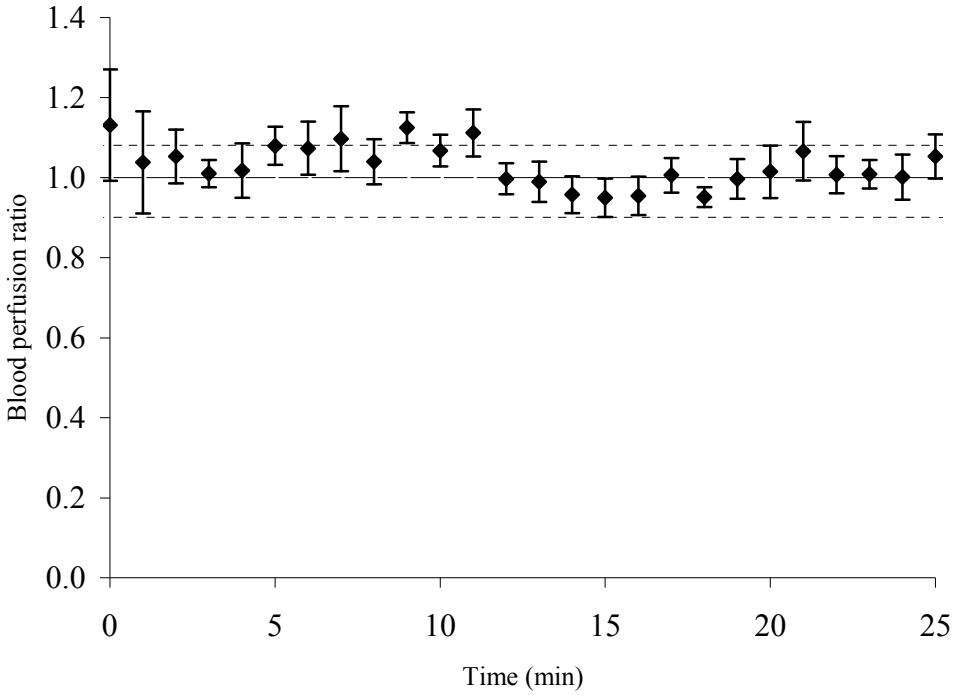

Figure 26. Effect of 70% ethanol on blood perfusion of the CAM (n = 5)

The accentuated cyclic trend, in which blood perfusion increased or decreased alternatively, indicated the existence of an auto-regulation mechanism in response to the initial increase stimulus in blood perfusion. Compensation for the initial increase in blood perfusion resulted in a decrease in blood perfusion before achieving baseline blood perfusion level once again. This study demonstrated that ethanol exerted an immediate effect on blood perfusion in the CAM and the effect was curbed by an auto-regulation mechanism. Such mechanisms, which may involve a host of biological factors, have been reported in humans where they play important roles in maintaining a stable system known as homeostasis (Guyton, 2000).

It was also possible that ethanol exhibited dual vasoconstrictive and vasodilative effects in the CAM. Ethanol first exerted a vasodilative effect on the CAM vessels, resulting in an increase in blood perfusion rate. High concentrations of ethanol had been found in another study to cause vasoconstriction, potentially through a redox sensitive and cyclo-oxygenase dependent pathways that affected the production of reactive oxygen species and Ca^{2+} signaling (Yogi et al., 2010). Hence, as more ethanol reached the CAM vessels over time, the receptors that caused vasoconstriction were possibly overactivated, resulting in the decrease in blood perfusion henceforth. Extrapolating from here, the diameters of the CAM vessels under the influence of 70% ethanol were further investigated and discussed in Section F.3. When used as a solvent, ethanol has the potential to trigger the auto-regulation mechanism or cause vasodilation and vasoconstriction. Thus, it is not an ideal solvent to be used in the perfusion study of drug substances.

E.6. N-Methyl-2-Pyrrolidone

The effect of NMP was also evaluated as it has been demonstrated to be a good permeation enhancer (Saw et al., 2005a, Saw et al., 2005b). Two concentrations of NMP (1 % w/v and 10 % w/v), were tested. A very distinct drop in blood perfusion was seen with 10 % v/v NMP but insignificant effect by 1 % v/v NMP were observed (Figure 27). The effect was seen immediately after application of 10 % v/v NMP. Blood perfusion decreased gradually over time and reached the minima around 10 min after application of NMP. Blood perfusion hovered at the low level for about 10 min before gradually recovering after the 20^{th} min time point, in a bid to re-establish the baseline blood perfusion albeit at a slightly lower level. The results illustrate that the permeation of NMP through the CAM was dependent on concentration. The effect

of 1 % v/v NMP on the CAM blood vessel diameters will be further discussed in Section F.4.

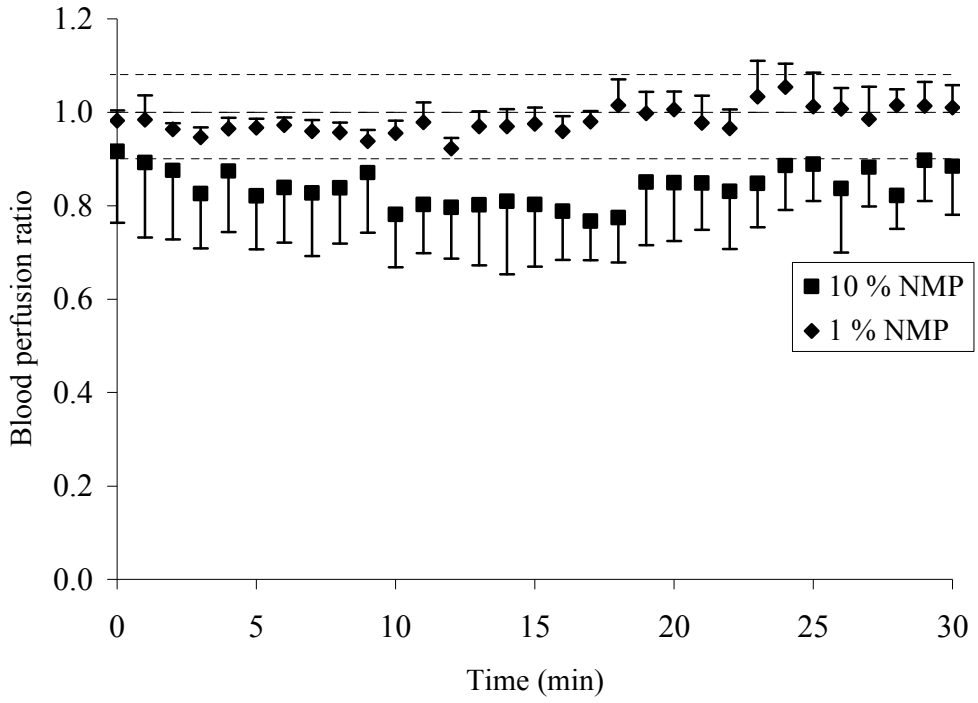

Figure 27. Effect of 1 % and 10 % v/v NMP solution on blood perfusion of the CAM (n = 5)

E.7. Propranolol

Propranolol is a β-blocker that affects both the $ß_1$ and $ß_2$ adrenoceptors. Resultant decrease in blood pressure in human subjects had been attributed to the reduction in cardiac output and decreased peripheral vascular resistance brought about by the action of propranolol. It was also found to act on the peripheral presynaptic adrenoceptors to decrease sympathetic vasoconstrictor nerve activity (Katzung, 2001). It is not known if $ß_1$ and $ß_2$ adrenoceptors are found in the chick embryo and whether propranolol would affect the function of the CAM. Experiments were therefore conducted to determine the effects of different concentrations of propranolol on blood

perfusion of the CAM. Three different doses of propranolol, 7.5, 15 and 30 mg/kg, were used in the first set of experiments. The highest dose is close to the LD50 in rats whilst the lowest dose is close to the high doses used in pediatrics (Lacy et al., 2004). The average weight of over 300 eggs was found to be 61.3g ± 4.1 g. This was rounded off to 60 g and used for the calculation of the amount of propranolol to be applied to the CAM. A slight increase in blood perfusion was seen when propranolol was administered, followed by a decrease in blood perfusion. The CAM tissues were also found to undergo hemorrhage and the embryo died about an hour after drug application.

As observed in the earlier irritancy assessment, propranolol in the dose range of 7.5 to 30 mg/kg was harmful to the CAM. From this perfusion study, it was further shown that propranolol was capable of increasing blood perfusion in the CAM, albeit a slight increase. The blood perfusion in the CAM gradually decreased despite the high dose, probably due to the harmful effects of the drug on the embryo.

It was thought that dosing propranolol by weight of the egg based on human doses might have resulted in harmful doses to the chick embryo. Hence, the amount of propranolol applied was recalculated, taking into account the total blood volume rather than weight of the egg. The total blood volume of the egg was reported to be 513 mm^3, which corresponds to about 0.5 mL (Kind, 1975). Further experiments were carried out with lower doses of propranolol, ranging from 50 ng/mL to 100 ng/mL which correspond to the therapeutic concentrations in human blood in hypertension management. Perfusion measurement intervals were shortened to 2 min over the duration of an hour after the application of propranolol. Surprisingly, a transient drop

in blood perfusion was seen after these lower doses of propranolol were applied to the CAM, followed by a small increase. Higher doses of propranolol of 150, 200 and 250 ng/mL were further tested and found to have insignificant effect on the blood perfusion. Response of the CAM blood perfusion to propranolol appeared complex.

In subsequent experiments, the test doses of propranolol were re-adjusted based on egg weight, covering a wide range that included 1, 2, 5, 10 and 15 mg/kg. With the dose of 1 mg/kg, there was only a slight increase in blood perfusion, followed by a very gradual decrease in blood perfusion with time. The other propranolol doses of 2 mg/kg and 5 mg/kg also showed similar trends. In contrast, the higher doses of 10 mg/kg and 15 mg/kg caused haemorrhage and the embryos died about an hour after the application of the drug. This confirmed the earlier observations for similar propranolol doses.

A plot of the blood perfusion ratio versus the concentration of propranolol used is shown in Figure 28. All of the propranolol doses caused an increase in blood perfusion. The extent of this increase reaches a maximum at the dose of 5 mg/kg, after which the magnitude of increase in blood perfusion drops. However, at these high concentrations, the change seen in blood perfusion might be complicated by their harmful effects to the CAM.

This is an interesting finding as propranolol had been reported to decrease peripheral vascular resistance in humans. It should therefore be inferred that the receptors found in the CAM are significantly different and less sensitive to propranolol. Due to the complexity and potential toxicity of propranolol, the use of propranolol as a marker drug for the assessment of blood perfusion may not be ideal. A marker drug should

not be toxic to the embryo and should preferably display reproducible change in blood perfusion that can be used to provide an accurate estimate of the influence of other variables on the absorption of the vasoactive marker drug.

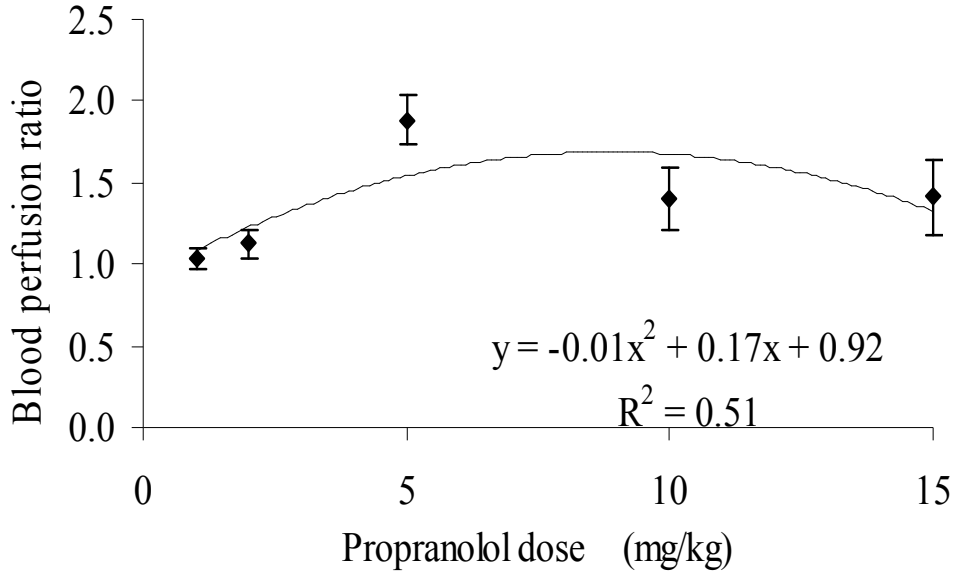

Figure 28. The relationship between blood perfusion ratio and propranolol dose (n = 3)

E.8. Theophylline

Theophylline, a methylxanthine bronchodilator, produces bronchodilation in human subjects through the inhibition of phosphodiesterase in the smooth muscle of the airway. The methylxanthines induce peripheral vasodilation. It was also reported to dilate coronary blood vessels (Bath, 2004). In addition, it stimulated the central nervous system by antagonizing adenosine and also produced cerebral vasoconstriction leading to a reduction in cerebral blood perfusion (Nehlig et al., 1992). It was employed for the treatment of ischemic stroke to produce cerebral vasoconstriction and increase blood perfusion to non-ischemic areas in the brain whilst increasing collateral blood perfusion to the ischemic region. The effect of

theophylline on the CAM has not been reported. Doses in the range of, 10, 20, 30, 40, 50, and 60 mcg/mL were tested. Blood perfusion readings were taken every minute for 25 min to capture any instantaneous change in blood perfusion. Readings were also taken at the 1^{st}, 2^{nd}, 3^{rd} and 4^{th} hour since theophylline concentration was previously found to reach a peak one to two hours after oral ingestion in humans (Lacy et al., 2004). Slight change in blood perfusion over time was observed with the theophylline doses used. However, the extent of change in blood perfusion was much smaller compared to propranolol and most likely, the measurements were of little clinical relevance to describe the drug's mode of action.

Further studies were carried out to investigate the influence of higher theophylline doses. The doses tested were equivalent to those recommended for pediatrics, 3.5, 3, 2.5, 2 and 1.5 mg/kg (Lacy et al., 2004). There did not appear to be any distinct relationship between the theophylline dose and blood perfusion. Theophylline did not demonstrate any substantial perfusion changes upon application. The lack of significant effect could possibly be due to the requirement of metabolic transformation of theophylline before exerting vasoactive methylxanthine effect (Bath, 2004). The metabolism of theophylline would result in the formation of metabolites such as caffeine. Hence, a further study was undertaken to establish if the CAM was more responsive to caffeine.

E.9. Caffeine

Vasodilation has been purported to be effected by increased cyclic adenosine monophosphate, inhibition of Ca^{2+} influx and inhibition of phosphodiesterase in humans. The binding of adenosine to adenosine receptors was found to cause

vasodilation (Lapeyre et al., 2004). Caffeine is a methylxanthine. It has been reported to exert competitive inhibition of adenosine binding to adenosine receptors, thereby causing vasoconstriction (Addicott et al., 2009). The effect of caffeine on the blood vessels of the CAM has not been reported. Vasoconstriction is expected to result in a decrease in blood perfusion. Hence, a decrease in blood perfusion with caffeine would suggest that caffeine causes constriction of blood vessels in the CAM.

The caffeine doses used in this study were 2, 4, 6, 8 and 10 mg/kg. These doses were chosen as they encompass the doses given to adults and children to treat various medical conditions. The choice of test dose also took into account the solubility of caffeine in normal saline. Blood perfusion in the CAM vessels was found to decrease in response to application of caffeine on the CAM surface. This suggests that caffeine exerted vasoconstrictive effect on the CAM vessels, similar to human vessels. The blood perfusion ratio with 6 mg/kg and 10 mg/kg of caffeine is shown in Figure 29.

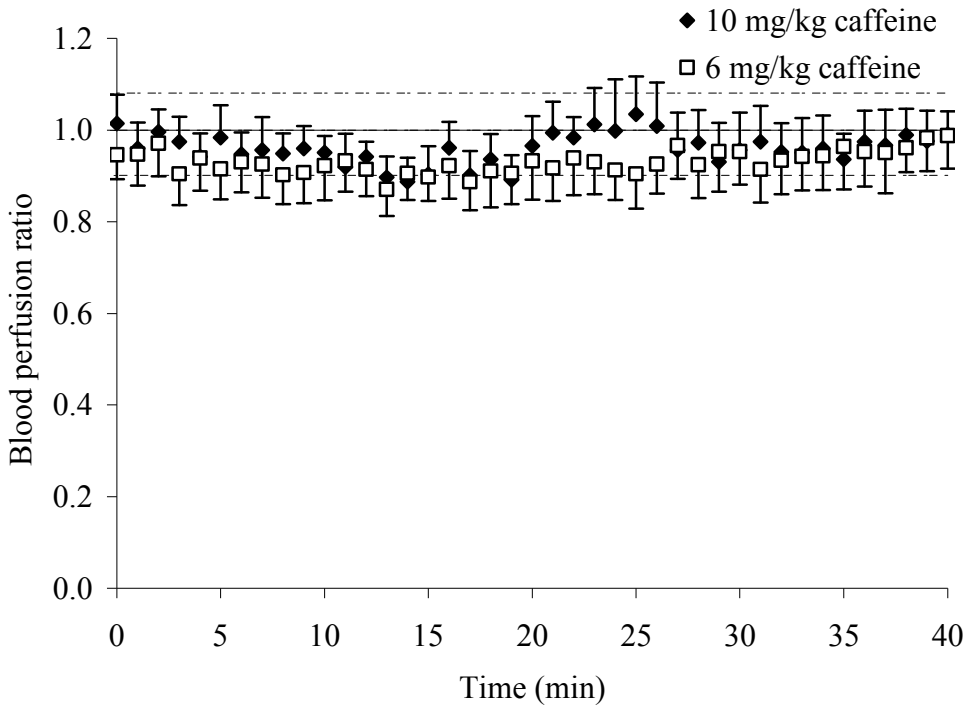

Figure 29. Change in blood perfusion with 6 mg/kg and 10 mg/kg of caffeine added at 0 min (n = 5)

A ratio of less than 1 indicates a drop in blood perfusion and a ratio greater than 1 indicates an increase in blood perfusion. The consistent ratio of value below 1 confirms that a drop in blood perfusion occurs with caffeine. Blood perfusion was found to decrease almost immediately after the administration of 6 mg/kg caffeine. This trend was also seen with the 2, 4, 8 and 10 mg/kg treatment groups. The blood perfusion levels started to rise toward the baseline level again after 30 - 35 min. Overall, the trend observed in changes in blood perfusion with respect to the baseline blood perfusion was consistent.

The degree of change in blood perfusion was higher than that seen with theophylline. These results were also comparable to the change in blood flow seen in humans in LDPI studies conducted with vasoconstrictive topical corticosteroids (Sommer et al.,

2003). Therefore, further analysis of the data was conducted, whereby the absolute decrease in blood perfusion was plotted against caffeine dose. This was done by obtaining the mean of the perfusion values prior to caffeine application and comparing that with the mean of the perfusion values that showed a decrease after caffeine application. The percentage change in blood perfusion was then plotted against the caffeine dose to eliminate the variability in baseline blood perfusion of the different eggs used (Figure 30). The relationship found was not straightforward. According to the Pearson's correlation test, it is non-linear ($p > 0.05$) and best described by a curve that initially appears linear before gradually attaining a plateau status toward the end of the curve. The magnitude of decrease in blood perfusion seemed to increase linearly from 2 mg/kg to 6 mg/kg of caffeine. Caffeine in concentrations beyond 6 mg/kg resulted in a gradual plateau in the graph. The presence of such a trend further illustrated the complicated effect of caffeine on the CAM blood perfusion. The effect of caffeine on vessel diameter is discussed in Section F.6.

The relationship of percentage change in blood perfusion with caffeine dose resembles the typical threshold model where the change in response reaches a maxima before leveling out. In the case of caffeine, the maxima is reached at the 10 mg/kg concentration point. Besides caffeine, other drugs such as pentobarbital and cocaine have been reported to display similar dose responses in pigeons and monkeys (Spealman et al., 1977).

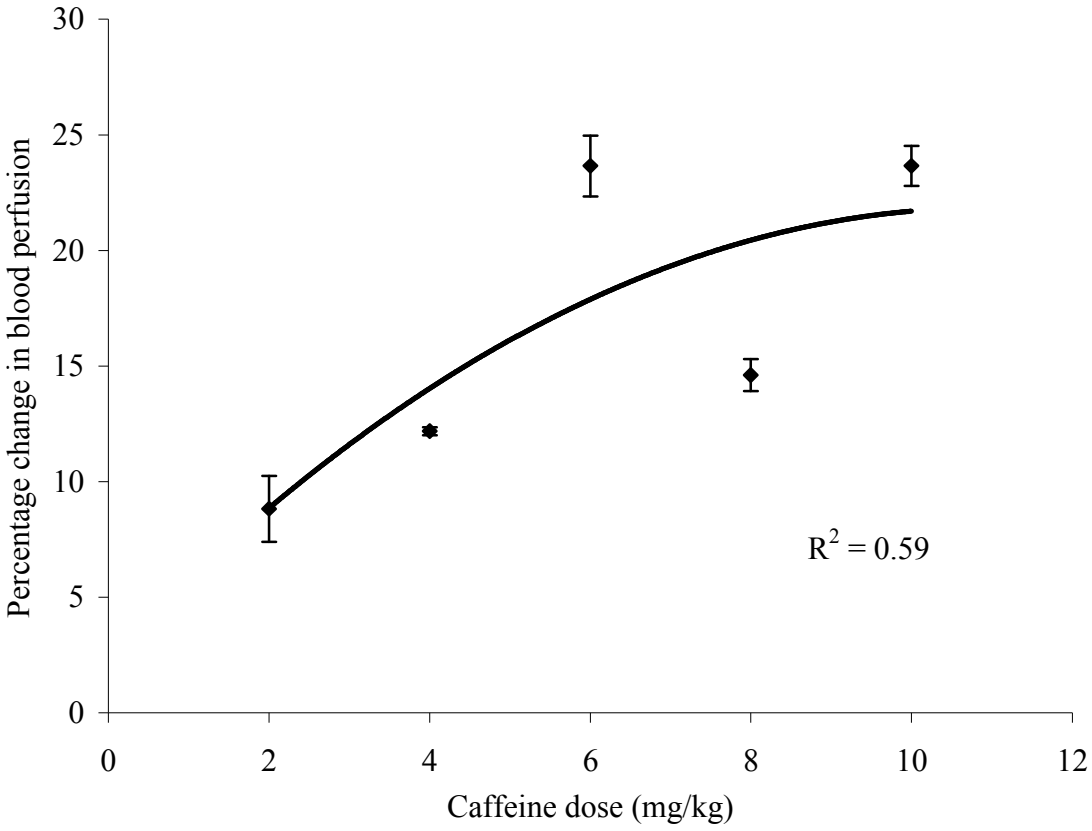

Figure 30. Relationship between caffeine concentration and change in blood perfusion (n = 5)

E.10. GTN

GTN is part of the nitrate family that releases nitric oxide in human vascular smooth muscle. Nitric oxide is a powerful vasodilator which elicits a rapid response from large arteries and veins. Venodilation, arterial-arteriolar dilation as well as dilation of vessels in the heart occur in the presence of GTN (Kelly et al., 2005). Veins are more sensitive than arteries to nitric oxide whilst arterioles are the least sensitive (Katzung, 2001). Owing to import restrictions, pure GTN was not available for this study. Two different types of GTN were used to investigate if the results were affected by the presence of formulation additives added to the GTN tablets as opposed to the GTN in injection form.

E.10.i. Tablet dosage form

GTN tablets were appropriately dissolved and diluted in normal saline to prepare the test solutions. Low doses of GTN were initially employed to determine the ability of GTN to elicit any vasoactive effects on the CAM model. Doses tested were 0.01, 0.0125, 0.025, 0.0375, 0.05, 0.075, 0.1, 0.12, 0.15, 0.2 and 0.25 mg/kg of the egg. These doses are close to the clinically used sublingual doses (Cossum and Roberts, 1985). Blood perfusion was found to decrease immediately after the application of GTN and this could be due to the reactive response of the CAM to the drug. The perfusion values before and after application of GTN were compared. The depression of blood perfusion in the CAM was seen to last for at least 15 min before blood perfusion level returned to the baseline (Figure 31). Blood perfusion was expected to increase following vasodilation with GTN, as vessel resistance is decreased and hence, blood perfusion enhanced. However, a decrease in blood perfusion after the application of GTN was observed in the majority of the concentrations used. A study using optical Doppler tomography to monitor blood perfusion in the CAM showed an increase in blood perfusion in the CAM arteries and a decrease in CAM veins following application of GTN (Chen et al., 1998). GTN resulted in dilation of both arteries and veins, and decreased the blood flow in arteries but increased the blood flow in veins. The mechanism behind this differing response to GTN is unknown. Arteries and veins can be distinguished by observing the direction of blood flow in the vessels with a stereo dissecting microscope (Fuchs and Lindenbaum, 1988, Shumko et al., 1988). On closer examination, the vessels measured were found to be brighter red in colour, suggesting that they were veins. CAM veins are equivalent to the pulmonary veins in humans. They bring oxygenated blood back to the embryo and would hence deliver blood that is brighter than those carried by the CAM arteries.

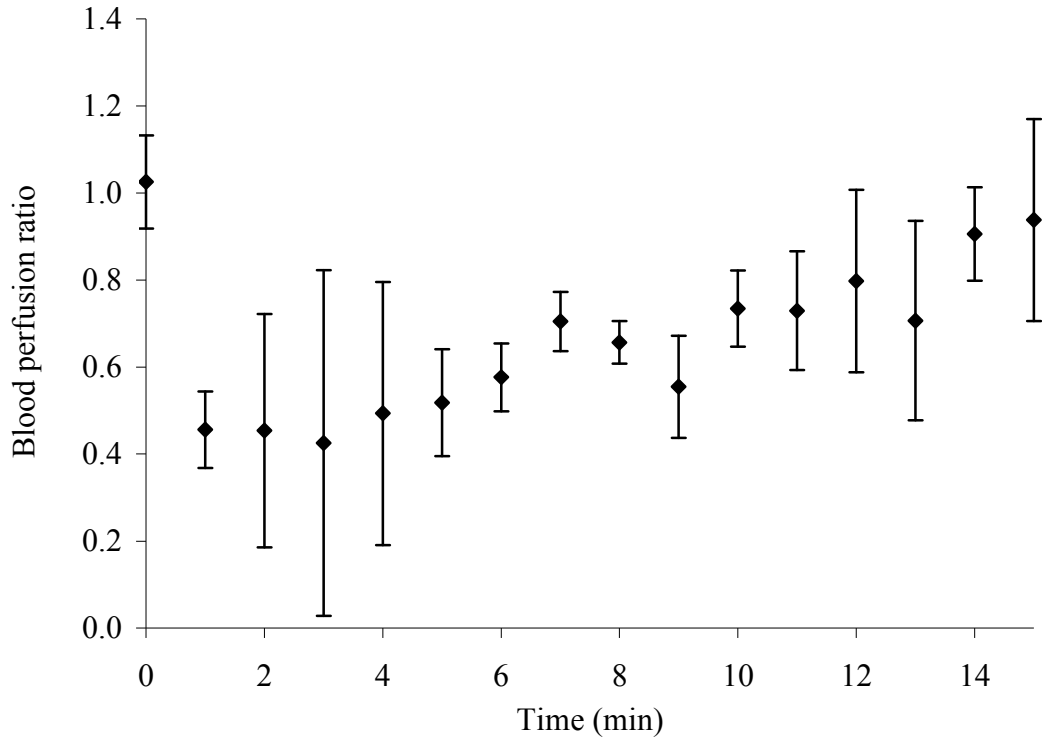

Figure 31. Blood perfusion ratios after application of GTN at time 0 min at dose of 0.25 mg/kg (n = 5)

This observation, coupled with the decrease in blood perfusion suggested that majority of the vessels measured were probably veins. This was further investigated and discussed in Section E.10.iii. The findings highlighted the significance of identifying whether the vessel measured was a vein or artery. It also showed that the CAM studied had more predominant veins than arteries.

In this study, blood perfusion decreased with all the GTN doses employed. The relationship was however not straightforward and it was of interest to determine a simple mathematical model that best describes the relationship. Hence, the data was further analyzed by plotting the GTN doses with the various derivatives of perfusion, i.e. perfusion change, percentage or log perfusion change and square root of perfusion

change. Except for the plots of GTN doses versus the square or square root of perfusion change, sine wave relationships were noted. Sine waves were also seen in the plot of the change in vessel diameter against GTN dose. This suggested that the manner by which GTN interacted with the relevant receptors was complex and/or compensatory mechanisms existed in response to GTN.

The plot of the square root of perfusion change versus GTN dose in the range of 0.01 mg/kg to 0.05 mg/kg showed a linear relationship with an R^2 value of 0.99 (Figure 32). Any subtle change in GTN dose within this range would be manifested by a proportional change in blood perfusion of the CAM. Hence, the effect of a formulation factor that result in a decrease or increase in GTN absorption within this range can be quantified. An estimation of the effect can be deduced from the change in blood perfusion. Although a wider concentration range is desirable, the 5-fold difference in concentration obtained for GTN is useful for evaluating the influence of formulation factors on drug absorption. The presence of various excipients in GTN tablets could have served as a confounding factor in the above study. Hence, the investigation was extended to include GTN injections to address this.

E.10.ii. Injection dosage form

GTN was diluted from a stock vial of GTN injection that consisted of GTN at a concentration of 1 mg/mL. This was carried out to determine if the presence of the excipients in the GTN sublingual tablet had any significant effect on blood perfusion. The doses tested were 0.01, 0.03, 0.05, 0.1, 0.15, 0.2 and 0.5 mg/kg of the egg weight, to correspond with the doses prepared from the GTN tablets (Figure 33). The trend obtained using the GTN injection was different (Figures 32 and 34), suggesting that

the excipients either in the GTN tablet or injection had affected the vasoactive effects of GTN on the CAM. As formulations of injections are generally simpler, it is most likely that interacting excipients are with the tablet dosage forms.

Another possible reason for these differing results could be due to the biphasic relaxant effect that had resulted from the action of GTN. It was proposed that 2 mechanisms of action existed for the biphasic response of GTN and that the metabolites of GTN also had an influence (Malta, 1989a, Malta, 1989b). However, there was little information with regard to this biphasic proposal, and is not readily available. However, the findings of this study suggested biphasic behaviour.

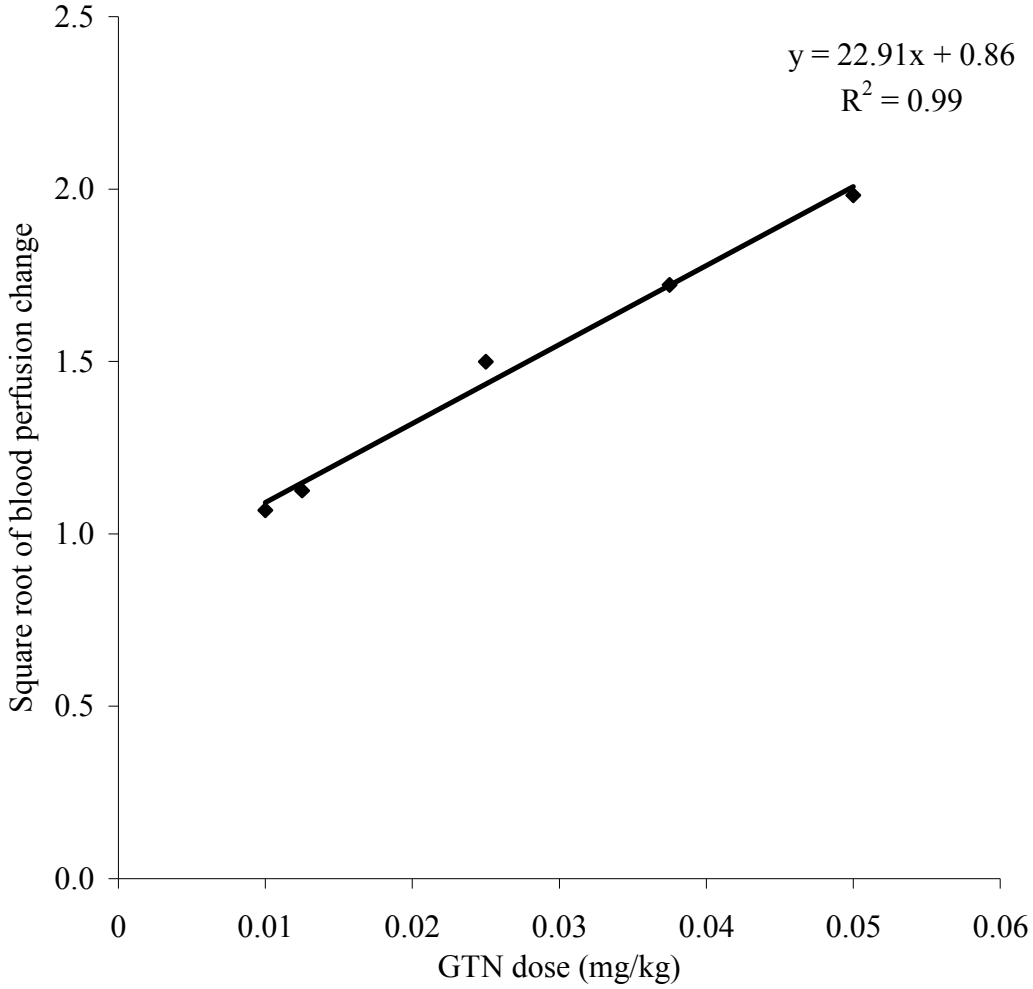

Figure 32. Relationship between square root of percentage change in blood perfusion and GTN dose, GTN from tablet dosage form (n = 3)

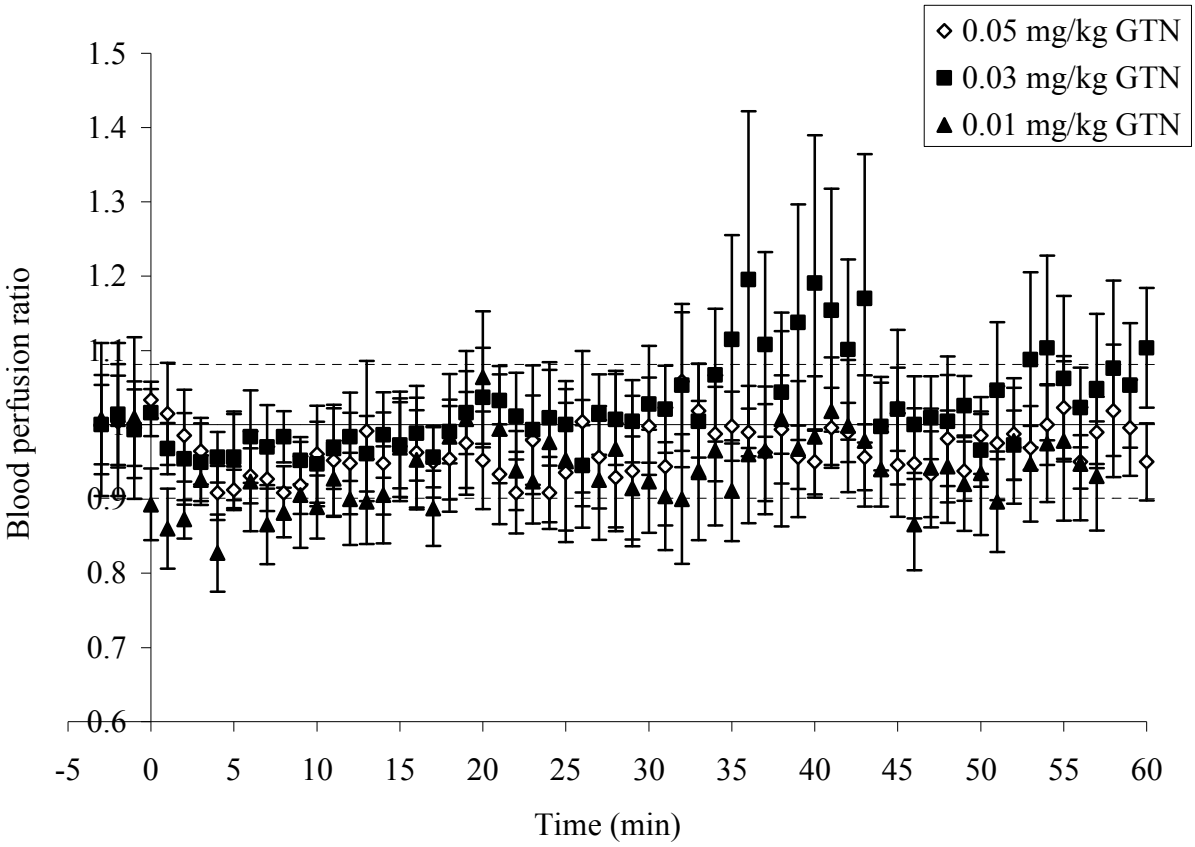

Figure 33. Blood perfusion profile of CAM with 0.01, 0.03 and 0.05 mg/kg GTN (n = 5)

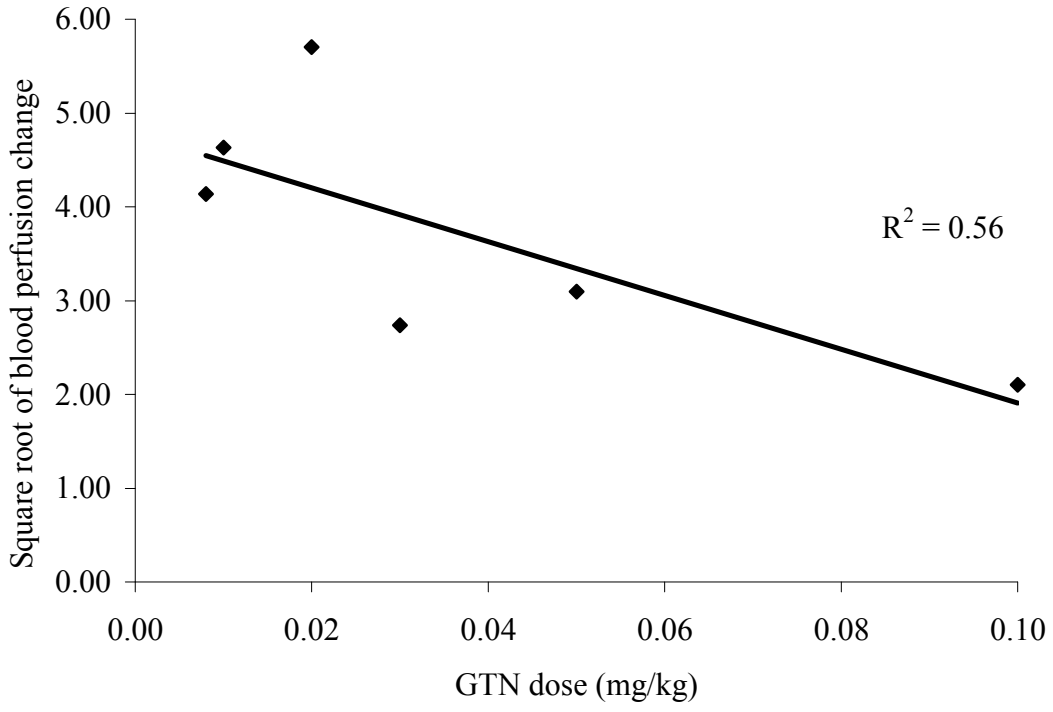

Figure 34. Effect of GTN dose on blood perfusion using GTN injection (n = 5)

E.10.iii. Blood perfusion in CAM veins and CAM arteries

Attempts were made to differentiate the veins from the arteries by their appearance. The blood perfusion in the respective veins and arteries in reponse to the different GTN doses was then determined (Figure 35).

The CAM arteries displayed vasodilation in response to GTN, as indicated by their greater blood perfusion with respect to the baseline. The reverse was exhibited by the CAM veins, indicating vasoconstriction. As most of the vessels measured previously were veins, an overall reduction in blood perfusion was obtained. The change in blood perfusion in the arteries was slightly increased by increasing GTN dose. Interestingly, the change in blood perfusion in the veins was decreased by increasing GTN and the

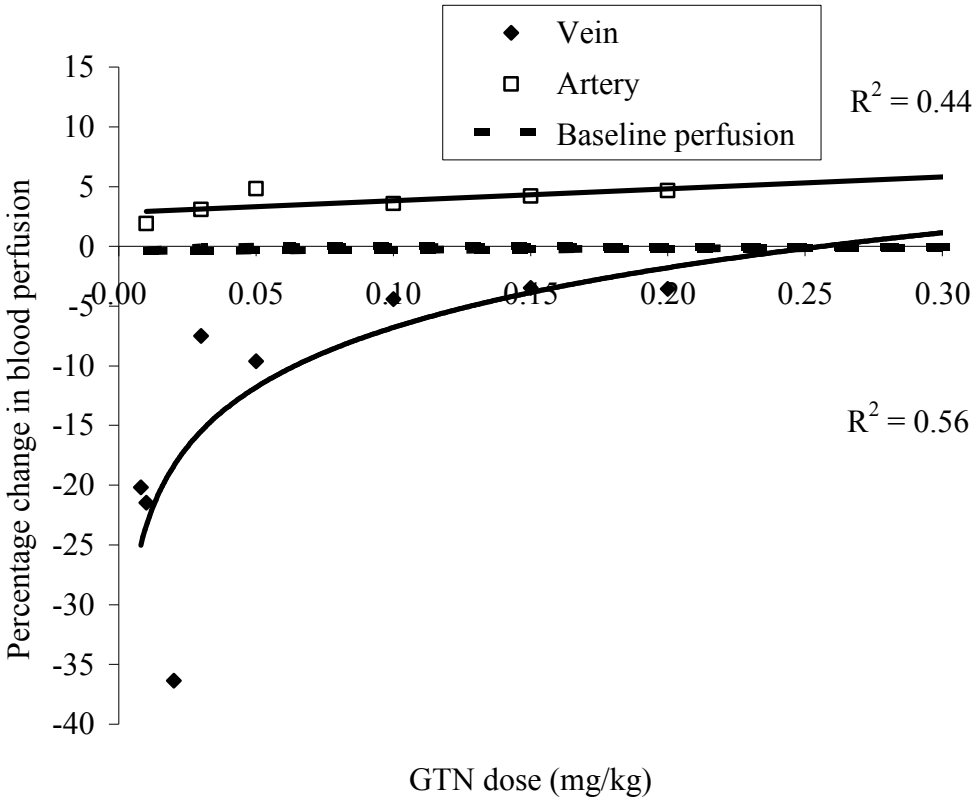

Figure 35**.** Relationship between GTN dose and blood perfusion change in CAM veins and arteries (n = 5)

effect was markedly greater. Such complexities in response of the blood vessels to GTN suggest the involvement of multiple factors and auto-regulation mechanisms.

E.11. Auto-regulation of blood perfusion

The results seen with caffeine and GTN indicated the existence of auto-regulation of blood perfusion by the CAM. Auto-regulation is an extremely complex array of mechanotransduction pathways (Olufsen et al., 2005, Sankaranarayanan et al., 2006). Blood perfusion has often been regarded as a crucial modulator of vascular tone. Combined effects of myogenic and metabolic regulation in response to the changes in blood flow have been reported (Carlson et al., 2008). In human skin, perfusion changes are dealt with by the action of reflex neural control. An increase in skin blood perfusion would result in the activation of sympathetic vasoconstrictor nerves and a decrease in skin blood perfusion would result in the activation of vasodilator nerves (Charkoudian, 2003). It has been postulated that this results from a process known as mechanoreception whereby the presence of mechanosensors located in endothelium would be triggered accordingly to result in either the release of hormones or various endothelium-derived relaxing and contracting factors (Rubanyi et al., 1990, Price, 1991). Other proposed mechanotransducers include ion channels, integrins, heterotrimeric G proteins and various others, although their mechanisms of action remain elusive (Hahn and Schwartz, 2009). Myogenic auto-regulation involves the vasoconstriction and vasodilation of the vessel to bring about an increase and decrease in resistance respectively. Metabolic regulation would result in the release of signal molecules to cause vasodilation and vasoconstriction accordingly. This would cause blood flow to change in accordance to the situation. It has been reported that the arteries in the CAM in the early stages of embryonic development adapt to the size of

their lumen in response to the blood that flows through in order to maintain mean shear stress at a constant level (Le Noble et al., 2005). Thus, in the CAM, changes in blood perfusion are also met with auto-regulation responses. Shear stress is related to both vessel diameter and the rate of blood flow. When the diameter of the vessel changes, blood perfusion would change and so would shear stress in response to blood perfusion changes. The changes in shear stress would then spark the regulation of vessel diameters to combat this change (Stasi et al., 2010). At higher concentrations of caffeine, the change in blood perfusion could have sparked a chain reaction in the CAM, resulting in a smaller extent of increase in blood perfusion compared to lower concentrations. As for the case of GTN, auto-regulation could have set in from the initial concentrations, but the combination of receptors' effects could have over ridden the auto-regulation effect, resulting in the decrease in the drop in blood perfusion at higher concentrations.

According to Poiseuille's Law, volume flow rate is directly proportional to the diameter of the tube, to the power of 4 as shown in Equation 4 (Silverthorn, 2001). Hence, an increase in diameter should cause blood perfusion to increase.

$$Q = \frac{\pi}{8}\frac{\Delta p r^4}{\eta L} \qquad \text{Equation 4}$$

where Q = volume flow rate, p = driving pressure, r = radius of the tube, η = fluid viscosity and L = vessel length

The impact of changing the diameter of blood vessels on perfusion may also be explained by the relationship between resistance and radius as depicted in Equation 5 (Guyton, 2000).

$$R = \frac{L\eta}{r^4} \qquad \text{Equation 5}$$

where R = resistance to blood flow.

An increase in diameter reduces the resistance to blood flow in the vessel. The reduction in resistance to flow would result in an increase in blood perfusion. Hence, an increase in diameter would increase blood perfusion.

Drugs that cause vasodilation could theoretically bring about an increase in blood flow. Poiseuille's law strictly applies to homogeneous fluids that do not have shear dependent changes in viscosity, move through a rigid tube and display non-pulsatile flow. This cannot be directly applied to the CAM, where blood flow occurs in a pulsatile manner through vessel walls that contain vascular smooth muscles that are capable of altering the vessel diameters and modifying blood flow rate. However, this law is still applicable to situations with pulsatile flow where mean flow rate does not change. As the results obtained did not show the theoretical trend, it was postulated that the auto-regulation of the CAM moderated the increase in blood perfusion by causing the blood perfusion to decrease in an over-compensatory manner.

F. Imaging studies

F.1. Effect of test substances on vessel size

The test substance was applied on the surface of the CAM and images captured at regular time intervals. The images captured were then analysed with a software to determine the vessel diameters (Figure 36). Different segments in a selected area for measurement were identified. The respective diameters of each vessel portion located in different segments were identified using the software. Using this procedure, the diameter of a specific vessel was determined automatically at each time point for the respective drug concentration. The change in vessel diameter for each concentration tested was then plotted to determine the concentration effect. This was done to illustrate the relationship between vessel diameter and blood perfusion, as well as to use the vessel diameter changes as a tool in the assessment of absorption of vasoactive drugs.

F.2. Controls

The distribution of the vessel diameter of the CAM was found to be normal ($p > 0.05$) according to the Kolmogorov-Smirnov test. Baseline changes in vessel diameter, i.e. control without the application of test substance were monitored over time. From the results obtained, it was apparent that the vessel diameters of the CAM at rest did not change significantly over time (Figure 37). Therefore, any change in vessel diameter seen in subsequent studies would most likely be attributed to the vasoactive effect of the test substance. Nevertheless, some small functions in blood vessel diameters were seen over time but these small fluctuations were relatively small and within a small range.

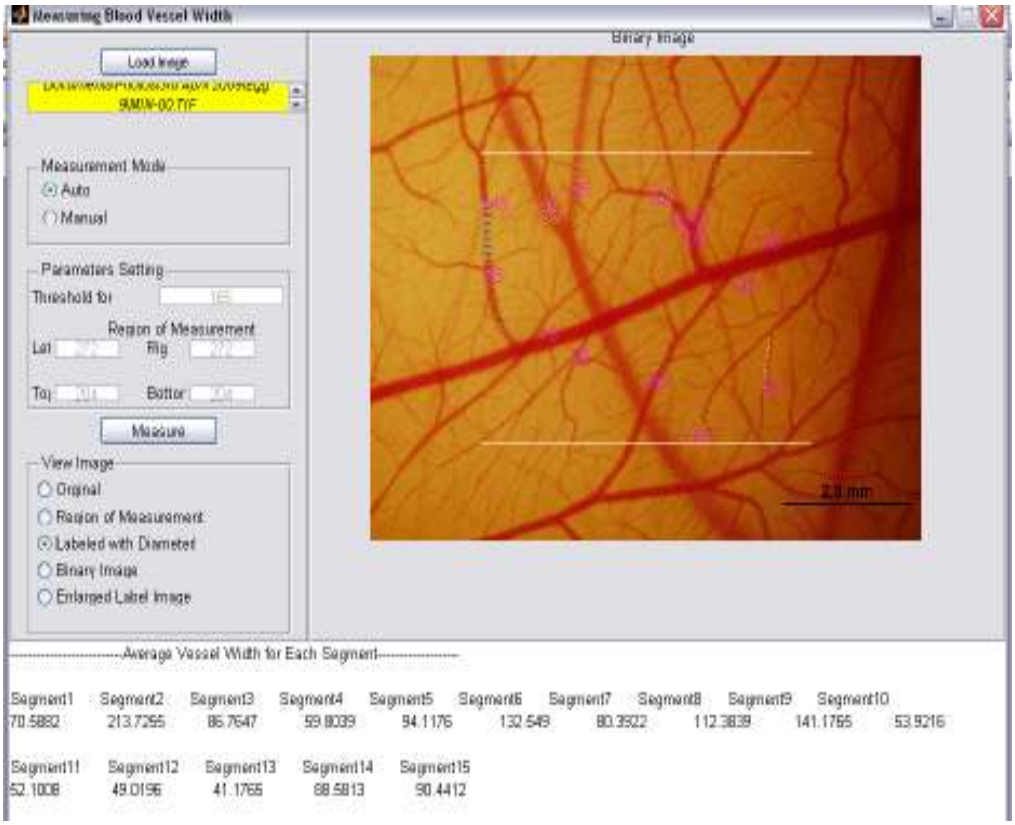

Figure 36. Vessel segments measured by imaging

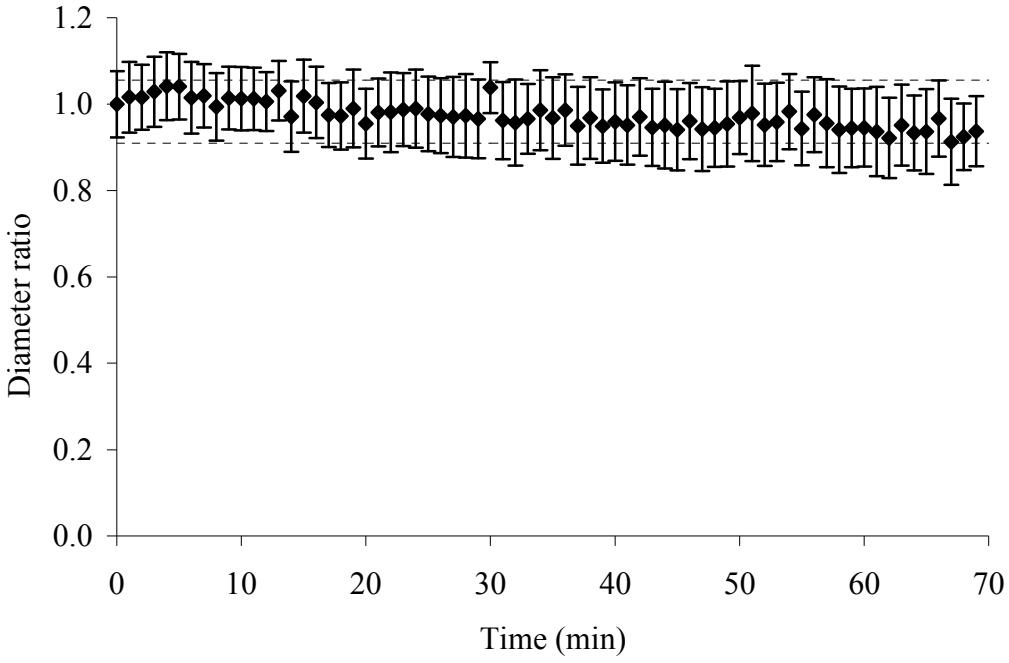

Figure 37. Vessel diameter of CAM over time (control) (n = 5)

F.3. 70 % v/v ethanol

Ethanol at concentration of 70 % v/v is commonly used as a solvent for drugs. Ethanol was reported to possess transdermal penetration enhancing action (Sinha and Kaur, 2000). Low doses of ethanol were found to increase the release of nitric oxide from the endothelium and hence augment vasodilation but high doses impaired relaxation of the endothelium (Puddey et al., 2001). Ethanol has been reported to cause both vasoconstriction (Altura et al., 1983, Yong et al., 1992, Zhang et al., 1993) and vasodilation (Altura et al., 1979, Mayhan and Didion, 1995).

The results show an immediate decrease in vessel diameter, followed by prolonged vasoconstriction in response to the ethanol administered (Figure 38). In an earlier study, blood perfusion increased immediately after the application of 70 % v/v ethanol, coinciding with the increase in vessel diameter. The subsequent vasoconstrictive effect of 70% ethanol lasted for at least an hour, occurring in tandem with reduced blood perfusion. In accordance with Poiseulle's Law, changes in vessel diameters had affected blood perfusion. As such, vessel diameters change would be the primary factor to ascertain if there was any vasoactive activity occurring in response to an external stimulus on the CAM vessels and changes in blood perfusion would hence be the secondary factor that had occurred as a result of changes in CAM vessel diameter values.

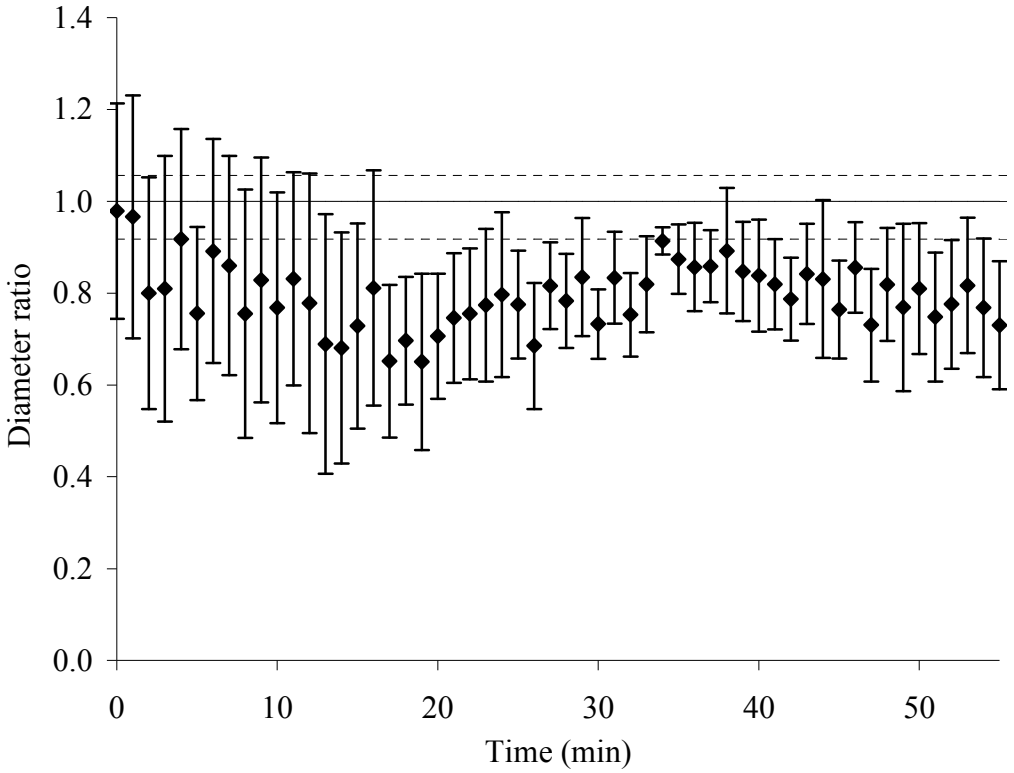

Figure 38. Effect of 70% ethanol on CAM vessel diameter when added at time 0 min (n = 5)

F.4. NMP

The change in vessel diameter with 10 % v/v NMP could not be further investigated as the CAM began to show haemorrhage and the resultant periphery blood obscured the visualization of the CAM vessels. The results showed that there was a slight drop in vessel diameter after application of 1 % v/v NMP, followed by a gradual increase in vessel diameter over time (Figure 39). As reported earlier, 1 % v/v NMP resulted in no discernible significant change in blood perfusion values. Hence, changes in blood perfusion of the CAM could not be solely attributed to changes in vessel diameter.

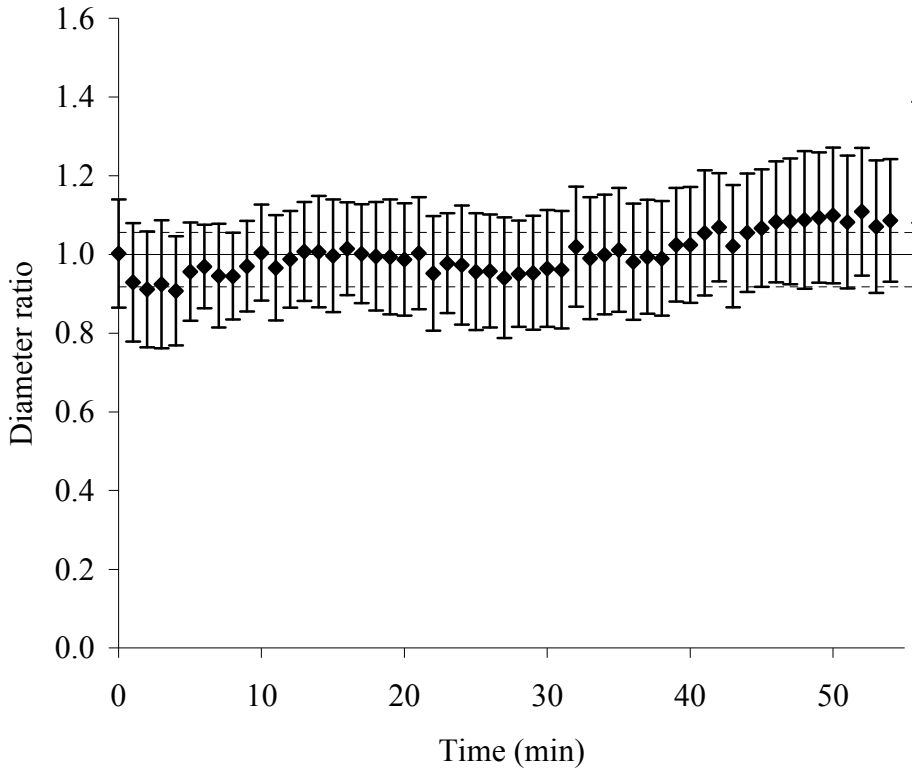

Figure 39. Change in vessel diameter over time with 1 % v/v NMP application on CAM (n = 5)

F.5. Glucagon

An increase in vessel diameter was seen with 1 mg/mL of glucagon after about 5 min of application to the CAM (Figure 40). The vasodilative action of glucagon was sustained and still evident even after an hour. However, the increase in vessel diameter was not accompanied by the expected increase in blood perfusion. A decrease in vessel diameter was accompanied by an increase in blood perfusion with 70 % v/v ethanol. A decrease in vessel diameter coupled with almost no change in blood perfusion was seen with the application of 1 % v/v NMP. A probable supposition is that changes in vessel diameter either need to reach a certain threshold before any discernable change in blood perfusion can be detected, or the expected changes in blood perfusion following vessel diameter changes are over-riden by auto-

regulation mechanisms of the CAM. In the case of glucagon, the increase in diameter may not have been adequate to result in blood perfusion change. Since the instilled compound produced vascular response, it was also likely to enter the circulatory system. Thus, besides effects on the local vasculature, there may be other systemic effects and changes in the cardiac contractile ability will certainly affect the overall perfusion rate. Hence, changes in vasculature may not sometimes reflect perfusion rate.

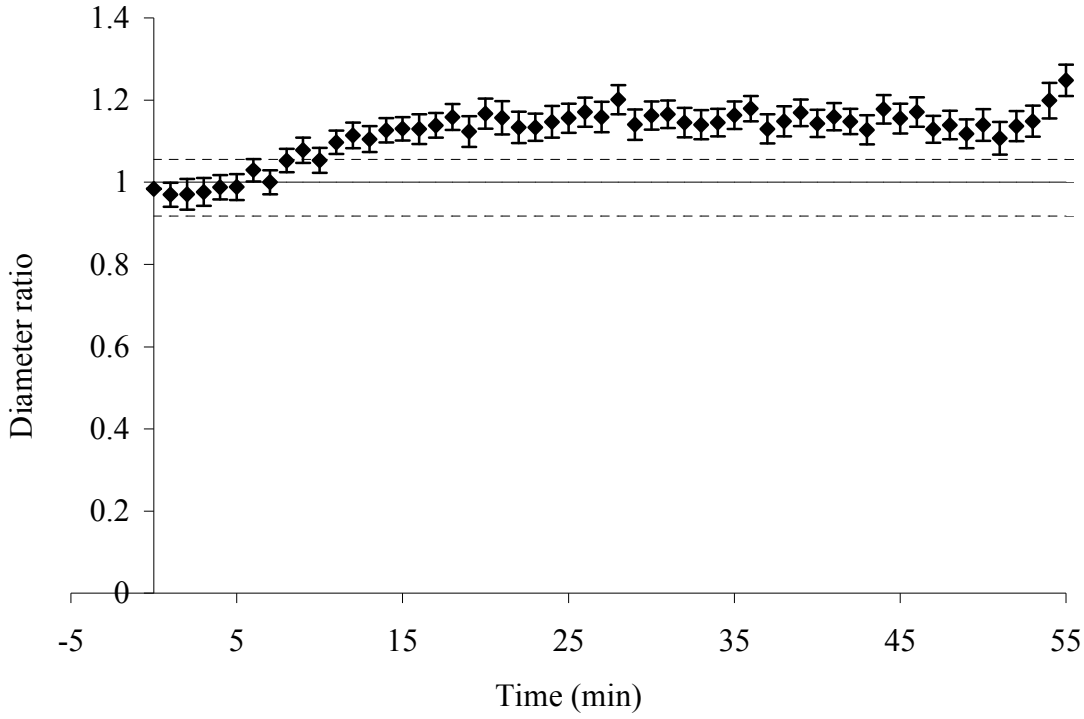

Figure 40. Change in vessel diameter over time after 1 mg/mL glucagon application on CAM (n = 5)

F.6. Caffeine

A marked increase in vessel diameter was obtained after the application of caffeine on the CAM surface for all the caffeine doses used. This observation suggested

consistent evidence of vasodilation (Figure 41). The standard error bars were omitted for a clearer view of the plot.

The plot of increase in vessel diameter ratio against caffeine concentration is shown in Figure 41. In an attempt to obtain a simple mathematical model to describe the effect of caffeine on vessel size, the caffeine dose was plotted against vessel derivatives of the change in vessel diameter. Derivatives employed include the percentage, log and square root values of the change in vessel diameter. According to the Pearson's correlation test, the relationship between increase in vessel diameter and caffeine concentration was non-linear ($p > 0.05$) and best described by a U shaped pattern, similar to the pattern seen with the plot of blood perfusion change against caffeine dose (Figure 42). According to the profile, the average change in vessel diameter increased from 2 mg/kg to 4 mg/kg caffeine. Caffeine in dose range of 4 mg/kg to 8 mg/kg showed similar effects on vessel diameter, resulting in a plateau on the graph. Further increase in caffeine concentration to 10 mg/kg increased vessel diameter significantly. Compared to blood perfusion, the vessel diameter was more sensitive to changes in caffeine dose. Change in vessel diameter has to reach a certain threshold before any discernable change in blood perfusion can be detected. This could possibly account for the greater response of vessel diameter to test substance in comparison to blood perfusion.

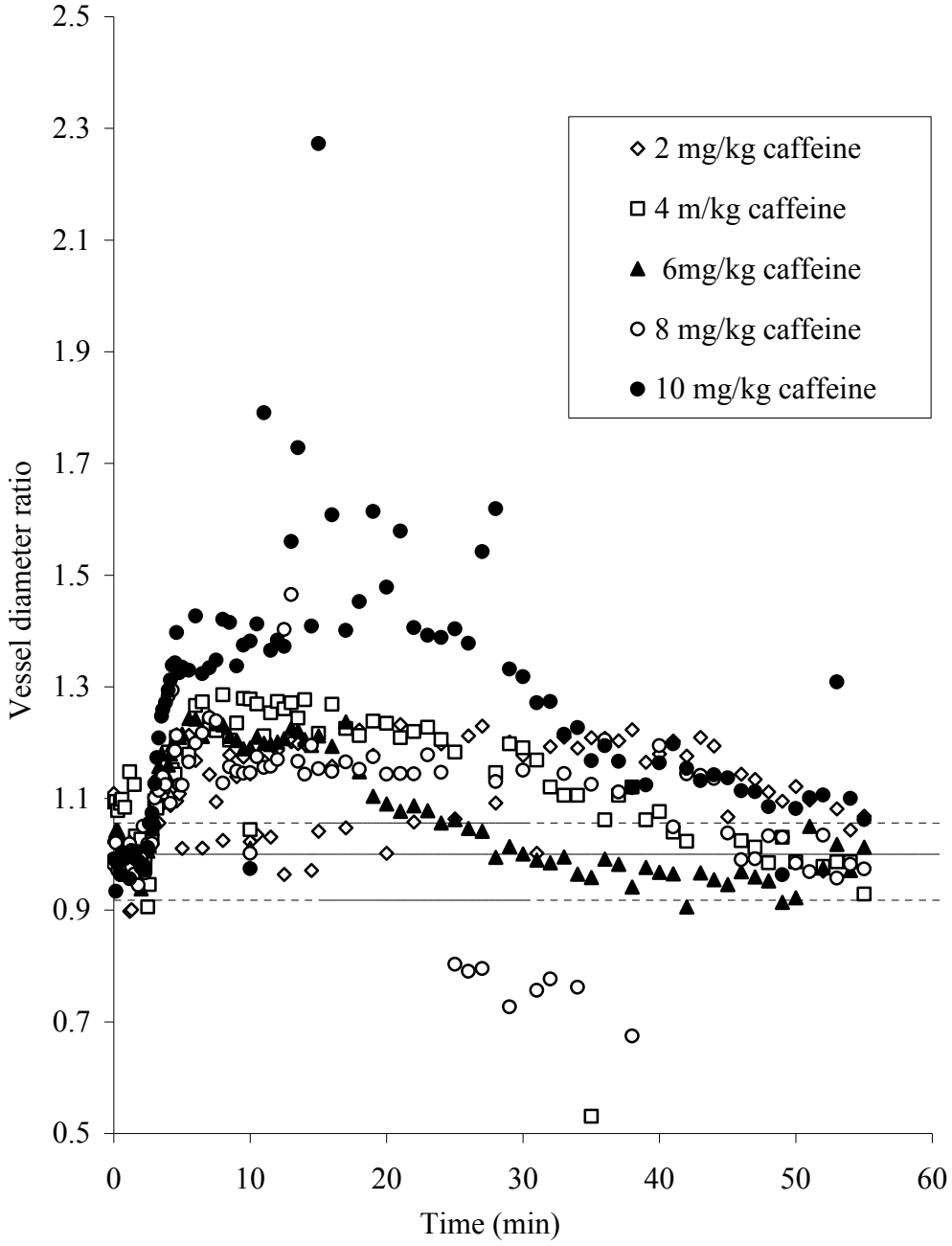

Figure 41. Time study of vessel diameter in response to different caffeine doses (n = 5)

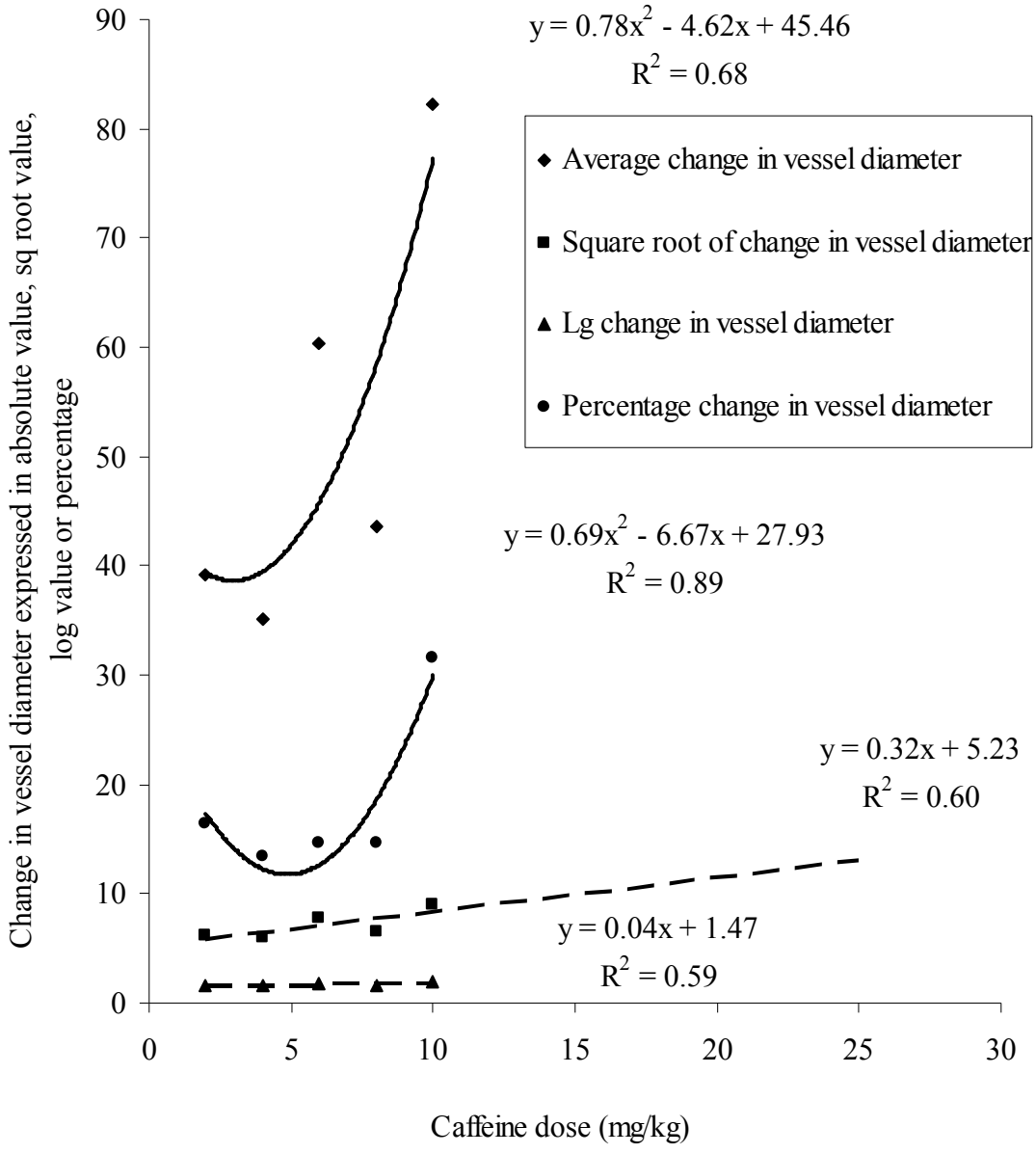

Figure 42. Relationship between caffeine dose and derivatives of change in vessel diameter

Auto-regulation could have set in and caused compensatory mechanisms so as to result in changes in vessel diameter to compensate for the decrease in blood perfusion. This would ensure that baseline perfusion and vessel diameter parameters are maintained so as to protect the well being of the foetus. Alternatively, hormesis could have resulted (Calabrese, 2009), which lead to a balance of vasodilation and

vasoconstriction factors that cumulated in the pattern seen with percentage change in vessel diameter, which decreases with dose before subsequently increasing gradually pass a certain dose. In addition, the binding of caffeine to different adenosine receptor subtypes (Riksen et al., 2008), which result in vasodilation or the antagonism of vasodilation, may also play a role in the results seen. If caffeine were to bind preferentially to either subtype, this could affect the balance of vessel diameter and cause vasodilation or vasoconstriction. At higher doses, the effect of the dominant receptor would be predominant (Szabadi, 1977).

Another possible explanation for the observed phenomenon is the concept of hormesis. There are two types of biphasic response. The first type illustrates a situation where the response variable increases above the baseline but subsequently decreases below the baseline as the drug dose increases. The second type demonstrates an opposite trend, where the response variable decreases below the baseline but subsequently increases above the baseline as the drug dose increases. An example of this time response plot is the hormesis model as shown in Figure 43. The hormetic dose response can perhaps provide a better explanation of the results in comparison with the threshold model (Calabrese and Baldwin, 2003). The inhibition and antagonism of adenosine by caffeine occur at the adenosine receptors. There are multiple subtypes of adenosine receptors that adenosine can bind and the consequence of selective binding results in either stimulatory or inhibitory effects on the vessels. At different concentrations, caffeine affects the binding of adenosine to the different receptors (Calabrese, 2008). A combination of these concepts can perhaps explain the trends observed. In the range of 2 – 4 mg/kg, caffeine appeared to be preferentially bound to the inhibitory adenosine receptors as indicated by the decreased blood vessel

diameter values. From 4 – 8 mg/kg, caffeine appeared to bind to the stimulatory and inhibitory receptors to similar extent as indicated by the constant change in blood vessel diameter. Above 8 mg/kg, the inhibitory receptors could have been saturated and the stimulatory effect predominated, resulting in an increase in vasodilation and hence, an increase in vessel diameter values. Hence, the use of caffeine as a model drug to investigate the influence of excipients on drug absorption should best be limited to the linear portion of the curve so as to provide an accurate estimation on the effect of the excipients through the change in vessel diameter by the caffeine absorbed.

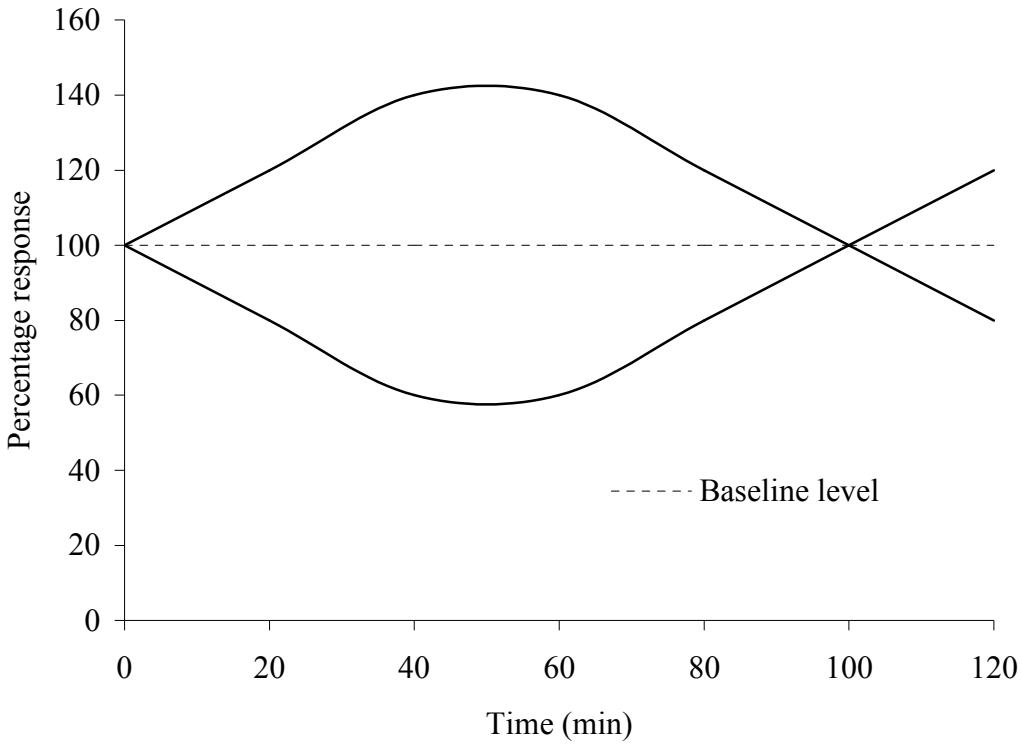

Figure 43. Two types of hormesis response curves (Adapted from Calabrese and Baldwin, 2003)

F.7. GTN

The majority of the vessels used in this study were veins with diameters in the range of 200 to 350 μm. The change in vessel diameter over time with 0.01, 0.03 and 0.05 mg/kg GTN is depicted in Figure 44. These concentrations were chosen as they produced changes in vessel diameter. The standard error bars were omitted to allow for clearer plots. Nitrates typically result in peak vasodilation 3 to 4 min after administration (Moens et al., 2005), and this trend was seen in the study.

According to the Pearson's correlation test, the relationship between change or percentage change in vessel diameter and GTN dose is non-linear ($p > 0.05$). The relationship is best described by the relationship depicted in Figure 45. The same trend was observed for change or percentage change in blood perfusion. The complex relationship between change in vessel diameter and GTN dose could be explained by the concept of hormesis.

The vasodilation effect of GTN may be attributed to more than one factor. Vasodilation may arise through the formation of nitric oxide prior to a series of complex pathways that begins with the activation of the intracellular enzyme, soluble guanylyl cylase (sGC) and results in a cascade pathway that involves cyclic guanosine-3',-5'-monophosphate (cGMP), cGMP-dependent protein kinase and protein phosphorylation that leads to the activation of Ca^{2+}. GTN is converted to nitric oxide following intracellular bioconversion, and this is the hypothesis that is commonly used to explain the subsequent vasoactive effects of GTN, through the mediating actions of nitric oxide. However, this may not be the only way that GTN causes vasodilation to occur. It is possible that GTN evokes vasodilation through another pathway that does not result in the formation of nitric oxide as a vasoactive

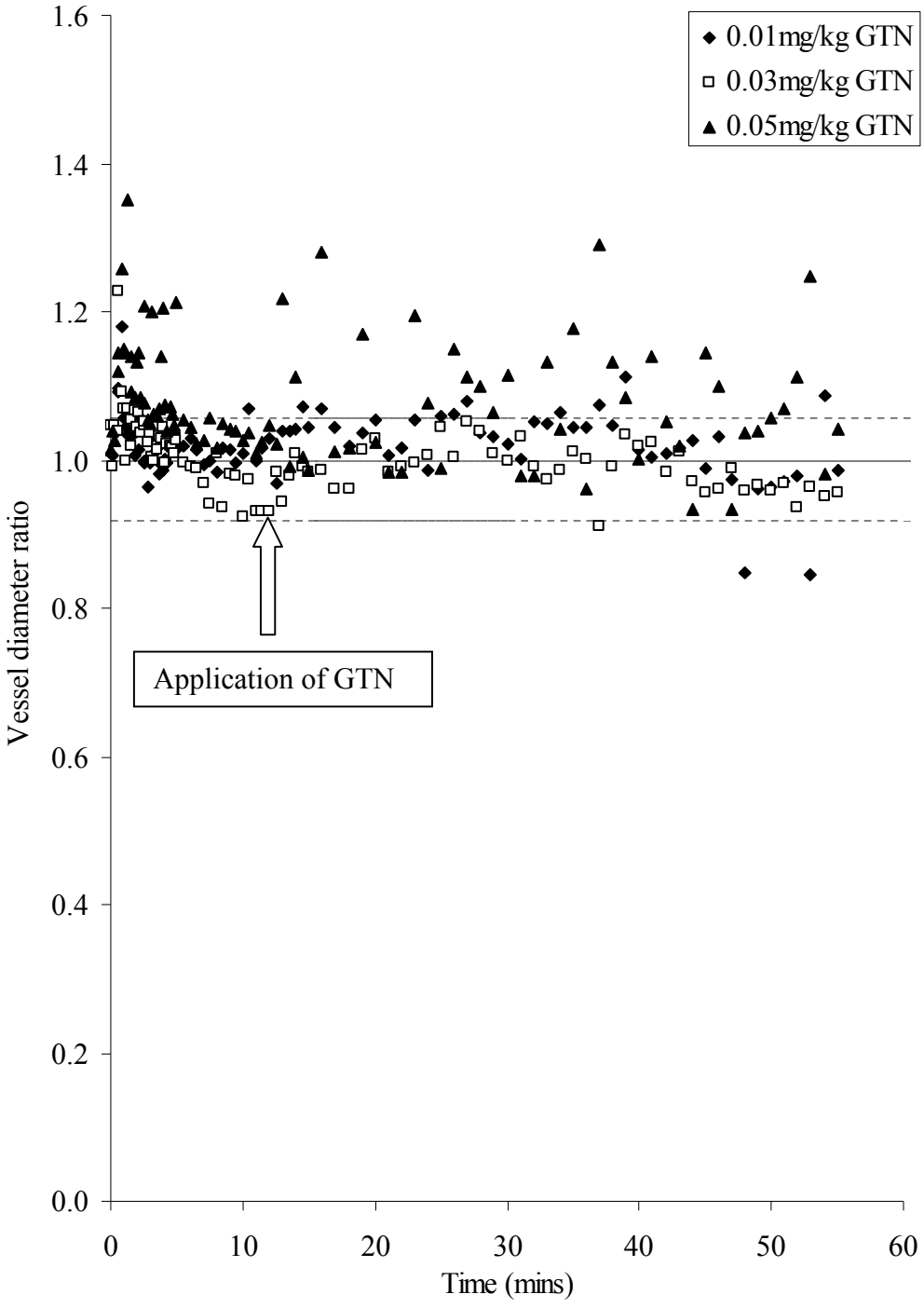

Figure 44. Change in vessel diameter over time with 0.01, 0.03 and 0.05 mg/kg GTN (n = 5)

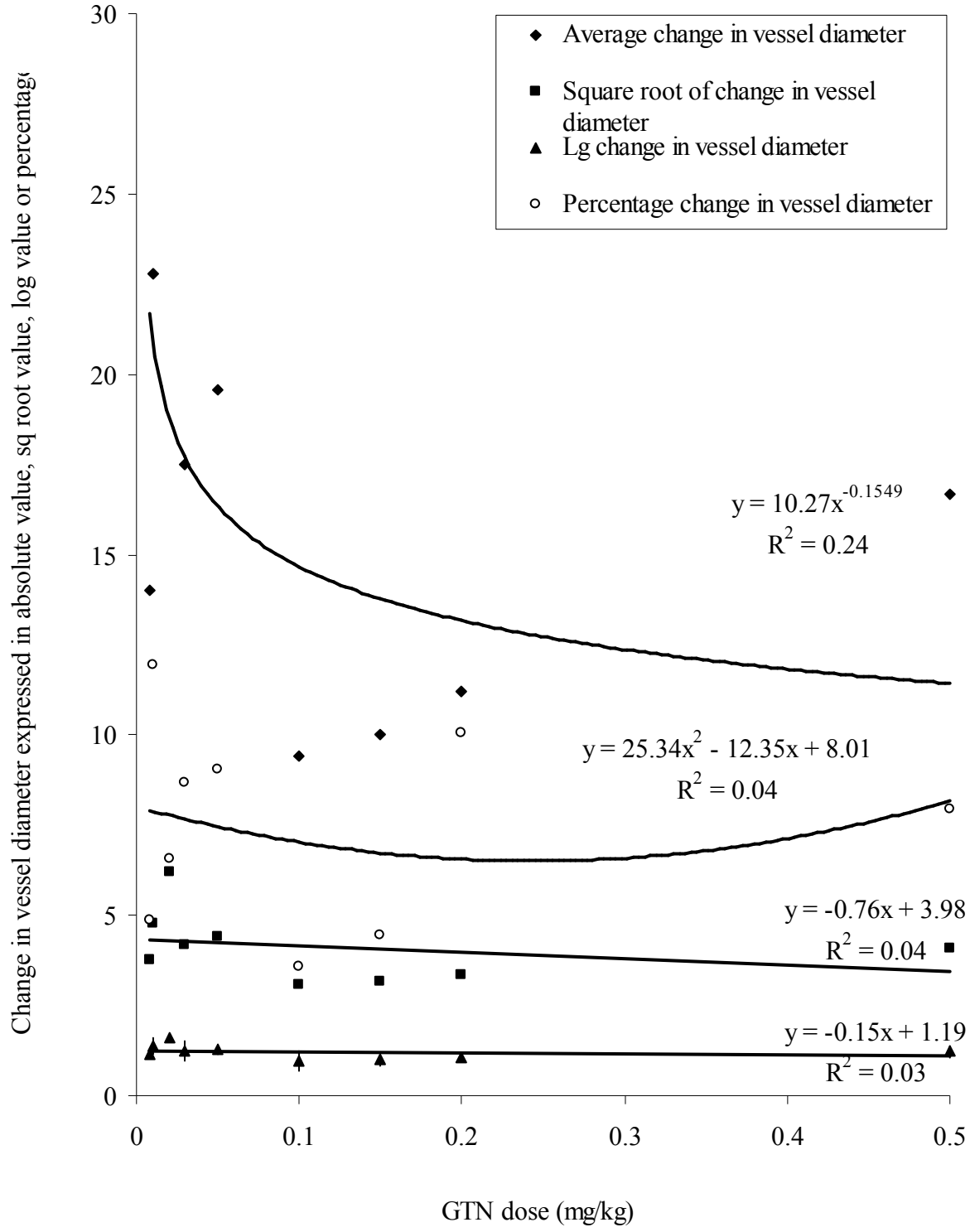

Figure 45. Relationship between GTN dose and derivatives of change in vessel diameter

mediator and instead, exerts vasoactivity via the activation of sGC through another pathway that is activated independently of the presence of nitric oxide (Kleschyov et al., 2003). In addition, GTN tolerance has been reported to have developed in the presence of high GTN concentrations or withdrawal of GTN. The mechanisms of the development of tolerance to GTN is complex and various mechanisms have been proposed (Abou-Mohamed et al., 2000). The decrease in extent of vasodilation seen at higher GTN doses could have been due to the presence of tolerance to the effect of GTN, hence resulting in the pattern seen.

F.8. Correlation between basal blood perfusion and vessel diameter of the CAM

CAM vessel diameters were plotted against the CAM basal perfusion levels to determine if there was any relationship between vessel diameter and blood perfusion. The spread of values in the 2D scatter plot showed extremely poor correlations (Figure 46). Further analysis using the Pearson's correlation test confirmed that the 2 parameters were not correlated (p value > 0.05). Hence, the size of the vessels used in this study had insignificant effect on the results. This allowed for meaningful interpretation of the results from blood perfusion studies.

Both GTN and caffeine are vasodilators (Kelly et al., 2005, Lapeyre et al., 2004). The doses of these 2 drugs used in the study generally produced vasodilation in the CAM. However, blood perfusion decreased instead of showing an increase that is expected with vasodilation. The inverse relationship is not in agreement with Poiseuille's Law that states that changes in blood perfusion should be proportional to changes in vessel diameter. Hence, there could be a different auto-regulatory response mechanism with

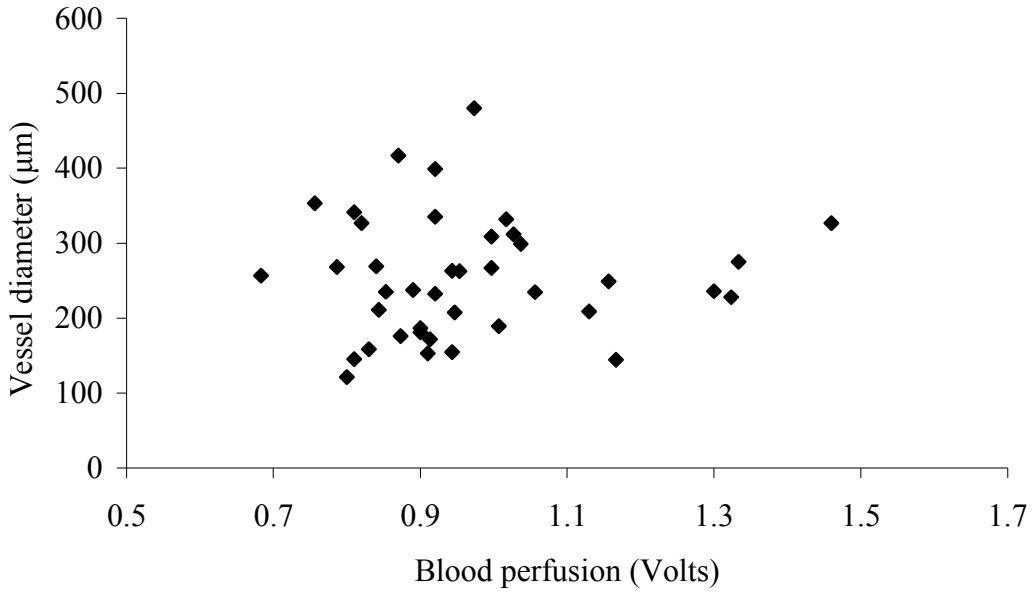

Figure 46. Lack of relationship between blood perfusion and vessel diameter

regards to vasodilation and vasoconstriction. Hyperoxia has been found to result in greater degree of angiogenic effect than hypoxia (Strick et al., 1991). Vasodilation resulted in a greater amount of blood perfusion. This could have resulted in the development of hyperoxia. As such, an enhanced angiogenic effect may have occurred. In response, a rebound reaction may have been triggered in an effort to restrict the hyperoxia. The rebound reaction thereby results in lower blood perfusion.

Caffeine was reported to result in varying changes on blood pressure (James, 2004, Engels et al., 1999). According to Poiseuille's Law, pressure is directly proportional to blood perfusion. Hence, any decrease in blood pressure due to the action of caffeine may cause blood perfusion values to decrease. Caffeine was also reported to increase vascular resistance (Hartley et al., 2004, James and Gregg, 2004). As mentioned previously, an increase in vascular resistance would result in a decrease in blood perfusion. In addition, caffeine was reported to alter cardiovascular performance in

embryos (Keller et al., 2007). Change in cardiovascular properties may alter pressure or output and hence affect blood perfusion of the CAM.

GTN was reported in numerous studies to decrease systolic, diastolic, mean arterial, and central aortic blood pressure (Kawakami et al., 1995, Conti et al., 1983). According to Poiseuille's Law, a decrease in pressure would result in a decrease in blood perfusion. GTN was also reported to cause a decrease in venous return, which would also decrease blood pressure and cardiac output (Kojda et al., 1996). A phenomenon known as the Bezold-Jarish reflex has been reported to cause hypotension as well as bradycardia in humans. It was postulated that the mechanism of action involved the stimulation of the cardioinhibitory receptors in the ventricle walls (Boyle, 2007) . High doses of nitric oxide arising from GTN was reported to reduce contractile response and blood pressure. The reduction in blood perfusion due to GTN could be attributed to the above mechanisms.

F.8.i. Caffeine

The change in vessel diameter that occurred under the influence of caffeine had an effect on the extent of change in blood perfusion. For each caffeine dose, the mean change in blood perfusion and corresponding change in vessel diameter were plotted (Figure 47). According to the Pearson's correlation test, the change in vessel diameter with caffeine concentration did not follow a linear relationship ($p > 0.05$). The relationship is best described by an inverted U-shaped curve. The initial part of the curve, which corresponds to dose range of 2 mg/kg to 6 mg/kg, shows a direct relationship between blood perfusion and vessel diameter Beyond vessel diameter of 35 μm, which corresponds to a dose of 6 mg/kg, the change in blood perfusion

decreases with increase in vessel diameter change. The last 2 points on the curve represent the 10 mg/kg and 8 mg/kg doses respectively. These findings implied that concentrations greater than 6 mg/kg resulted in a smaller change in blood perfusion that was not dose-dependent. This may have been a result of oversaturation of the receptors. The complex relationship between change in vessel diameter and caffeine doses clearly demonstrated the importance of hormesis in a biological system.

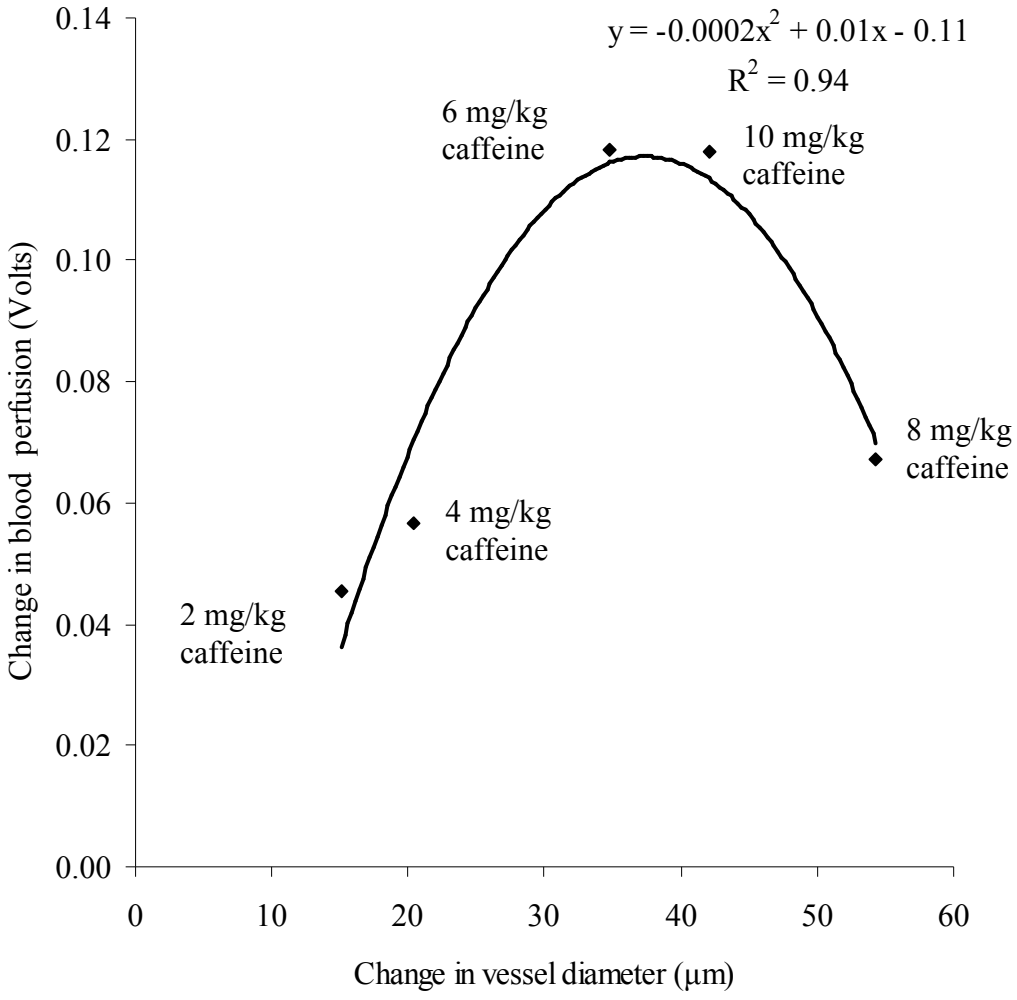

Figure 47. Relationship between blood perfusion and vessel diameter changes with caffeine

F.8.ii. GTN

The change in vessel diameter that occurred under the influence of GTN also had an effect on the extent of change in blood perfusion. For each GTN dose, the mean change in blood perfusion and corresponding change in vessel diameter were plotted (Figure 48). According to the Pearson's correlation test, the change in vessel diameter with GTN dose did not follow a linear relationship ($p > 0.05$). Interestingly, the relationship followed a U-shaped curve, which is direct contrast to the inverted U-shaped curve obtained for caffeine. The initial part of the curve shows a linear relationship between blood perfusion and vessel diameter. The linear relationship lasted till the threshold value of 15 μm. After the threshold value, the change in blood perfusion plateaued and then increased with an increase in vessel diameter. This relationship did not occur concurrently with the doses of GTN applied topically to the CAM. Low concentrations of GTN were shown to result in greater changes in vessel diameter as opposed to the higher concentrations of GTN used. The low GTN concentrations such as 0.008 mg/kg and 0.02 mg/kg also resulted in the greatest change in blood perfusion compared to the other GTN concentrations. Hence, this shows that blood perfusion change in the CAM is more sensitive to low concentrations of GTN and would react in accordance to this sensitivity. With the exception of the lowest GTN concentration of 0.008 mg/kg, the low range of GTN concentrations cause an increased change in vessel diameter in contrast to the higher range of GTN concentrations. However, the change does not occur in a dose dependent manner. There is a possibility of the receptors being saturated at higher concentrations of GTN. The use of GTN as a model drug would be appropriate if the low ranges of concentrations are used. The complex relationship between change in

vessel diameter and GTN concentration could be explained by the concept of hormesis.

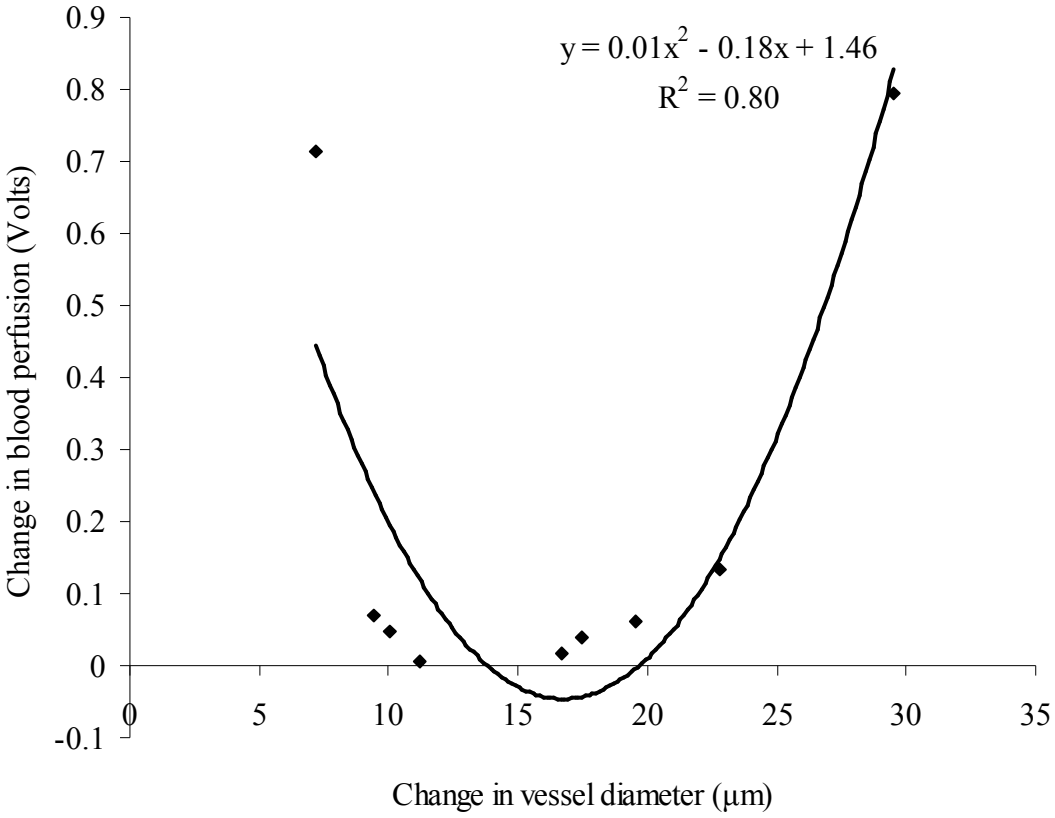

Figure 48. Relationship between blood perfusion and vessel diameter changes with GTN. The points from left to right refer to the concentration of 0.008 mg/kg, 0.1 mg/kg, 0.15 mg/kg, 0.2 mg/kg, 0.5 mg/kg, 0.03 mg/kg, 0.05 mg/kg, 0.01 mg/kg and 0.02 mg/kg respectively

F.9. Diameter ratio

F.9.i. Caffeine

The diameter ratios obtained for caffeine showed a dose dependent trend (Figure 49). Diameter ratio increased when the concentration of caffeine was increased. This meant that an increase in caffeine dose resulted in a greater increase in vessel diameter of the CAM. Perfusion ratio versus dose was also plotted on the same graph.

A downward sloping line was obtained, however, it was almost horizontal, signifying that there was little change in perfusion ratio with caffeine dose.

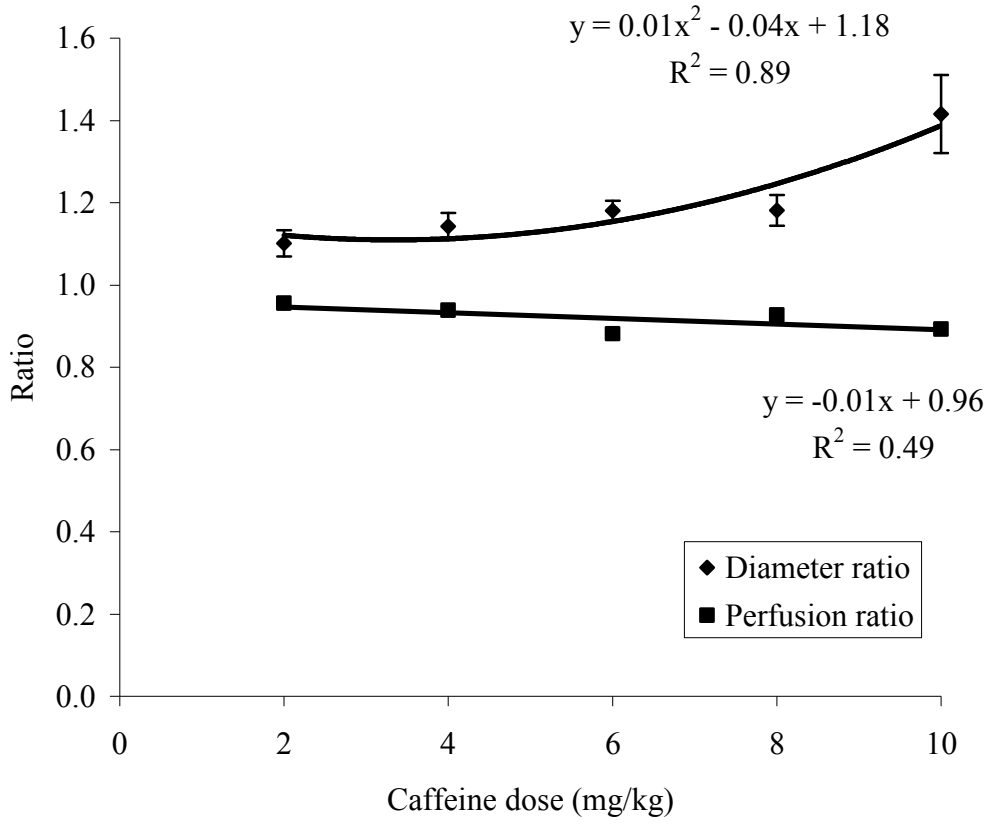

Figure 49. Effect of caffeine dose on perfusion ratio and diameter ratio

F.9.ii. GTN

The diameter ratios obtained for GTN showed a dose dependent trend (Figure 50). The values of the diameter ratio increased gradually when the dose of GTN was increased. The plot of perfusion ratio with GTN dose showed an almost horizontal line, indicating that GTN has little effect on the perfusion ratio. The vasodilation exerted by caffeine was of greater magnitude than the vasodilation caused by GTN. Hence, caffeine may be a better choice to act as a model drug in studies focused on vessel diameter change.

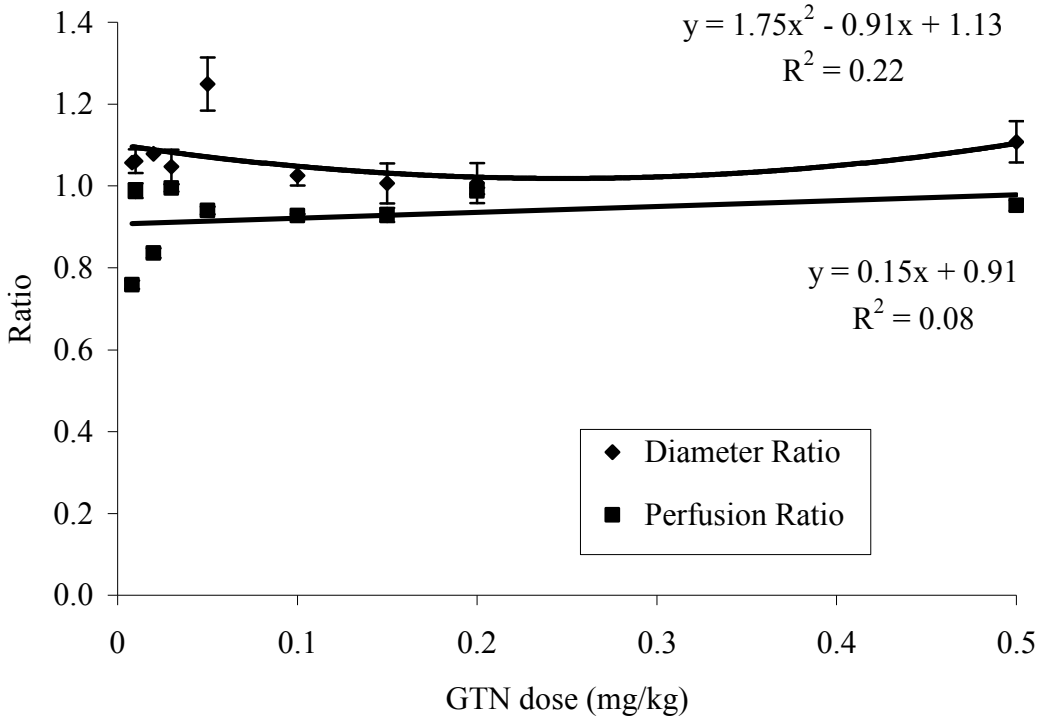

Figure 50. Effect of GTN concentration on perfusion ratio and diameter ratio

G. Permeation studies

G.1. Permeation studies with the Franz diffusion cell

Nicotine was used as the model drug as it possesses good solubility in both polar and non-polar solvents. Its low molecular weight also aligns it to be a good penetrator (Zorin et al., 1999). In addition, GTN was chosen for its clinical relevance to buccal mucosa. Photographs of the CAM, snake skin and pig skin are shown in Figure 51.

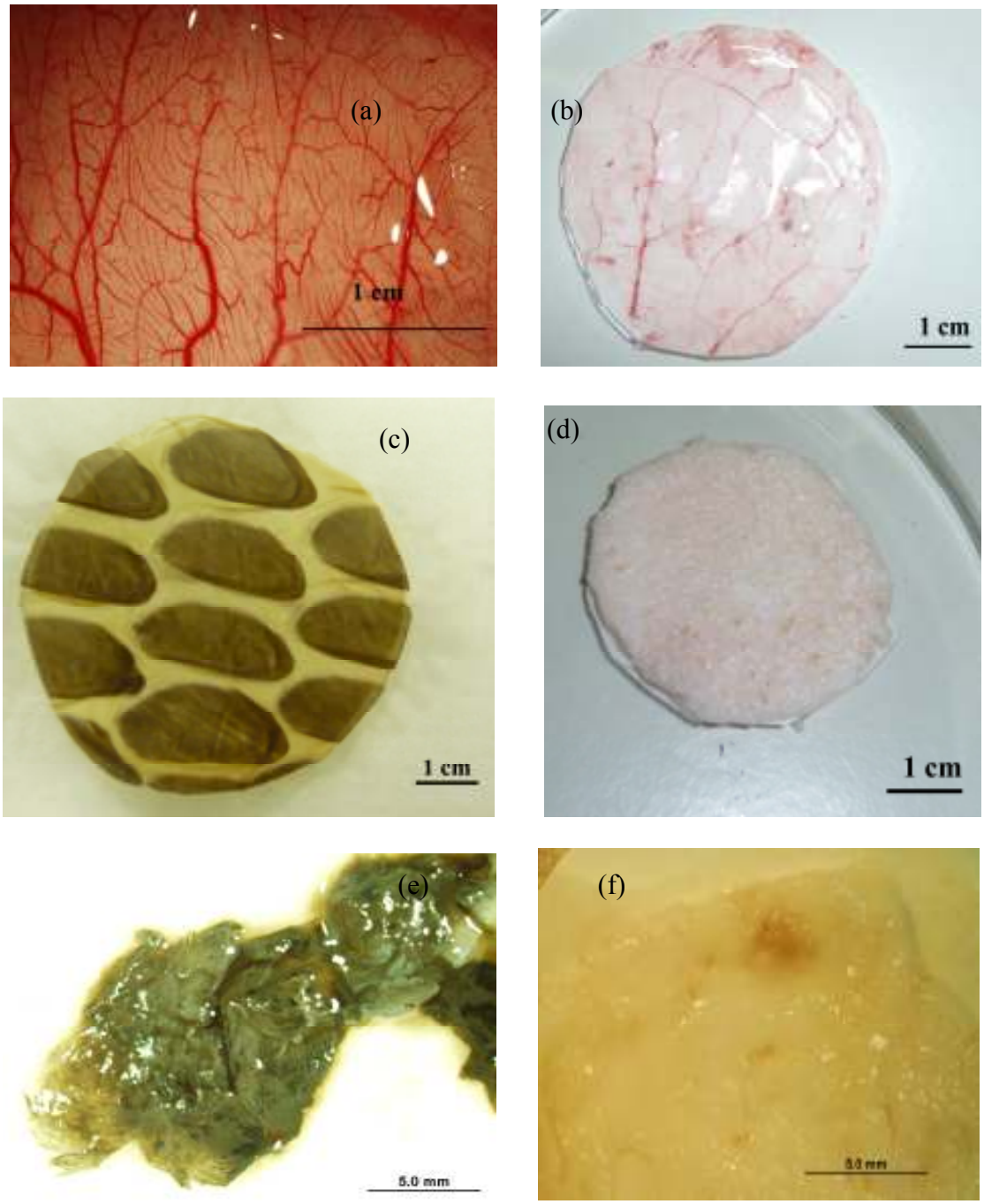

Figure 51. Photographs of (a) CAM in egg, (b) CAM specimen, (c) snake skin specimen, (d) pig skin specimen, (e) pig retina and (f) pig buccal mucosa

G.2. Influence of partition coefficient and molecular weight of drug on permeation through the CAM

The model drugs used possess different partition coefficients (nicotine, 1.17 and GTN, 1.62) and molecular weights (nicotine, 162.2 and GTN, 227.1). Using the skin as a guide, a drug with a $\log_{10}$ partition coefficient value of less than or equals to 2 is considered as a potential candidate to penetrate the skin (Beetge et al., 2000). The partition coefficient refers to the ratio of the solubility of the compound in octanol over the solubility of the compound in water. A drug requires a balance in order to be able to permeate through the skin and subsequently into the systemic circulation. In the case of the CAM, the drug would need to partition through the mesoderm of the CAM and penetrate the extracellular matrix which is composed of many different types of material such as laminin, collagen type IV, fibronectin and various glycosaminoglycans (Ribatti, 2008). GTN has a partition coefficient that falls within the proposed optimum range of values that are less than or equal to 2. This probably explains its rapid action in the CAM as quick responses were observed. However, propranolol which has a partition coefficient outside the stated range, also affected blood flow and caused hemorrhage in the CAM. This shows that propranolol (with a partition coefficient value of 3.48) was accessible to the blood vessels in the CAM, probably to a lower extent in comparison with GTN. Furthermore, theophylline has partition coefficient (-0.02) and molecular weight (198.2) comparable to those of caffeine (partition coefficient value and molecular weight of -0.07 and 194.2 respectively). A molecular weight of less than 600 Daltons is more permeable through the skin (Aulton, 2001). Unlike caffeine, theophylline was unable to elicit a response in the CAM blood perfusion measurements. As discussed earlier, metabolism of theophylline to caffeine is a prerequisite before it can exert its effects on blood

perfusion. The enzymes required for this metabolism to take place are found in human skin but not in the CAM. Therefore, the CAM may not be an ideal model for the human skin but for biological membranes. Such possible membranes probably include the non-keratinised retina tissue of the eye or the buccal mucosa, based on the structural characteristics of these membranes in comparison with the CAM (Table 2). The suitability of the CAM to mimic human membrane was further investigated.

G.3. Nicotine

G.3.i. Synthetic membrane

In a separate control study, the synthetic membranes were placed onto the receptor compartment without any biological membrane to determine the effect of the synthetic membrane on the drug release profile. The synthetic membrane served to provide structural support to the test membrane. Hydrophobic membranes were avoided as they were found to be poorly wetted by the receptor fluid. Poor wetting of the membrane was found to affect the release of nitroglycerin (Shargel, 2005). The compatibility of the membrane with the buffer solutions rendered it to be suitable for use, as it did not dissolve or degrade on contract with the buffer solution. The CAM was supported on the synthetic membrane and the release rate of nicotine through the CAM determined. In a preliminary study, the amount of nicotine that permeated through the synthetic membrane reached a plateau within an hour. Furthermore, the amount of drug that permeated through the synthetic membrane was higher than the amount of drug that eventually permeated through the combination of test membranes and synthetic membrane, except for pig retina. This showed that the presence of the synthetic membrane did not pose a barrier to drug permeation and hinder the rate at which nicotine permeated through the other biological membranes (Figure 52).

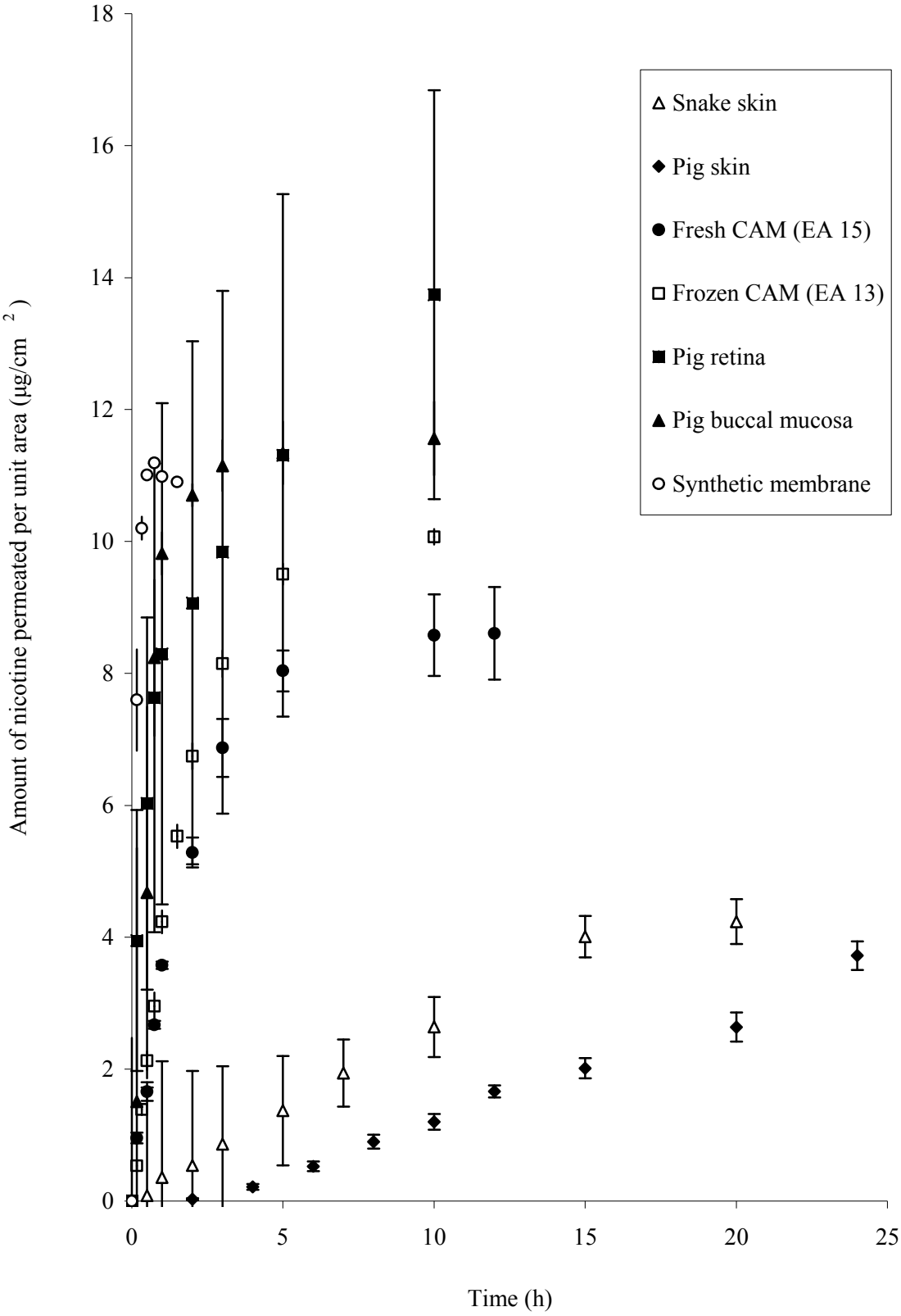

Figure 52**.** Permeation profiles of nicotine through different membranes (n = 3)

G.3.ii. Fresh CAM

G.3.ii.a Influence of CAM thickness

The thickness of the CAM obtained from fertilized eggs of different age was measured. The thickness of the CAM was found to increase linearly with embryo age in an exponential manner (r^2 0.94) (Figure 53). The standard error values are so small that they cannot be seen on the graph, indicating the robustness and reproducibility of CAM thickness with embryo age. The values are in agreement with reported CAM thickness values of between 100 – 150 μm (Kurz et al., 1994). The thickness of the CAM can be attributed to the increase in vascularity as well as the changing cell compositions in the CAM layers that result in the formation of intercellular spaces, vacuolation of cytoplasm and accumulation of excretory waste. No definite trend was observed between CAM thickness and the permeation profile of nicotine through the CAM at different EAs (Figure 54). Hence, CAM thickness was not a determining factor of permeation through the CAM.

G.3.ii.b. Permeation properties through fresh CAM

It would be optimal to employ fresh CAM in experiments as it has been found that freshly harvested animal skin retained most of the characteristics of living skin (Yazdanian, 1994). The typical permeation profile of nicotine through the CAM is depicted in Figure 52. Irrespective of embryo age, the total amount of nicotine that permeated through the CAM reached a plateau after about 5 h. Some examples are shown in Figure 55. However, the permeation coefficient of the CAM was found to vary with embryo age (p value < 0.05) (Table 13). This suggested that the composition of the CAM that varied with age may play a role in affecting permeation

Table 13. K_p values of test membranes with nicotine

	Embryo Age	Permeability Coefficient, K_p	Coefficient of Variance
Fresh CAM	9	0.129	4.98
	10	0.180	15.9
	11	0.181	17.7
	12	0.152	23.5
	13	0.127	10.9
	14	0.170	29.2
	15	0.130	28.7
	16	0.156	14.8
	17	0.130	24.8
	18	0.132	21.2
Frozen CAM	9	0.188	5.06
	10	0.202	11.5
	11	0.357	4.53
	12	0.292	11.3
	13	0.217	7.58
	14	0.199	2.96
	15	0.238	24.3
	16	0.291	0.758
	17	0.334	2.12
	18	0.307	1.86
Snake skin		0.011	36.8
Pig Skin		0.003	13.4
Pig retina		0.473	57.9
Pig buccal mucosa		0.133	47.1

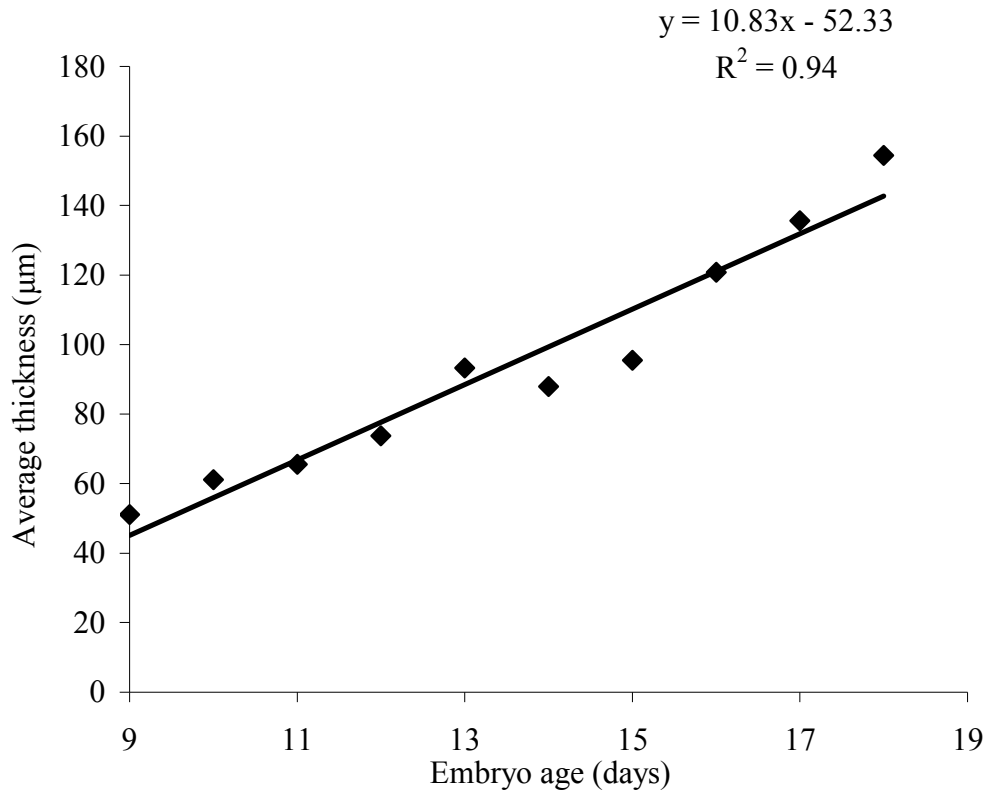

Figure 53. Average thickness of CAM at different embryo age (n = 3)

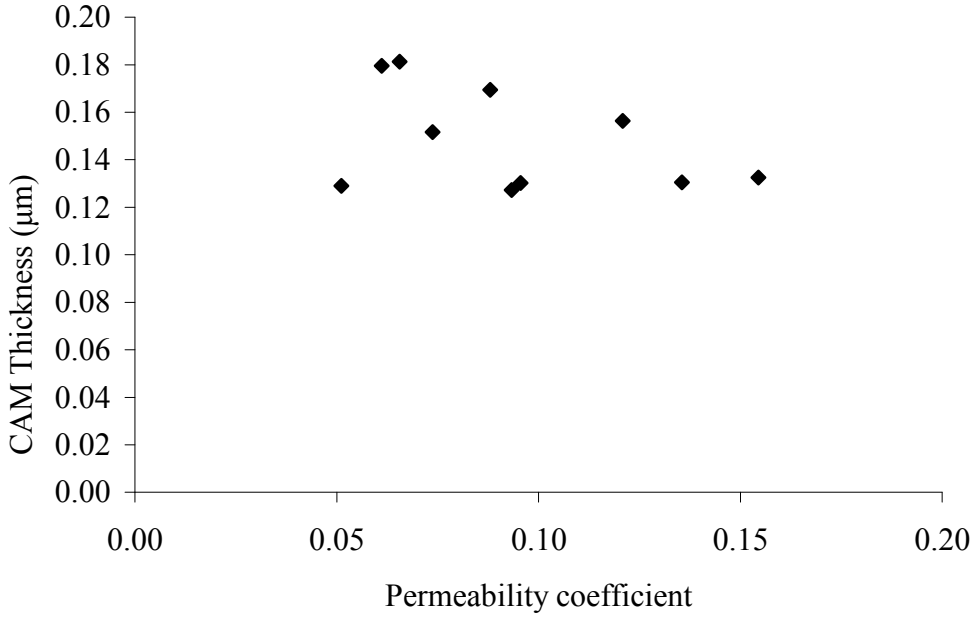

Figure 54. Relationship between CAM thickness and permeability coefficient

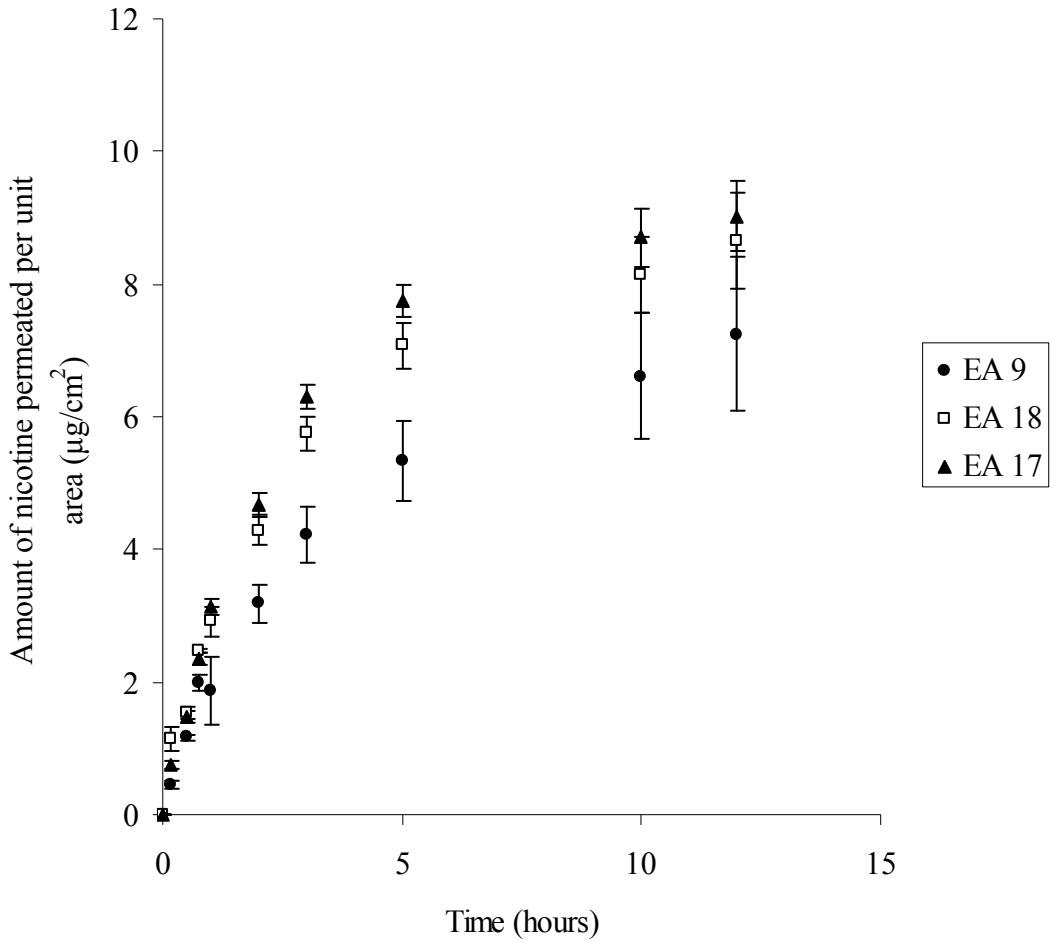

Figure 55. Permeation profiles of nicotine through CAM of different EA (n = 3)

through the CAM. The properties of fresh CAM, in comparison with the other biological membranes, will be discussed in subsequent sections.

The CAM consists of three layers as mentioned in the introduction. The ectoderm, mesoderm and endoderm, which grow at different rates and exhibit different morphological characteristics. The ectoderm is made up of a majority of cuboidal cells while the mesoderm is composed of a matrix which consists of blood vessels and cells with fibrillar material. The endoderm consists of squamous and cuboidal cells. As the egg matures, these cells change to columnar type and large intercellular spaces

appear after EA 16. Light and electron microscopy have shown the ectoderm layer to be the densest with the most closely packed cells. Hence, it is likely that the greatest barrier to permeation through the CAM would be the ectoderm layer. After EA 10, the ectoderm proliferates non-uniformly until it is at least 8 cells thick. It reaches a maximum thickness at EA 14 and disappears after EA 15. As such, gradual decrease in K_p value after EA 10 and minimum K_p value at EA 14 would be expected.

According to the results, the change in K_p values with embryo age could be roughly accounted by the morphological change of the ectoderm (Table 13). The K_p value of fresh CAM was seen to decrease after EA 10 and reaches a minimum at EA 13 before increasing at EA 14, decreasing at EA 15 before increasing again at EA 16 and finally reaching a plateau at EA17 and EA 18 (Figure 56). However, the K_p values from EA 15 to EA 18 can almost be regarded as similar because of the overlapping standard error. The slight deviation from the expected trend showed that the mesoderm and endoderm also affected the permeation of nicotine, but to a smaller extent. There was an increase in the endothelium of the larger vessels in the mesoderm after EA 15 (Romanoff, 1960, Shumko et al., 1988). This increase in endothelium, which may pose a barrier to permeation could account for the lower K_p values after EA 14 instead of the expected increase.

The K_p of nicotine for each EA of fresh and frozen CAM as well as that for pig skin, snake skin, pig buccal mucosa and pig retina tissue was calculated from the flux values obtained (Table 13).

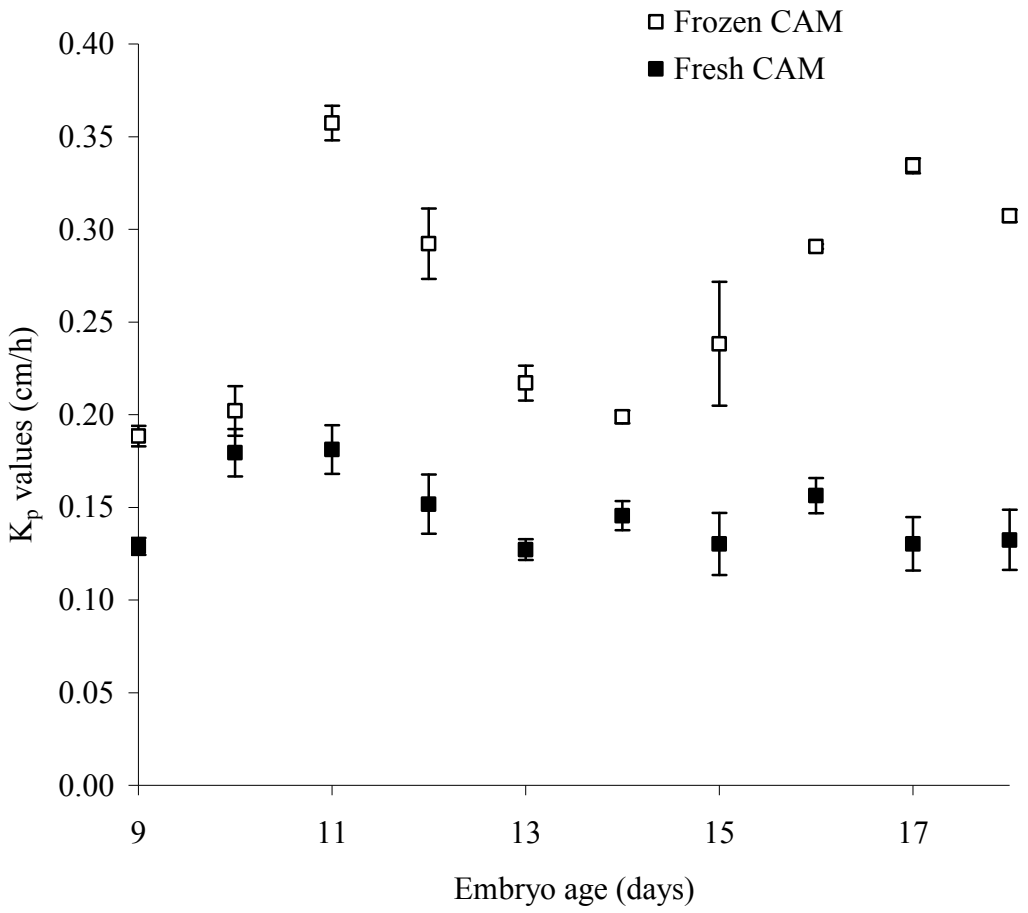

Figure 56. Plots of EA versus K_p for nicotine through frozen and fresh CAMs (n = 3)

G.3.iii. Frozen CAM

Permeation study was also conducted using frozen CAM of EA 9 to EA 18 so as to investigate the effect of freezing on the permeability profile of nicotine through the CAM. The permeability profile of nicotine through the frozen CAM is shown in Figure 52. In comparison with the permeability profile of freshly harvested CAM, the amount that eventually permeated through the frozen CAM is higher.

The plot of K_p versus EA is shown in Figure 56 for fresh CAM and frozen CAM. Irrespective of the embryo age, the shapes of both graphs are roughly similar.

The K_p values of frozen CAM are higher than the values obtained for fresh CAM. Statistically significant differences in flux values between fresh and frozen porcine buccal mucosa were also reported (Van Eyk and Van der Biijl, 2006). Freezing has been found to cause an increase in permeability through the skin. This is a result of the formation of ice crystals from water in the skin as well as disorganization of lipids that damages the keratinocytes and the lipid matrix of the rate – limiting stratum corneum (Ahlstrom et al., 2007, Babu et al., 2003, Kemppainen et al., 1986, Swarbrick et al., 1982). Mechanical damage and osmotic effects have also been proposed as possible mechanisms of destruction (Schafer and Kaufmann, 1999). These changes to the diffusion pathway would result in an increase in the permeability of the skin, affecting the pathways through which the drugs pass through. Similar effects are likely to occur to other tissues.

Hence, freezing should be avoided so as to prevent formation of ice crystals and changes to lipid structure of the CAM. However, fresh CAM, especially those of specific EA, may not be readily available. In the event that frozen CAM is used, the results should be interpreted appropriately with respect to the trends seen with frozen CAM.

G.3.iv. Pig skin

Pig skin is regarded as one of the most well-suited animal models for human skin (Barbero and Frasch, 2009, Lin et al., 1992). The K_p value obtained for pig skin was similar to that obtained from previous studies which compared pig skin to human skin (Maibach and Bronaugh, 2002). The permeation profile of nicotine through pig skin shows that the total amount of permeated nicotine was lower than that of fresh and

frozen CAM. In addition, it took a longer time for nicotine to reach a plateau in pig skin as compared to the CAM (Figure 52). These K_p values of the pig skin were significantly lower than those of fresh and frozen CAMs but similar to the K_p value of 0.0039 cm/h for human skin (Berner et al., 1992). This indicates that the permeation profile through pig skin resembles that of human skin, but not the CAM. Hence, the CAM would not be suitable as a skin model. The metabolizing capabilities of the skin is largely attributed to the viable epidermis (Zwadlo-Klarwasser et al., 2001). In this case, the pig skin was frozen prior to use and the tissue was not viable, hence metabolism of nicotine could not have occurred. The stratum corneum is 13 - 17 μm thick, consisting of 10 – 20 layers of keratin rich corneocytes and lipid layers. The corneocytes are embedded in an extracellular lipid matrix that is arranged in an orderly manner. This complex arrangement of corneocytes and lipids is referred to as the brick and mortar model and accounts for the main barrier to drug permeation through the skin. (Dupuis et al., 1984). In addition, a full thickness specimen of pig skin was used. The presence of the stratum corneum in the pig skin could have posed a permeation barrier and accounted for the significantly lower amount of nicotine that permeated through as compared to the CAM which does not possess a stratum corneum.

G.3.v. Snake skin

A slower rate of permeation of nicotine was observed, which is in agreement with the findings from a previous study (Pongjanyakul et al., 2002). This demonstrates the reproducibility of permeation experiments through snake skin. The K_p value of the snake skin was significantly lower than those of the fresh and frozen CAMs but higher than that of pig skin. Snake skin is easily available without causing harm to the

snake as a relatively large amount of skin is shed from the same snake periodically. Shed snake skin consists of 3 layers of non-living pure stratum corneum that do not contain hair follicles. It has a beta keratin rich outermost layer, alpha keratin and lipid rich intermediate mesos layer and finally an alpha keratin rich innermost layer. It is the intermediate mesos layer, which has three to five layers of cornified cells enclosed by intercellular lipids that accounts for the similarity to human stratum corneum. The stratum corneum components such as glycosphinolipids and ceramides, as well as the vascular structures and collageneous connective tissues are similar in both snake and human skin (Godin and Touitou, 2007). Snake skin has been used as a model for human skin due to its similarity to the stratum corneum of the human skin (Takahashi and Rytting, 2001). However, the absence of hair follicles accounts for snake skin being less permeable than human skin because hair follicles contribute to an increase in permeability (Barbero and Frasch, 2009). The K_p value of snake skin is higher than that of pig skin. The stratum corneum layer in pig skin (26.4 ± 0.4 μm) is thicker compared to the stratum corneum in the snake skin (10 - 20 μm) (Maibach and Bronaugh, 2002, Itoh et al., 1990). Hence, the difference in permeability of the snake skin and pig skin may be due to the thicker stratum corneum in pig skin. Therefore, snake skin may not be a suitable model for human skin.

G.3.vi. Retina tissue

The organs and membranes of pigs have been considered structurally similar to human parts. The permeation profile of nicotine through retina tissue showed that the total amount of permeated nicotine was significantly higher than that of fresh and frozen CAM. The average K_p value of the retina was significantly higher than those of fresh and frozen CAM. Some of the retina samples still retained the pigments at the

time of experimentation. The retinal pigment epithelium and endothelial membrane of the retinal vessels possess tight junctions that are non-leaky (Cunhavaz, 1980). The CAM is of comparable thickness to human retina, which is approximately 100 – 300 μm. Furthermore, the tissue responses of *in vitro* CAM have been found to be similar to *in vivo* rabbit retina (Leng et al., 2004). The preparation process was tedious and required careful handling as the retina is a very delicate piece of tissue. There could have been holes in the retina tissue that resulted from the preparation procedure that were not visible to the naked eye. The presence of holes could have lead to a higher K_p value as compared to the other biological membranes as well as higher standard error values. However, it is more likely that the absence of the retinal pigmented epithelium was responsible for the higher K_p value. The retinal pigmented epithelium exhibits tight junctions which form a barrier to molecules into the retina (Duvvuri et al., 2003). The process of removing the retina and soaking it in isotonic phosphate buffer resulted in the loss of the retinal pigmented epithelium. Hence, more nicotine was able to permeate through the piece of retina, resulting in a higher K_p value.

G.3.vii. Buccal mucosa

The permeation profile of nicotine through pig buccal mucosa showed that the total amount of nicotine that permeated through the buccal mucosa was higher than those through fresh CAM. However, the K_p values of the buccal mucosa and fresh CAM were comparable. The pig buccal mucosa in this study has been found to be 44 times more permeable than the pig skin, which is widely used as a human skin model. The buccal mucosa is suitable for the delivery of macromolecules and hydrophilic compounds (Tanojo et al., 1999). The pig buccal mucosa was chosen as an alternative to human buccal mucosa because of the similarities in structure. Rabbit buccal

mucosa is the closest to human buccal mucosa in terms of structure. However, keratinization occurs in the rabbit tissue in patchy areas. This leads to limited areas available for permeation studies. Hamster buccal epithelium is also another viable option, however the available area for experimentation is too small (Tavakoli-Saberi and Audus, 1989). The next best option is pig buccal mucosa. Pig buccal mucosa is the most commonly used model for human buccal mucosa to date due to its availability and low cost (Obradovic and Hidalgo, 2008). The presence of membrane coating granules located in the upper third portion of the epithelium has been attributed to causing the permeability barrier in oral mucosa. The pH of the phosphate buffer in the Franz diffusion cell is also similar to the pH of saliva which ranges from 5.5 to 8 depending on the flow rate of saliva (Shojaei, 1998). Human buccal tissue allows only a few milligrams of drug to pass through (Zhang et al., 2002) and in this respect, the permeation profile through pig buccal mucosa is similar to that of human buccal tissue. Studies with nicotine have shown that nicotine from chewing gum reaches a peak plasma concentration at 30 minutes after the gum is first chewed. In this study, nicotine reached peak amount permeated through at close to 30 minutes. Drug is presumed to pass through human buccal mucosa through the paracellular and transcellular routes particularly for hydrophilic and hydrophobic compounds respectively. Since nicotine is hydrophilic, the passage of nicotine through the CAM could potentially be through the paracellular route and by passive diffusion (Adrian et al., 2006). Although the average thickness of the buccal mucosa is 500 – 600 μm, and much thicker than the CAM (Nicolazzo and Finnin, 2008), the similarity between CAM and buccal mucosa permeation profile paves the possibility of the CAM being used as a substitute for human buccal mucosa instead of pig buccal mucosa. Cell cultures of human buccal mucosa are available but limited information and studies

have been done on them. The prospect of the CAM being a human buccal model has many advantages over the pig buccal mucosa. There is the possibility of tissue damage to the buccal mucosa that may occur when the pig masticates and accidentally bites the buccal mucosa. The CAM is kept in a protected environment in the egg away from physical assaults from the environment. Tissue acquisition from pigs is also a more laborious and time intensive procedure as opposed to harvesting the CAM. More costs are incurred with the maintenance of pigs to suitable age for experimentation and also to sacrifice them in a humane manner. Most importantly, there is the lack of ethical issues surrounding the use of CAM that are less than EA 10 in age.

G.4. GTN

The similarity between the CAM and buccal mucosa provided the impetus to investigate the permeation profile of a drug commonly used on the buccal mucosa. The most commonly used drug for buccal delivery is GTN for rapid treatment of acute attacks of angina pectoris. GTN is employed as a sublingual tablet administered to the surface of the buccal mucosa. The blood perfusion studies have indicated that the formulation additives present in GTN tablets may be an influencing factor. Hence, the injection form was used in a bid to overcome the formulation effects.

The HPLC standards of GTN were problematical. The limit of detection of GTN with the HPLC was higher than the amount of GTN present in the samples withdrawn from the Franz cell. The limiting factor was the maximum concentration of the stock GTN solution that was added to the CAM surface when it was introduced into the donor compartment of the Franz cell. Such analytical difficulties with regards to the

detection of GTN have been documented (Cossum and Roberts, 1985). GTN solutions could not be reconstituted as GTN was not available in powder form as it is considered to be an explosive and its import and sale are highly controlled.

The results from this study shows that the CAM *in vivo* model is still more sensitive that the *in vitro* model. The topical application of GTN on the CAM demonstrated changes in blood perfusion and vessel diameter studies. The CAM is able to detect the minute concentration of GTN that was not detectable with HPLC. The CAM tissue was used fresh after being sacrificed. Hence, the CAM tissue could have still been viable in the early part of the study. GTN has been reported to be metabolized by epidermal enzymes into 1,2 – and 1,3 – glyceryldinitrate metabolites (Higo et al., 1992). This could indicate the presence of enzymes in the CAM that could have depleted the amount of GTN to low levels that was not accurately detected with HPLC. In the *in vivo* studies, it was possible that either the blood perfusion and vessel diameter responses occurred before the metabolism of GTN or that metabolism did occur but therapeutically sufficient levels of GTN were still present to induce vessel diameter and blood perfusion changes in the CAM.

In summary, the application of the CAM has been shown to be most suitable for use as a model for the pig buccal biological membrane in the assessment of drug permeation. As pig buccal mucosa is commonly used as a model for human buccal mucosa, it would thus be feasible that the CAM may be employed to mimic human buccal mucosa.

CONCLUSIONS

CONCLUSIONS

The aim of this project was to develop an alternative *in vivo / in vitro* model for assessing drug absorption in pharmaceutical product development.

The CAM was employed successfully as a screening tool for irritation effects. Thus, it was able to screen for suitable drugs and solvents to be used in subsequent blood perfusion and diameter measurements.

Two imaging based-*in vivo* CAM models that involved blood perfusion and vessel dimensions of the CAM were developed. The CAM was successfully prepared by a partial deshelling method. The age of the CAM was an important consideration as it was harder to perform the deshelling process with older embryos. Younger embryos were prone to succumbing after the deshelling process. Diameters of the CAM blood vessels could be measured accurately using high resolution video imaging and image analysis system with customized software. Blood perfusion of the CAM could be measured by the non-invasive LDPI method rapidly. The readings were significantly affected by amplitude and threshold. The relationships of blood perfusion and vessel size with drug concentration were generally complex due to auto-regulation mechanisms. Change in vessel size was a better indication of drug absorption than blood perfusion.

The CAM was also evaluated as an *in vitro* model for drug permeation using the Franz diffusion cell. The CAM was easily removed from the egg at EA 13. The frozen CAM was more permeable than the fresh CAM. The CAM was also most similar to the buccal mucosa as opposed to skin or retina tissue in terms of permeation profile

and permeability coefficient values. Hence, the CAM shows promise and potential as as an *in vitro* buccal model. It is also potentially useful as a "live" *in vivo* model for assessing formulations and drug absorption for buccal delivery.

Further studies using formulation variables are recommended to verify this model established. However, this is beyond the time available for this current work.

REFERENCES

Abou-Mohamed, G., Kaesemeyer, W. H., Caldwell, R. B. & Caldwell, R. W. (2000) Role of L-arginine in the vascular actions and development of tolerance to nitroglycerin. *Br J Pharmacol,* 130**,** 211-8.

Addicott, M. A., Yang, L. L., Peiffer, A. M., Burnett, L. R., Burdette, J. H., Chen, M. Y., Hayasaka, S., Kraft, R. A., Maldjian, J. A. & Laurienti, P. J. (2009) The effect of daily caffeine use on cerebral blood flow: How much caffeine can we tolerate? *Hum Brain Mapp,* 30**,** 3102-14.

Adrian, C. L., Olin, H. B., Dalhoff, K. & Jacobsen, J. (2006) In vivo human buccal permeability of nicotine. *Int J Pharm,* 311**,** 196-202.

Ahlstrom, L. A., Cross, S. E. & Mills, P. C. (2007) The effects of freezing skin on transdermal drug penetration kinetics. *J Vet Pharmacol Ther,* 30**,** 456-63.

Akomeah, F. K., Martin, G. P. & Brown, M. B. (2007) Variability in human skin permeability in vitro: Comparing penetrants with different physicochemical properties. *Journal of Pharmaceutical Sciences,* 96**,** 824-834.

Allen, D. D., Caviedes, R., Caedenas, A. M., Shimahara, T., Segura-Aguilar, J. & Caviedes, P. A. (2008) Cell lines as in vitro models for drug screening and toxicity studies (vol 31, pg 757, 2005). *Drug Development and Industrial Pharmacy,* 34**,** 234-234.

Allen, D. D., Caviedes, R., Cardenas, A. M., Shimahara, T., Segura-Aguilar, J. & Caviedes, P. A. (2005) Cell lines as in vitro models for drug screening and toxicity studies. *Drug Development and Industrial Pharmacy,* 31**,** 757-768.

Alsenz, J. & Haenel, E. (2003) Development of a 7-day, 96-well Caco-2 permeability assay with high-throughput direct UV compound analysis. *Pharmaceutical Research,* 20**,** 1961-1969.

Altura, B. M., Altura, B. T. & Gebrewold, A. (1983) Alcohol-Induced Spasms of Cerebral Blood-Vessels - Relation to Cerebrovascular Accidents and Sudden-Death. *Science,* 220**,** 331-333.

Altura, B. M., Ogunkoya, A., Gebrewold, A. & Altura, B. T. (1979) Effects of ethanol on terminal arterioles and muscular venules: direct observations on the microcirculation. *J Cardiovasc Pharmacol,* 1**,** 97-113.

Andrews, K., Baranowski, A. & Kinnman, E. (1999) Sensory threshold changes without initial pain or alterations in cutaneous blood flow, in the area of secondary hyperalgesia caused by topical application of capsaicin in humans. *Neurosci Lett,* 266**,** 45-8.

Arildsson, M., Asker, C. L., Salerud, E. G. & Stromberg, T. (2000a) Skin capillary appearance and skin microvascular perfusion due to topical application of analgesia cream. *Microvasc Res,* 59**,** 14-23.

Arildsson, M., Nilsson, G. E. & Stromberg, T. (2000b) Effects on skin blood flow by provocation during local analgesia. *Microvasc Res,* 59**,** 122-30.

Audus, K. L., Bartel, R. L., Hidalgo, I. J. & Borchardt, R. T. (1990) The Use of Cultured Epithelial and Endothelial-Cells for Drug Transport and Metabolism Studies. *Pharmaceutical Research,* 7**,** 435-451.

Aulton, M. E. (2001) *Pharmaceutics : the science of dosage form design,* Edinburgh ; New York :, Churchill Livingstone.

Ausprunk, D. H., Knighton, D. R. & Folkman, J. (1974) Differentiation of vascular endothelium in the chick chorioallantois: a structural and autoradiographic study. *Dev Biol,* 38**,** 237-48.

Avila, C. P., Jr., Bartsch, D. U., Bitner, D. G., Cheng, L., Mueller, A. J., Karavellas, M. P. & Freeman, W. R. (1998) Retinal blood flow measurements in branch retinal vein occlusion using scanning laser Doppler flowmetry. *Am J Ophthalmol,* 126**,** 683-90.

Babu, R. J., Kanikkannan, N., Kikwai, L., Ortega, C., Andega, S., Ball, K., Yim, S. & Singh, M. (2003) The influence of various methods of cold storage of skin on the permeation of melatonin and nimesulide. *Journal of Controlled Release,* 86**,** 49-57.

Balls, M. (2009) Animal experimentation and the Three Rs: time for honest answers to some leading questions. *Altern Lab Anim,* 37**,** 229-32.

Barbero, A. M. & Frasch, H. F. (2009) Pig and guinea pig skin as surrogates for human in vitro penetration studies: A quantitative review. *Toxicology in Vitro,* 23**,** 1-13.

Bartholomew, R. B. & Crawley, F. E. (1980) *Science Laboratory Techniques,* United States of America, Addison-Weseley Publishing Company.

Bath, P. M. (2004) Theophylline, aminophylline, caffeine and analogues for acute ischaemic stroke. *Cochrane Database Syst Rev***,** CD000211.

Beetge, E., Du Plessis, J., Muller, D. G., Goosen, C. & Van Rensburg, F. J. (2000) The influence of the physicochemical characteristics and pharmacokinetic properties of selected NSAID's on their transdermal absorption. *Int J Pharm,* 193**,** 261-4.

Berardesca, E., Elsner, P. & Maibach, H. I. (1995) *Bioengineering of the skin: cutaneous blood flow and erthyema,* Boca Raton, CRC Press.

Berner, B., Mazzenga, G. C., Gargiulo, P. M. & Steffens, R. (1992) A transdermal nicotine system: feasibility studies. *Journal of Controlled Release,* 20**,** 13-19.

Bhogal, N. (2009) 21st century drug development: advances, opportunities and challenges. *Altern Lab Anim,* 37**,** 335-9.

Binzoni, T., Leung, T. S., Boggett, D. & Delpy, D. (2003) Non-invasive laser Doppler perfusion measurements of large tissue volumes and human skeletal muscle blood RMS velocity. *Phys Med Biol,* 48**,** 2527-49.

Bircher, A. J. (1995) Laser Doppler Measurement of Skin Blood Flux: Variation and Validation. IN SERUP, J. & JEMEC, B. E. (Eds.) *Handbook of non-invasive methods and the skin.* Florida, CRC Press.

Bjarnason, B., Flosadottir, E. & Fischer, T. (1999) Objective non-invasive assessment of patch tests with the laser Doppler perfusion scanning technique. *Contact Dermatitis,* 40**,** 251-60.

Borges, J., Tegtmeier, F. T., Padron, N. T., Mueller, M. C., Lang, E. M. & Stark, G. B. (2003) Chorioallantoic membrane angiogenesis model for tissue engineering: a new twist on a classic model. *Tissue Eng,* 9**,** 441-50.

Bornmyr, S., Castenfors, J., Evander, E., Olsson, G., Hjortsberg, U. & Wollmer, P. (2001) Effect of local cold provocation on systolic blood pressure and skin blood flow in the finger. *Clinical Physiology,* 21**,** 570-575.

Boyle, M. J. (2007) A dramatic drop in blood pressure following prehospital GTN administration. *Emerg Med J,* 24**,** 225-6.

Brain, K. R., Green, D. M., Dykes, P. J., Marks, R. & Bola, T. S. (2006) The role of menthol in skin penetration from topical formulations of ibuprofen 5% in vivo. *Skin Pharmacology and Physiology,* 19**,** 17-21.

Brand, M., Lamande, N., Larger, E., Corvol, P. & Gasc, J. M. (2006) Angiotensinogen impairs angiogenesis in the chick chorioallantoic membrane. *J Mol Med*.

Brantner, A. H., Quehenberger, F., Chakraborty, A., Polligger, J., Sosa, S. & Della Loggia, R. (2002) HET-CAM bioassay as in vitro alternative to the croton oil test for investigating steroidal and non-steroidal compounds. *Altex,* 19**,** 51-6.

Bray, R., Forrester, K., Leonard, C., Mcarthur, R., Tulip, J. & Lindsay, R. (2003) Laser Doppler imaging of burn scars: a comparison of wavelength and scanning methods. *Burns,* 29**,** 199-206.

Broekhuizen, M. L. A., Bouman, H. G. A., Mast, F., Mulder, P. G., Groot, A. C. G.-D. & Wladimiroff, J. W. (1995) Hemodynamic Changes in HH Stage 34 Chick Embryos after Treatment with All-*trans*-retinoic Acid. *Pediatric Research,* 38**,** 342 - 348.

Burton, F. G. & Tullett, S. G. (1985) Respiration of avian embryos. *Comparative Biochemistry and Physiology Part A: Physiology,* 82**,** 735-744.

Cai, H., Stoner, C., Reddy, A., Freiwald, S., Smith, D., Winters, R., Stankovic, C. & Surendran, N. (2006) Evaluation of an integrated in vitro-in silico PBPK (physiologically based pharmacokinetic) model to provide estimates of human bioavailability. *Int J Pharm,* 308**,** 133-9.

Calabrese, E. J. (2008) Hormesis and medicine. *Br J Clin Pharmacol,* 66**,** 594-617.

Calabrese, E. J. (2009) Getting the dose-response wrong: why hormesis became marginalized and the threshold model accepted. *Arch Toxicol,* 83**,** 227-47.

Calabrese, E. J. & Baldwin, L. A. (2003) The hormetic dose-response model is more common than the threshold model in toxicology. *Toxicol Sci,* 71**,** 246-50.

Carlson, B. E., Arciero, J. C. & Secomb, T. W. (2008) Theoretical model of blood flow autoregulation: roles of myogenic, shear-dependent, and metabolic responses. *American Journal of Physiology-Heart and Circulatory Physiology,* 295**,** H1572-H1579.

Charkoudian, N. (2003) Skin blood flow in adult human thermoregulation: How it works, when it does not, and why. *Mayo Clinic Proceedings,* 78**,** 603-612.

Chen, Z., Milner, T. E., Wang, X., Srinivas, S. & Nelson, J. S. (1998) Optical Doppler tomography: imaging in vivo blood flow dynamics following pharmacological intervention and photodynamic therapy. *Photochem Photobiol,* 67**,** 56-60.

Chernyavsky, I. L., Jensen, O. E. & Leach, L. (2010) A mathematical model of intervillous blood flow in the human placentone. *Placenta,* 31**,** 44-52.

Chin, W., Lau, W., Lay, S. L., Wei, K. K. & Olivo, M. (2004) Photodynamic-induced vascular damage of the chick chorioallantoic membrane model using perylenequinones. *Int J Oncol,* 25**,** 887-91.

Clough, G. & Gush, R. (2009) Is it important to model the impact of blood flow on the dose of drugs delivered transcutaneously? *J Vasc Res,* 46**,** 267-9.

Cobb, G. P., Bargar, T. A., Pepper, C. B., Norman, D. M., Houlis, P. D. & Anderson, T. A. (2003) Using chorioallantoic membranes for non-lethal assessment of persistent organic pollutant exposure and effect in oviparous wildlife. *Ecotoxicology,* 12**,** 31-45.

Conti, C. R., Feldman, R. L., Pepine, C. J., Hill, J. A. & Conti, J. B. (1983) Effect of glyceryl trinitrate on coronary and systemic hemodynamics in man. *Am J Med,* 74**,** 28-32.

Cossum, P. A. & Roberts, M. S. (1985) Nitroglycerin Disposition in Human-Blood. *European Journal of Clinical Pharmacology,* 29**,** 169-175.

Cryan, S. A., Sivadas, N. & Garcia-Contreras, L. (2007) In vivo animal models for drug delivery across the lung mucosal. *Advanced Drug Delivery Reviews,* 59**,** 1133-1151.

Cunhavaz, J. G. (1980) Blood-Retinal Barriers in Health and Disease. *Transactions of the Ophthalmological Societies of the United Kingdom,* 100**,** 337-340.

Curren, R. D. & Harbell, J. W. (2002) Ocular safety: a silent (in vitro) success story. *Altern Lab Anim,* 30 Suppl 2**,** 69-74.

Czernin, J. & Waldherr, C. (2003) Cigarette smoking and coronary blood flow. *Progress in Cardiovascular Diseases,* 45**,** 395-404.

Dash, A. K., Miller, D. W., Huai-Yan, H., Carnazzo, J. & Stout, J. R. (2001) Evaluation of creatine transport using Caco-2 monolayers as an in vitro model for intestinal absorption. *Journal of Pharmaceutical Sciences,* 90**,** 1593-1598.

Daston, G. P. & Mcnamee, P. (2005) Alternatives to Toxicity Testing in Animals: Challenges and Opportunities.

Davis, G. & Johns, E. J. (1990) The effect of angiotensin II and vasopressin on renal haemodynamics. *J Med Eng Technol,* 14**,** 197-200.

Dayal, P., Pillay, V., Babu, R. J. & Singh, M. (2005) Box-Behnken experimental design in the development of a nasal drug delivery system of model drug hydroxyurea: Characterization of viscosity, in vitro drug release, droplet size, and dynamic surface tension. *Aaps Pharmscitech,* 6.

Debbasch, C., Ebenhahn, C., Dami, N., Pericoi, M., Van Den Berghe, C., Cottin, M. & Nohynek, G. J. (2005) Eye irritation of low-irritant cosmetic formulations: correlation of in vitro results with clinical data and product composition. *Food Chem Toxicol,* 43**,** 155-65.

Defouw, D. O., Rizzo, V. J., Steinfeld, R. & Feinberg, R. N. (1989) Mapping of the microcirculation in the chick chorioallantoic membrane during normal angiogenesis. *Microvasc Res,* 38**,** 136-47.

Dias, M., Farinha, A., Faustino, E., Hadgraft, J., Pais, J. & Toscano, C. (1999) Topical delivery of caffeine from some commercial formulations. *International Journal of Pharmaceutics,* 182**,** 41-47.

Dimitropoulou, C., Malkusch, W., Fait, E., Maragoudakis, M. E. & Konerding, M. A. (1998) The vascular architecture of the chick chorioallantoic membrane: sequential quantitative evaluation using corrosion casting. *Angiogenesis,* 2**,** 255-63.

Donos, N., D'aiuto, F., Retzepi, M. & Tonetti, M. (2005) Evaluation of gingival blood flow by the use of laser Doppler flowmetry following periodontal surgery. A pilot study. *J Periodontal Res,* 40**,** 129-37.

Drenkhahn, M., Gescher, D. M., Wolber, E. M., Meyhoefer-Malik, A. & Malik, E. (2004) Expression of angiopoietin 1 and 2 in ectopic endometrium on the chicken chorioallantoic membrane. *Fertil Steril,* 81 Suppl 1**,** 869-75.

Dressman, J. B., Thelen, K. & Jantratid, E. (2008) Towards quantitative prediction of oral drug absorption. *Clinical Pharmacokinetics,* 47**,** 655-667.

Droog, E. J., Steenbergen, W. & Sjoberg, F. (2001) Measurement of depth of burns by laser Doppler perfusion imaging. *Burns,* 27**,** 561-8.

Dunn, L. K., Gruenloh, S. K., Dunn, B. E., Reddy, D. S., Falck, J. R., Jacobs, E. R. & Medhora, M. (2005) Chick chorioallantoic membrane as an in vivo model to study vasoreactivity: characterization of development-dependent hyperemia induced by epoxyeicosatrienoic acids (EETs). *Anat Rec A Discov Mol Cell Evol Biol,* 285**,** 771-80.

Dupuis, D., Rougier, A., Roguet, R., Lotte, C. & Kalopissis, G. (1984) In vivo relationship between horny layer reservoir effect and percutaneous absorption in human and rat. *J Invest Dermatol,* 82**,** 353-6.

Duvvuri, S., Majumdar, S. & Mitra, A. K. (2003) Drug delivery to the retina: challenges and opportunities. *Expert Opin Biol Ther,* 3**,** 45-56.

Engels, H. J., Wirth, J. C., Celik, S. & Dorsey, J. L. (1999) Influence of caffeine on metabolic and cardiovascular functions during sustained light intensity cycling and at rest. *Int J Sport Nutr,* 9**,** 361-70.

Ernest, J. T. (1980) Blood-Flow in Normal and Abnormal Retinal-Vessels. *Transactions of the Ophthalmological Societies of the United Kingdom,* 100**,** 343-345.

Farah, A. E. (1983) Glucagon and the circulation. *Pharmacol Rev,* 35**,** 181-217.

Ferrell, W. R., Balint, P. V. & Sturrock, R. D. (2000) Novel use of laser Doppler imaging for investigating epicondylitis. *Rheumatology (Oxford),* 39**,** 1214-7.

Festing, S. (2008) Animal experimentation: the need for deliberation and challenge. *Altern Lab Anim,* 36**,** 1-4.

Fitzgerald, M. E., Wildsoet, C. F. & Reiner, A. (2002) Temporal relationship of choroidal blood flow and thickness changes during recovery from form deprivation myopia in chicks. *Exp Eye Res,* 74**,** 561-70.

Flick, B., Talsness, C. E., Jackh, R., Buesen, R. & Klug, S. (2009) Embryotoxic potential of N-methyl-pyrrolidone (NMP) and three of its metabolites using the rat whole embryo culture system. *Toxicol Appl Pharmacol,* 237**,** 154-67.

Flyckt, V. M. M., Raaymakers, B. W. & Lagendijk, J. J. W. (2006) Modelling the impact of blood flow on the temperature distribution in the human eye and the orbit: fixed heat transfer coefficients versus the Pennes bioheat model versus discrete blood vessels. *Physics in Medicine and Biology,* 51**,** 5007-5021.

Forough, R., Wang, X., Martinez-Lemus, L. A., Thomas, D., Sun, Z., Motamed, K., Parker, J. L. & Meininger, G. A. (2003) Cell-based and direct gene transfer-induced angiogenesis via a secreted chimeric fibroblast growth factor-1 (sp-FGF-1) in the chick chorioallantoic membrane (CAM). *Angiogenesis,* 6**,** 47-54.

Forough, R., Weylie, B., Patel, C., Ambrus, S., Singh, U. S. & Zhu, J. (2005) Role of AKT/PKB signaling in fibroblast growth factor-1 (FGF-1)-induced angiogenesis in the chicken chorioallantoic membrane (CAM). *J Cell Biochem,* 94**,** 109-16.

Freccero, C., Holmlund, F., Bornmyr, S., Castenfors, J., Johansson, A. M., Sundkvist, G., Svensson, H. & Wollmer, P. (2003) Laser Doppler perfusion monitoring of skin blood flow at different depths in finger and arm upon local heating. *Microvasc Res,* 66**,** 183-9.

Fuchs, A. & Lindenbaum, E. S. (1988) The two- and three-dimensional structure of the microcirculation of the chick chorioallantoic membrane. *Acta Anat (Basel),* 131**,** 271-5.

Fulcher, S. M., Koman, L. A., Smith, B. P., Holden, M. & Smith, T. L. (1998) The effect of transdermal nicotine on digital perfusion in reformed habitual smokers. *J Hand Surg [Am],* 23**,** 792-9.

Fuller, V. J. & Kolb, R. W. (1968) Comparison of titrations on the chorioallantoic membrane of chick embryos with the rabbit scarification technique for the potency assay of smallpox vaccines. *Appl Microbiol,* 16**,** 458-62.

Fullerton, A., Rode, B. & Serup, J. (2002a) Skin irritation typing and grading based on laser Doppler perfusion imaging. *Skin Res Technol,* 8**,** 23-31.

Fullerton, A., Rode, B. & Serup, J. (2002b) Studies of cutaneous blood flow of normal forearm skin and irritated forearm skin based on high-resolution laser Doppler perfusion imaging (HR-LDPI). *Skin Res Technol,* 8**,** 32-40.

Gabrielli, M. G., Cox, J. V., Materazzi, G. & Menghi, G. (2004) Cell type-specific and developmentally regulated expression of the AE1 anion exchanger in the chicken chorioallantoic membrane. *Histochem Cell Biol,* 121**,** 189-99.

Gabrielli, M. G., Materazzi, G., Bondi, A. M. & Menghi, G. (2003) Developmental expression of glycocomponents in the chick chorioallantoic membrane. *Anat Embryol (Berl),* 207**,** 63-71.

Galanzha, E. I., Tuchin, V. V. & Zharov, V. P. (2007) Advances in small animal mesentery models for in vivo flow cytometry, dynamic microscopy, and drug screening. *World J Gastroenterol,* 13**,** 192-218.

Gigli, I., Cushman, R. A., Wahl, C. M. & Fortune, J. E. (2005) Evidence for a role for anti-Mullerian hormone in the suppression of follicle activation in mouse ovaries and bovine ovarian cortex grafted beneath the chick chorioallantoic membrane. *Mol Reprod Dev,* 71**,** 480-8.

Godin, B. & Touitou, E. (2007) Transdermal skin delivery: Predictions for humans from in vivo, ex vivo and animal models. *Advanced Drug Delivery Reviews,* 59**,** 1152-1161.

Goode, T. L. & Klein, H. J. (2002) Miniaturization: an overview of biotechnologies for monitoring the physiology and pathophysiology of rodent animal models. *Ilar J,* 43**,** 136-46.

Goon, A. T., Leow, Y. H., Chan, Y. H. & Goh, C. L. (2004) Correlation between laser Doppler perfusion imaging and visual scoring of patch test sites in subjects with experimentally induced allergic and irritant contact reactions. *Skin Res Technol,* 10**,** 64-6.

Gottfried, V., Davidi, R., Averguj, C. & Kimel, S. (1995) In vivo damage to chorioallantoic membrane blood vessels by porphycene-induced photodynamic therapy. *J Photochem Photobiol B,* 30**,** 115-21.

Gow, N. A., Knox, Y., Munro, C. A. & Thompson, W. D. (2003) Infection of chick chorioallantoic membrane (CAM) as a model for invasive hyphal growth and pathogenesis of Candida albicans. *Med Mycol,* 41**,** 331-8.

Grams, Y. Y., Whitehead, L., Cornwell, P. & Bouwstra, J. A. (2004) On-line visualization of dye diffusion in fresh unfixed human skin. *Pharmaceutical Research,* 21**,** 851-859.

Gush, R. J., Thompson, J. M. & Weiss, J. B. (1990) Measurement of blood flow in the chick egg yolk sac membrane. *J Med Eng Technol,* 14**,** 205-209.

Guyton, A. C. (2000) *Textbook of medical physiology,* Philadelphia :, Saunders.

Hadgraft, J. (1999) Passive enhancement strategies in topical and transdermal drug delivery. *International Journal of Pharmaceutics,* 184**,** 1-6.

Hahn, C. & Schwartz, M. A. (2009) Mechanotransduction in vascular physiology and atherogenesis. *Nat Rev Mol Cell Biol,* 10**,** 53-62.

Hahon, N. (1959) Survival of variola virus in chorioallantoic membrane preparations. *J Bacteriol,* 78**,** 731-3.

Hamburger, V. & Hamilton, H. L. (1992) A series of normal stages in the development of the chick embryo. 1951. *Dev Dyn,* 195**,** 231-72.

Hammer-Wilson, M. J., Cao, D., Kimel, S. & Berns, M. W. (2002) Photodynamic parameters in the chick chorioallantoic membrane (CAM) bioassay for photosensitizers administered intraperitoneally (IP) into the chick embryo. *Photochem Photobiol Sci,* 1**,** 721-8.

Handley, R. C., Essex, T. & Pooley, J. (1990) Laser Doppler flowmetry and bone blood flow in an isolated perfused preparation. *J Med Eng Technol,* 14**,** 201-4.

Harrison, D. K., Abbot, N. C., Beck, J. S. & Mccollum, P. T. (1993) A preliminary assessment of laser Doppler perfusion imaging in human skin using the tuberculin reaction as a model. *Physiol Meas,* 14**,** 241-52.

Hartley, T. R., Lovallo, W. R. & Whitsett, T. L. (2004) Cardiovascular effects of caffeine in men and women. *Am J Cardiol,* 93**,** 1022-6.

Haruyama, T. (2006) Cellular biosensing: chemical and genetic approaches. *Anal Chim Acta,* 568**,** 211-6.

Harvell, J. D. & Maibach, H. I. (1998) In vitro skin toxicity assays for predicting cosmetic-induced irritancy. IN BARAN, R. & MAIBACH, H. I. (Eds.) *Textbook of cosmetic dermatology.* United States of America Martin Dunitz.

Hidalgo, I. J. (2001) Assessing the absorption of new pharmaceuticals. *Curr Top Med Chem,* 1**,** 385-401.

Higo, N., Hinz, R. S., Lau, D. T. W., Benet, L. Z. & Guy, R. H. (1992) Cutaneous Metabolism of Nitroglycerin Invitro .1. Homogenized Versus Intact Skin. *Pharmaceutical Research,* 9**,** 187-191.

Hjortsjo, C., Saxegaard, E., Young, A. & Dahl, J. E. (2009) In vivo and in vitro irritation testing of low concentrations of hydrofluoric acid. *Acta Odontol Scand***,** 1-6.

Hochel, J., Akiyama, R., Masuko, T., Pearson, J. T., Nichelmann, M. & Tazawa, H. (1998) Development of heart rate irregularities in chick embryos. *Am J Physiol,* 275**,** H527-33.

Hoff, D. A., Gregersen, H. & Hatlebakk, J. G. (2009) Mucosal blood flow measurements using laser Doppler perfusion monitoring. *World J Gastroenterol,* 15**,** 198-203.

Hoffmann, K., Auer, T., Stucker, M., Hoffmann, A. & Altmeyer, P. (1998) Comparison of skin atrophy and vasoconstriction due to mometasone furoate, methylprednisolone and hydrocortisone. *J Eur Acad Dermatol Venereol,* 10**,** 137-42.

Hugger, E. D., Audus, K. L. & Borchardt, R. T. (2002) Effects of poly(ethylene glycol) on efflux transporter activity in Caco-2 cell monolayers. *Journal of Pharmaceutical Sciences,* 91**,** 1980-1990.

Humeau, A., Steenbergen, W., Nilsson, H. & Stromberg, T. (2007) Laser Doppler perfusion monitoring and imaging: novel approaches. *Med Biol Eng Comput,* 45**,** 421-35.

Ingels, F. M. & Augustijns, P. F. (2003) Biological, pharmaceutical, and analytical considerations with respect to the transport media used in the absorption screening system, Caco-2. *Journal of Pharmaceutical Sciences,* 92**,** 1545-1558.

Issachar, N., Gall, Y., Borrel, M. T. & Poelman, M. C. (1998) Correlation between percutaneous penetration of methyl nicotinate and sensitive skin, using laser Doppler imaging. *Contact Dermatitis,* 39**,** 182-6.

Itoh, T., Xia, J., Magavi, R., Nishihata, T. & Rytting, J. H. (1990) Use of Shed Snake Skin as a Model Membrane for Invitro Percutaneous Penetration Studies - Comparison with Human Skin. *Pharmaceutical Research,* 7**,** 1042-1047.

Jacobi, U., Kaiser, M., Koscielny, J., Schutz, R., Meinke, M., Sterry, W. & Lademann, J. (2006) Comparison of blood flow to the cutaneous temperature and redness after topical application of benzyl nicotinate. *J Biomed Opt,* 11**,** 014025.

James, J. E. (2004) Critical review of dietary caffeine and blood pressure: a relationship that should be taken more seriously. *Psychosom Med,* 66**,** 63-71.

James, J. E. & Gregg, M. E. (2004) Hemodynamic effects of dietary caffeine, sleep restriction, and laboratory stress. *Psychophysiology,* 41**,** 914-23.

Johannes Frank, Vijay S. Gorantla, Gary L. Anderson, Luis Laurentin-Perez, Claudio Maldonado & Barker, J. H. (2001) Microcirculation Research for Microsurgeons: Basic Concepts and Potential Applications. *European Journal of Trauma,* 4**,** 153 - 162.

Kang, F. R. & Singh, J. (2005) Preparation, in vitro release, in vivo absorption and biocompatibility studies of insulin-loaded microspheres in rabbits. *Aaps Pharmscitech,* 6.

Katzung, B. G. (2001) *Basic & Clinical Pharmacology,* United States of America, The McGraw-Hill Companies.

Kawakami, H., Sumimoto, T., Hamada, M., Mukai, M., Shigematsu, Y., Matsuoka, H., Abe, M. & Hiwada, K. (1995) Acute effect of glyceryl trinitrate on systolic blood pressure and other hemodynamic variables. *Angiology,* 46**,** 151-6.

Keller, B. B., Liu, L. J., Tinney, J. P. & Tobita, K. (2007) Cardiovascular developmental insights from embryos. *Ann N Y Acad Sci,* 1101**,** 377-88.

Kelly, E. A., Ahmed, R. M. & Horowitz, J. D. (2005) Withdrawal of intravenous glyceryl trinitrate: absence of rebound phenomena with transition to oral isosorbide dinitrate. *Clin Exp Pharmacol Physiol,* 32**,** 269-72.

Kemppainen, B. W., Riley, R. T., Pace, J. G. & Hoerr, F. J. (1986) Effects of Skin Storage-Conditions and Concentration of Applied Dose on [H-3] T-2 Toxin Penetration through Excised Human and Monkey Skin. *Food and Chemical Toxicology,* 24**,** 221-227.

Kernick, D. P. & Shore, A. C. (2000) Characteristics of laser Doppler perfusion imaging in vitro and in vivo. *Physiol Meas,* 21**,** 333-40.

Kikwai, L., Babu, R. J., Prado, R., Kolot, A., Armstrong, C. A., Ansel, J. C. & Singh, M. (2005) In vitro and in vivo evaluation of topical formulations of Spantide II. *Aaps Pharmscitech,* 6.

Kind, C. (1975) The development of the circulating blood volume of the chick embryo. *Anat Embryol (Berl),* 147**,** 127-32.

Kleschyov, A. L., Oelze, M., Daiber, A., Huang, Y., Mollnau, H., Schulz, E., Sydow, K., Fichtlscherer, B., Mulsch, A. & Munzel, T. (2003) Does nitric oxide mediate the vasodilator activity of nitroglycerin? *Circ Res,* 93**,** e104-12.

Klueh, U., Dorsky, D. I., Moussy, F. & Kreutzer, D. L. (2003) Ex ova chick chorioallantoic membrane as a novel model for evaluation of tissue responses to biomaterials and implants. *J Biomed Mater Res A,* 67**,** 838-43.

Kojda, G., Kottenberg, K., Nix, P., Schluter, K. D., Piper, H. M. & Noack, E. (1996) Low increase in cGMP induced by organic nitrates and nitrovasodilators improves contractile response of rat ventricular myocytes. *Circ Res,* 78**,** 91-101.

Krogstad, A. L., Lonnroth, P., Larson, G. & Wallin, B. G. (1999) Capsaicin treatment induces histamine release and perfusion changes in psoriatic skin. *Br J Dermatol,* 141**,** 87-93.

Kunzi-Rapp, K., Ruck, A. & Kaufmann, R. (1999) Characterization of the chick chorioallantoic membrane model as a short-term in vivo system for human skin. *Arch Dermatol Res,* 291**,** 290-5.

Kurz, H., Wilting, J. & Christ, B. (1994) Multivariate Characterization of Blood Vessel Morphogenesis in the Avian Chorioallantoic Membrane (CAM): Cell Proliferation, Length Density and Fractal Dimension. IN T.F. NONNENMACHER, G.A. LOSA & WEIBEL, E. R. (Eds.) *Fractals in biology and medicine.* Boston, Birkh8auser Verlag.

Lacy, C. F., Armstrong, L. L., Goldman, M. P. & Lance, L. L. (2004) *Drug Information Handbook International*, Lexi-Comp Inc.

Lagarto, A., Vega, R., Guerra, I. & Gonzalez, R. (2006) In vitro quantitative determination of ophthalmic irritancy by the chorioallantoic membrane test with trypan blue staining as alternative to eye irritation test. *Toxicol In Vitro,* 20**,** 699-702.

Lam, F. Y. & Ferrell, W. R. (1993) Acute inflammation in the rat knee joint attenuates sympathetic vasoconstriction but enhances neuropeptide-mediated vasodilatation assessed by laser Doppler perfusion imaging. *Neuroscience,* 52**,** 443-9.

Lantsberg, L. & Goldman, M. (1990) Lower limb sympathectomy assessed by laser Doppler blood flow and transcutaneous oxygen measurements. *J Med Eng Technol,* 14**,** 182-3.

Lapeyre, A. C., 3rd, Goraya, T. Y., Johnston, D. L. & Gibbons, R. J. (2004) The impact of caffeine on vasodilator stress perfusion studies. *J Nucl Cardiol,* 11**,** 506-11.

Le Noble, F., Fleury, V., Pries, A., Corvol, P., Eichmann, A. & Reneman, R. S. (2005) Control of arterial branching morphogenesis in embryogenesis: go with the flow. *Cardiovasc Res,* 65**,** 619-28.

Leighton, J., Nassauer, J. & Tchao, R. (1985) The chick embryo in toxicology: an alternative to the rabbit eye. *Food Chem Toxicol,* 23**,** 293-8.

Leng, T., Miller, J. M., Bilbao, K. V., Palanker, D. V., Huie, P. & Blumenkranz, M. S. (2004) The chick chorioallantoic membrane as a model tissue for surgical retinal research and simulation. *Retina,* 24**,** 427-34.

Lewis, J. D., Destito, G., Zijlstra, A., Gonzalez, M. J., Quigley, J. P., Manchester, M. & Stuhlmann, H. (2006) Viral nanoparticles as tools for intravital vascular imaging. *Nat Med,* 12**,** 354-60.

Li Kam Wa, T. C., Almond, N. E., Cooke, E. D. & Turner, P. (1990) Skin blood flow changes following intradermal bradykinin injections measured by laser Doppler flowmetry: comparison with weal and flare. *J Med Eng Technol,* 14**,** 190-3.

Li, L., Ke, Z., Tong, K. Y. & Ying, M. (2010) Evaluation of cerebral blood flow changes in focal cerebral ischemia rats by using transcranial Doppler ultrasonography. *Ultrasound Med Biol,* 36**,** 595-603.

Liebsch, M. & Spielmann, H. (2002) Currently available in vitro methods used in the regulatory toxicology. *Toxicol Lett,* 127**,** 127-34.

Lin, M., Marshall, C. T., Qi, Y., Johnston, S. M., Badea, C. T., Piantadosi, C. A. & Johnson, G. A. (2009) Quantitative blood flow measurements in the small animal cardiopulmonary system using digital subtraction angiography. *Med Phys,* 36**,** 5347-58.

Lin, S. Y., Hou, S. J., Hsu, T. H. S. & Yeh, F. L. (1992) Comparisons of Different Animal Skins with Human Skin in Drug Percutaneous Penetration Studies. *Methods and Findings in Experimental and Clinical Pharmacology,* 14**,** 645-654.

Luepke, N. P. (1985) Hens Egg Chorioallantoic Membrane Test for Irritation Potential. *Food and Chemical Toxicology,* 23**,** 287-291.

Lugassy., C., Vernon., S. E. & Barnhill, R. L. (2006) The shell-less CAM (chicken chorioallantoic membrane) assay: A model for studying melanoma angiotropism and extravascular migratory metastasis. *Miami Nature Biotechnology Winter Symposia.* Miami.

Maeda, Y. & Noda, M. (2003) Coordinated development of embryonic long bone on chorioallantoic membrane in ovo prevents perichondrium-derived suppressive signals against cartilage growth. *Bone,* 32**,** 27-34.

Maibach, H. I. & Bronaugh, R. L. (2002) *Topical absorption of dermatological products,* New York, Marcel Dekker.

Malkia, A., Murtomaki, L., Urtti, A. & Kontturi, K. (2004) Drug permeation in biomembranes in vitro and in silico prediction and influence of physicochemical properties. *European Journal of Pharmaceutical Sciences,* 23**,** 13-47.

Malta, E. (1989a) Biphasic relaxant curves to glyceryl trinitrate in rat aortic rings. Evidence for two mechanisms of action. *Naunyn Schmiedebergs Arch Pharmacol,* 339**,** 236-43.

Malta, E. (1989b) Studies on the biphasic relaxant curve of glyceryl trinitrate in rat aorta: role of GTN metabolites. *Clin Exp Pharmacol Physiol,* 16**,** 829-35.

Mancebo, A., Hernandez, O., Gonzalez, Y., Aldana, L. & Carballo, O. (2008) Assessment of skin and eye irritation of 14 products under the stepwise approach of the OECD. *Cutan Ocul Toxicol,* 27**,** 173-85.

Mandagere, A. K., Thompson, T. N. & Hwang, K. K. (2002) Graphical model for estimating oral bioavailability of drugs in humans and other species from their Caco-2 permeability and in vitro liver enzyme metabolic stability rates. *J Med Chem,* 45**,** 304-11.

Manka, D. R., Gilson, W., Sarembock, I., Ley, K. & Berr, S. S. (2000) Noninvasive in vivo magnetic resonance imaging of injury-induced neointima formation in the carotid artery of the apolipoprotein-E null mouse. *Journal of Magnetic Resonance Imaging,* 12**,** 790-794.

Mathieu, F., Galmier, M. J., Pognat, J. F., Petit, J. & Lartigue, C. (1999) Transepithelial transport of bepridil in the human intestinal cell line, Caco-2, using two media, DMEMc and HBSS. *International Journal of Pharmaceutics,* 181**,** 203-217.

Mayhan, W. G. & Didion, S. P. (1995) Acute Effects of Ethanol on Responses of Cerebral Arterioles. *Stroke,* 26**,** 2097-2101.

Mayrovitz, H. N., Brown-Cross, D. & Washington, Z. (2007) Skin tissue water and laser Doppler blood flow during a menstrual cycle. *Clinical Physiology and Functional Imaging,* 27**,** 54-59.

Mccormick, J. F., Nassauer, J., Bielunas, J. & Leighton, J. (1984) Anatomy of the chick chorioallantoic membrane relevant to its use as a substrate in bioassay systems. *Scan Electron Microsc***,** 2023-30.

Mcphee, D. A., Parsonson, I. M., Della-Porta, A. J. & Jarrett, R. G. (1984) Teratogenicity of Australian Simbu serogroup and some other Bunyaviridae viruses: the embryonated chicken egg as a model. *Infect Immun,* 43**,** 413-20.

Melkonian, G., Wang, J. L., Chung, J., Munoz, N. & Talbot, P. (2004) CD44 and tenascin play critical roles in growth and vascular development of the chick chorioallantoic membrane and are targets of cigarette smoke. *Anat Embryol (Berl),* 208**,** 109-20.

Miyai, N., Terada, K., Sakaguchi, S., Minami, Y., Tomura, T., Yamamoto, H., Tomida, K. & Miyashita, K. (2005) Preliminary study on the assessment of peripheral vascular response to cold provocation in workers exposed to hand-arm vibration using laser Doppler perfusion imager. *Ind Health,* 43**,** 548-55.

Miyajima, T., Yokoyama, H., Taira, H. & Tsuji, Y. (2005) Quantitative estimation of renal blood flow by power Doppler ultrasonography in renovascular hypertensive dogs. *Kidney Int,* 68**,** 2781-6.

Moens, A. L., Goovaerts, I., Claeys, M. J. & Vrints, C. J. (2005) Flow-mediated vasodilation - A diagnostic instrument, or an experimental tool? *Chest,* 127**,** 2254-2263.

Monnet, E., Pelsue, D. & Macphail, C. (2006) Evaluation of laser Doppler flowmetry for measurement of capillary blood flow in the stomach wall of dogs during gastric dilatation-volvulus. *Vet Surg,* 35**,** 198-205.

Morales, F., Graaff, R., Smit, A. J., Bertuglia, S., Petoukhova, A. L., Steenbergen, W., Leger, P. & Rakhorst, G. (2005) How to assess post-occlusive reactive hyperaemia by means of laser Doppler perfusion monitoring: application of a standardised protocol to patients with peripheral arterial obstructive disease. *Microvasc Res,* 69**,** 17-23.

Mori, M., Stokes, K. Y., Vowinkel, T., Watanabe, N., Elrod, J. W., Harris, N. R., Lefer, D. J., Hibi, T. & Granger, D. N. (2005) Colonic blood flow responses in experimental colitis: time course and underlying mechanisms. *Am J Physiol Gastrointest Liver Physiol,* 289**,** G1024-9.

Murase, K. & Miyazaki, S. (2007) Error analysis of tumor blood flow measurement using dynamic contrast-enhanced data and model-independent deconvolution analysis. *Physics in Medicine and Biology,* 52**,** 2791-2805.

Murase, K., Yamazaki, Y. & Shinohara, M. (2003) Autoregressive moving average (ARMA) model applied to quantification of cerebral blood flow using dynamic susceptibility contrast-enhanced magnetic resonance imaging. *Magn Reson Med Sci,* 2**,** 85-95.

Murray, A. K., Herrick, A. L. & King, T. A. (2004) Laser Doppler imaging: a developing technique for application in the rheumatic diseases. *Rheumatology (Oxford),* 43**,** 1210-8.

Mysliveckova, A. & Rychter, Z. (1975) Electron microscopy analysis of differentiation of the wall and capillary bed of the chick embryo allantochorion. *Folia Morphol (Praha),* 23**,** 306-19.

Nakase, H., Kaido, T., Okuno, S., Hoshida, T. & Sakaki, T. (2002) Novel intraoperative cerebral blood flow monitoring by laser-Doppler scanner. *Neurol Med Chir (Tokyo),* 42**,** 1-4.

Nakazawa, M., Miyagawa, S., Takao, A., Clark, E. B. & Hu, N. (1986) hemodynamic Effects of Environmental Hyperthermia in Stage 18, 21, and 24 Chick Embryos. *Pediatric Research,* 20**,** 1213 - 1215.

Nap, A. W., Dunselman, G. A., De Goeij, A. F., Evers, J. L. & Groothuis, P. G. (2004) Inhibiting MMP activity prevents the development of endometriosis in the chicken chorioallantoic membrane model. *Hum Reprod,* 19**,** 2180-7.

Nap, A. W., Dunselman, G. A., Griffioen, A. W., Mayo, K. H., Evers, J. L. & Groothuis, P. G. (2005) Angiostatic agents prevent the development of endometriosis-like lesions in the chicken chorioallantoic membrane. *Fertil Steril,* 83**,** 793-5.

Nap, A. W., Groothuis, P. G., Demir, A. Y., Maas, J. W., Dunselman, G. A., De Goeij, A. F. & Evers, J. L. (2003) Tissue integrity is essential for ectopic implantation of human endometrium in the chicken chorioallantoic membrane. *Hum Reprod,* 18**,** 30-4.

Navarro, M., Deruiter, M. C., Carretero, A. & Ruberte, J. (2003) Microvascular assembly and cell invasion in chick mesonephros grafted onto chorioallantoic membrane. *J Anat,* 202**,** 213-25.

Nehlig, A., Daval, J. L. & Debry, G. (1992) Caffeine and the central nervous system: mechanisms of action, biochemical, metabolic and psychostimulant effects. *Brain Res Brain Res Rev,* 17**,** 139-70.

Nico, B., Ennas, M. G., Crivellato, E., Frontino, A., Mangieri, D., De Giorgis, M., Roncali, L. & Ribatti, D. (2004) Desmin-positive pericytes in the chick embryo chorioallantoic membrane in response to fibroblast growth factor-2. *Microvasc Res,* 68**,** 13-9.

Nicolazzo, J. A. & Finnin, B. C. (2008) In vivo and in vitro models for assessing drug absorption across the buccal mucosa. *Biotechnology: Pharmaceutical Aspects.* Springer.

Nicoletti, P., Trevisani, M., Manconi, M., Gatti, R., De Siena, G., Zagli, G., Benemei, S., Capone, J. A., Geppetti, P. & Pini, L. A. (2008) Ethanol causes neurogenic vasodilation by TRPV1 activation and CGRP release in the trigeminovascular system of the guinea pig. *Cephalalgia,* 28**,** 9-17.

Nielsen, H. M. & Rassing, M. R. (2000) TR146 cells grown on filters as a model of human buccal epithelium: IV. Permeability of water, mannitol, testosterone and beta-adrenoceptor antagonists. Comparison to human, monkey and porcine buccal mucosa. *International Journal of Pharmaceutics,* 194**,** 155-167.

Niwayama, J. & Sanaka, T. (2005) Development of a new method for monitoring blood purification: the blood flow analysis of the head and foot by laser Doppler blood flowmeter during hemodialysis. *Hemodial Int,* 9**,** 56-62.

Noon, J. P., Evans, C. E., Haynes, W. G., Webb, D. J. & Walker, B. R. (1996) A comparison of techniques to assess skin blanching following the topical application of glucocorticoids. *Br J Dermatol,* 134**,** 837-42.

Obradovic, T. & Hidalgo, I. J. (2008) In vitro models for investigations of buccal drug permeation and metabolism. *Biotechnology: Pharmaceutical Aspects.* Springer.

Olufsen, M. S., Ottesen, J. T., Tran, H. T., Ellwein, L. M., Lipsitz, L. A. & Novak, V. (2005) Blood pressure and blood flow variation during postural change from sitting to standing: model development and validation. *J Appl Physiol,* 99**,** 1523-37.

Pandey, P. & Turton, R. (2005) Movement of different-shaped particles in a pan-coating device using novel video-imaging techniques. *Aaps Pharmscitech,* 6.

Patan, S., Haenni, B. & Burri, P. H. (1997) Implementation of intussusceptive microvascular growth in the chicken chorioallantoic membrane (CAM). *Microvasc Res,* 53**,** 33-52.

Pawar, P. K. & Majumdar, D. K. (2006) Effect of formulation factors on in vitro permeation of moxifloxacin from aqueous drops through excised goat, sheep, and buffalo corneas. *Aaps Pharmscitech,* 7.

Pegaz, B., Debefve, E., Ballini, J. P., Wagnieres, G., Spaniol, S., Albrecht, V., Scheglmann, D. V., Nifantiev, N. E., Van Den Bergh, H. & Konan-Kouakou, Y. N. (2006) Photothrombic activity of m-THPC-loaded liposomal formulations: pre-clinical assessment on chick chorioallantoic membrane model. *Eur J Pharm Sci,* 28**,** 134-40.

Pemp, B., Maar, N., Weigert, G., Luksch, A., Resch, H., Garhofer, G., Orgul, S. & Schmetterer, L. (2009) Strategies for reducing variance in laser Doppler flowmetry measurements. *Graefes Archive for Clinical and Experimental Ophthalmology,* 247**,** 67-71.

Pendleton, N., Pazouki, S., Heerkens, E., Smither, R. L., Chisholm, D. M., Moore, J. V., Howell, A., Horan, M. A. & Schor, A. M. (1998) Relationships between different measurements of vascularity and clinico-pathological parameters in breast cancer. *Anticancer Res,* 18**,** 4565-8.

Pongjanyakul, T., Prakongpan, S., Panomsuk, S., Puttipipatkhachorn, S. & Priprem, A. (2002) Shed king cobra and cobra skins as model membranes for in-vitro nicotine permeation studies. *J Pharm Pharmacol,* 54**,** 1345-50.

Pontiroli, A. E., Perfetti, M. G., Fattor, B. & Pozza, G. (1989) Effect of intranasal growth hormone-releasing hormone and corticotropin-releasing hormone administration on growth hormone and cortisol release: improved bioavailability by means of sodium-glycocholate. *J Clin Endocrinol Metab,* 68**,** 821-4.

Price, J. M. (1991) Influence of pressure and flow on constriction of blood vessels. *J Fla Med Assoc,* 78**,** 825-7.

Pu, X., Lee, L. S., Galinsky, R. E. & Carlson, G. P. (2004) Evaluation of a rat model versus a physiologically based extraction test for assessing phenanthrene bioavailability from soils. *Toxicol Sci,* 79**,** 10-7.

Puddey, I. B., Zilkens, R. R., Croft, K. D. & Beilin, L. J. (2001) Alcohol and endothelial function: A brief review. *Clinical and Experimental Pharmacology and Physiology,* 28**,** 1020-1024.

Qian, M., Yan, L., Niu, L., Jin, Q., Ling, T., Chen, Y. & Zheng, H. (2009) Micro-ultrasound biofluid imaging and multi-component velocity measurement with micro echo particle image velocimetry technique. *Conf Proc IEEE Eng Med Biol Soc,* 2009**,** 451-4.

Qvist, M. H., Hoeck, U., Kreilgaard, B., Madsen, F. & Frokjaer, S. (2000) Evaluation of Gottingen minipig skin for transdermal in vitro permeation studies. *Eur J Pharm Sci,* 11**,** 59-68.

Rahn, H., Paganelli, C. V. & Ar, A. (1987) Pores and gas exchange of avian eggs: a review. *J Exp Zool Suppl,* 1**,** 165-72.

Rajan, V., Varghese, B., Van Leeuwen, T. G. & Steenbergen, W. (2008) Review of methodological developments in laser Doppler flowmetry. *Lasers Med Sci*.

Rapedius, M. & Blanchard, J. (2001) Comparison of the hanson microette and the Van Kel apparatus for in vitro release testing of topical semisolid formulations. *Pharm Res,* 18**,** 1440-7.

Reizis, A., Hammel, I. & Ar, A. (2005) Regional and developmental variations of blood vessel morphometry in the chick embryo chorioallantoic membrane. *J Exp Biol,* 208**,** 2483-8.

Remky, A., Arend, O., Beausencourt, E., Elsner, A. E. & Bertram, B. (1996) [Retinal vessels before and after photocoagulation in diabetic retinopathy. Determining the diameter using digitized color fundus slides]. *Klin Monatsbl Augenheilkd,* 209**,** 79-83.

Ribatti, D. (2008) Chick embryo chorioallantoic membrane as a useful tool to study angiogenesis. *Int Rev Cell Mol Biol,* 270**,** 181-224.

Ribatti, D., De Falco, G., Nico, B., Ria, R., Crivellato, E. & Vacca, A. (2003) In vivo time-course of the angiogenic response induced by multiple myeloma plasma cells in the chick embryo chorioallantoic membrane. *J Anat,* 203**,** 323-8.

Ribatti, D., Nico, B., Vacca, A., Roncali, L. & Presta, M. (1999) Endogenous and exogenous fibroblast growth factor-2 modulate wound healing in the chick embryo chorioallantoic membrane. *Angiogenesis,* 3**,** 89-95.

Ribatti, D., Vacca, A., Roncali, L. & Dammacco, F. (2000) The chick embryo chorioallantoic membrane as a model for in vivo research on anti-angiogenesis. *Curr Pharm Biotechnol,* 1**,** 73-82.

Richardson, M. & Singh, G. (2003) Observations on the use of the avian chorioallantoic membrane (CAM) model in investigations into angiogenesis. *Curr Drug Targets Cardiovasc Haematol Disord,* 3**,** 155-85.

Richardson, M., Wong, D., Lacroix, S., Stanisz, J. & Singh, G. (2005) Inhibition by doxycycline of angiogenesis in the chicken chorioallantoic membrane (CAM). *Cancer Chemother Pharmacol,* 56**,** 1-9.

Riksen, N. P., Rongen, G. A., Yellon, D. & Smits, P. (2008) Human in vivo research on the vascular effects of adenosine. *Eur J Pharmacol,* 585**,** 220-7.

Romanoff, A. L. (1960) *The Avian Embryo; Structural and functional development,* New York, The Macmillan Company.

Romanoff, A. L. (1967) *Biochemistry of the Avian Embryo,* United States of America, John Wiley & Sons Inc.

Rubanyi, G. M., Freay, A. D., Kauser, K., Johns, A. & Harder, D. R. (1990) Mechanoreception by the endothelium: mediators and mechanisms of pressure- and flow-induced vascular responses. *Blood Vessels,* 27**,** 246-57.

Sakaguchi, M., Hosie, K. B., Gourevitch, D., Tudor, R., Hioki, K., Yamamoto, M., Young, H. L. & Keighley, M. R. (1990) Laser Doppler assessment of human colonic blood flow. *J Med Eng Technol,* 14**,** 188-9.

Samkoe, K. S. & Cramb, D. T. (2003) Application of an ex ovo chicken chorioallantoic membrane model for two-photon excitation photodynamic therapy of age-related macular degeneration. *J Biomed Opt,* 8**,** 410-7.

Sankaranarayanan, M., Ghista, D. N., Poh, C. L., Seng, T. Y. & Kassab, G. S. (2006) Analysis of blood flow in an out-of-plane CABG model. *Am J Physiol Heart Circ Physiol,* 291**,** H283-95.

Saw, C. L., Heng, P. W., Chin, W. W., Soo, K. C. & Olivo, M. (2005a) Enhanced photodynamic activity of hypericin by penetration enhancer N-methyl pyrrolidone formulations in the chick chorioallantoic membrane model. *Cancer Lett*.

Saw, C. L., Olivo, M., Chin, W. W., Soo, K. C. & Heng, P. W. (2005b) Transport of hypericin across chick chorioallantoic membrane and photodynamic therapy vasculature assessment. *Biol Pharm Bull,* 28**,** 1054-60.

Saw, C. L., Olivo, M., Chin, W. W., Soo, K. C. & Heng, P. W. (2007a) Superiority of N-methyl pyrrolidone over albumin with hypericin for fluorescence diagnosis of human bladder cancer cells implanted in the chick chorioallantoic membrane model. *J Photochem Photobiol B,* 86**,** 207-18.

Saw, C. L. L., Heng, P. W. S. & Olivo, M. (2007b) Potentiation of the photodynamic action of hypericin. *Journal of Environmental Pathology Toxicology and Oncology,* 27**,** 23-33.

Saw, C. L. L., Olivo, M., Chin, W. W. L., Soo, K. C. & Heng, P. W. S. (2005c) Transport of hypericin across chick chorioallantoic membrane and photodynamic

therapy vasculature assessment. *Biological & Pharmaceutical Bulletin,* 28**,** 1054-1060.

Saw, C. L. L., Olivo, M., Chin, W. W. L., Soo, K. C. & Heng, P. W. S. (2007c) Superiority of N-methyl pyrrolidone over albumin with hypericin for fluorescence diagnosis of human bladder cancer cells implanted in the chick chorioallantoic membrane model. *Journal of Photochemistry and Photobiology B-Biology,* 86**,** 207-218.

Saw, C. L. L., Olivo, M., Wohland, T., Fu, C. Y., Kho, K. W., Soo, K. C. & Heng, P. W. S. (2007d) Effects of n-methyl pyrrolidone on the uptake of hypericin in human bladder carcinoma and co-staining with DAPI investigated by confocal microscopy. *Technology in Cancer Research & Treatment,* 6**,** 383-394.

Schafer, A. T. & Kaufmann, J. D. (1999) What happens in freezing bodies? Experimental study of histological tissue change caused by freezing injuries. *Forensic Sci Int,* 102**,** 149-58.

Schmid, G. F., Papastergiou, G. I., Nickla, D. L., Riva, C. E., Lin, T., Stone, R. A. & Laties, A. M. (1996) Validation of laser Doppler interferometric measurements in vivo of axial eye length and thickness of fundus layers in chicks. *Curr Eye Res,* 15**,** 691-6.

Senel, S. & Hincal, A. A. (2001) Drug permeation enhancement via buccal route: possibilities and limitations. *J Control Release,* 72**,** 133-44.

Shargel, L. W.-P., Susanna; Yu, Andrew B.C. (2005) *Applied Biopharmaceutics and Pharmacokinetics,* United States of America, The McGraw-Hill Companies.

Shojaei, A. H. (1998) Buccal mucosa as a route for systemic drug delivery: a review. *J Pharm Pharm Sci,* 1**,** 15-30.

Shumko, J. Z., Defouw, D. O. & Feinberg, R. N. (1988) Vascular histodifferentiation in the chick chorioallantoic membrane: a morphometric study. *Anat Rec,* 220**,** 179-89.

Silverthorn, D. U. (2001) *Human physiology : an integrated approach,* Upper Saddle River, NJ :, Prentice Hall.

Sinha, V. R. & Kaur, M. P. (2000) Permeation enhancers for transdermal drug delivery. *Drug Development and Industrial Pharmacy,* 26**,** 1131-1140.

Snyder, G. K. & Birchard, G. F. (1982) Water loss and survival in embryos of the domestic chicken. *J Exp Zool,* 219**,** 115-7.

Sommer, A., Lucassen, G. W., Houben, A. J. & Neumann, M. H. (2003) Vasoconstrictive effect of topical applied corticosteroids measured by laser doppler imaging and reflectance spectroscopy. *Microvasc Res,* 65**,** 152-9.

Sommer, A., Veraart, J., Neumann, M. & Kessels, A. (1998) Evaluation of the vasoconstrictive effects of topical steroids by laser-Doppler-perfusion-imaging. *Acta Derm Venereol,* 78**,** 15-8.

Sorensen, J., Bengtsson, M., Malmqvist, E. L., Nilsson, G. & Sjoberg, F. (1996) Laser Doppler perfusion imager (LDPI)--for the assessment of skin blood flow changes following sympathetic blocks. *Acta Anaesthesiol Scand,* 40**,** 1145-8.

Spealman, R. D., Goldberg, S. R., Kelleher, R. T., Goldberg, D. M. & Charlton, J. P. (1977) Some effects of cocaine and two cocaine analogs on schedule-controlled behavior of squirrel monkeys. *J Pharmacol Exp Ther,* 202**,** 500-9.

Spielmann, H., Liebsch, M., Moldenhauer, F., Holzhutter, H. G., Bagley, D. M., Lipman, J. M., Pape, W. J., Miltenburger, H., De Silva, O., Hofer, H. & Steiling, W. (1997) IRAG working group 2. CAM-based assays. Interagency Regulatory Alternatives Group. *Food Chem Toxicol,* 35**,** 39-66.

Stasi, M. A., Scioli, M. G., Arcuri, G., Mattera, G. G., Lombardo, K., Marcellini, M., Riccioni, T., De Falco, S., Pisano, C., Spagnoli, L. G., Borsini, F. & Orlandi, A. (2010) Propionyl-L-carnitine improves postischemic blood flow recovery and arteriogenetic revascularization and reduces endothelial NADPH-oxidase 4-mediated superoxide production. *Arterioscler Thromb Vasc Biol,* 30**,** 426-35.

Staton, C. A., Reed, M. W. & Brown, N. J. (2009) A critical analysis of current in vitro and in vivo angiogenesis assays. *Int J Exp Pathol,* 90**,** 195-221.

Straughan, D. W., Fentem, J. H., Balls, M., José, V. C. & María José, G.-L. (1996) Replacement Alternative and Complementary In Vitro Methods in Pharmaceutical Research. *In Vitro Methods in Pharmaceutical Research.* San Diego, Academic Press.

Strick, D. M., Waycaster, R. L., Montani, J. P., Gay, W. J. & Adair, T. H. (1991) Morphometric measurements of chorioallantoic membrane vascularity: effects of hypoxia and hyperoxia. *Am J Physiol,* 260**,** H1385-9.

Stucker, M., Heese, A., Hoffmann, K., Rochling, A. & Altmeyer, P. (1995) Precision of laser Doppler scanning in clinical use. *Clin Exp Dermatol,* 20**,** 371-6.

Stucker, M., Hugler, P., Von Kobyletzki, G., Reuther, T., Hoffmann, K., Laubenthal, H. & Altmeyer, P. (1997) Intracutaneous histamine injection can detect damage of cutaneous afferent fibres in postherpetic neuralgia. *Dermatology,* 195**,** 311-6.

Subramanian, N., Ray, S., Ghosal, S. K., Bhadra, R. & Moulik, S. P. (2004) Formulation design of self-microemulsifying drug delivery systems for improved oral bioavailability of celecoxib. *Biol Pharm Bull,* 27**,** 1993-9.

Sutinen, R., Paronen, P., Saano, V. & Urtti, A. (2000) Water-activated, pH-controlled patch in transdermal administration of timolol. II. Drug absorption and skin irritation. *Eur J Pharm Sci,* 11**,** 25-31.

Svedman, C., Cherry, G. W., Strigini, E. & Ryan, T. J. (1998) Laser Doppler imaging of skin microcirculation. *Acta Derm Venereol,* 78**,** 114-8.

Swarbrick, J., Lee, G. & Brom, J. (1982) Drug Permeation through Human-Skin .1. Effect of Storage-Conditions of Skin. *Journal of Investigative Dermatology,* 78**,** 63-66.

Szabadi, E. (1977) A model of two functionally antagonistic receptor populations activated by the same agonist. *J Theor Biol,* 69**,** 101-12.

Takahashi, K. & Rytting, J. H. (2001) Novel approach to improve permeation of ondansetron across shed snake skin as a model membrane. *Journal of Pharmacy and Pharmacology,* 53**,** 789-794.

Tanaka, T., Riva, C. & Ben-Sira, B. (1974) Blood velocity measurements in human retinal vessels. *Science,* 186**,** 830-1.

Tanojo, H., Boelsma, E., Junginger, H. E., Ponec, M. & Bodde, H. E. (1999) In vivo human skin permeability enhancement by oleic acid: a laser Doppler velocimetry study. *J Control Release,* 58**,** 97-104.

Tavakoli-Saberi, M. R. & Audus, K. L. (1989) Cultured buccal epithelium: an in vitro model derived from the hamster pouch for studying drug transport and metabolism. *Pharm Res,* 6**,** 160-6.

Tavaszi, J. & Budai, P. (2007) The use of HET-CAM test in detecting the ocular irritation. *Commun Agric Appl Biol Sci,* 72**,** 137-41.

Thompson, W. D. & Brown, F. I. (1987) Quantitation of histamine-induced angiogenesis in the chick chorioallantoic membrane: mode of action of histamine is indirect. *Int J Microcirc Clin Exp,* 6**,** 343-57.

Thorfinn, J., Sjoberg, F., Sjostrand, L. & Lidman, D. (2006) Perfusion of the skin of the buttocks in paraplegic and tetraplegic patients, and in healthy subjects after a short and long load. *Scandinavian Journal of Plastic and Reconstructive Surgery and Hand Surgery,* 40**,** 153-160.

Tillmann, U., Pollet, D. & Miltenburger, H. G. (1989) Scoring of Cytotoxicity by Image-Analysis Using Animal-Cell Cultures. *Atla-Alternatives to Laboratory Animals,* 17**,** 109-127.

Tuan, R. S. (1980) Calcium transport and related functions in the chorioallantoic membrane of cultured shell-less chick embryos. *Dev Biol,* 74**,** 196-204.

Tufan., A. C., Akdogan., I. & Adiguzel., E. (2004) Shell-less culture of the chick embryo as a model system in the study of developmental neurobiology. *Neuroanatomy,* 3**,** 8-11.

Uchil, J., Pattabi, M. & Shripathi, T. (2004) Dielectric studies on the chicken egg membrane deposited with CdS nanoparticles. *Solar Energy Materials and Solar Cells,* 81**,** 313-322.

Valdes, T. I., Klueh, U., Kreutzer, D. & Moussy, F. (2003) Ex ova chick chorioallantoic membrane as a novel in vivo model for testing biosensors. *J Biomed Mater Res A,* 67**,** 215-23.

Valdes, T. I., Kreutzer, D. & Moussy, F. (2002) The chick chorioallantoic membrane as a novel in vivo model for the testing of biomaterials. *J Biomed Mater Res,* 62**,** 273-82.

Van Der Schueren, B. J., Rogiers, A., Vanmolkot, F. H., Van Hecken, A., Depre, M., Kane, S. A., De Lepeleire, I., Sinclair, S. R. & De Hoon, J. N. (2008) Calcitonin gene-related peptide(8-37) antagonizes capsaicin-induced vasodilation in the skin: Evaluation of a human in vivo pharmacodynamic model. *Journal of Pharmacology and Experimental Therapeutics,* 325**,** 248-255.

Van Eyk, A. D. & Van Der Biijl, P. (2006) Comparative permeability of fresh and frozen/thawed porcine buccal mucosa towards various chemical markers. *Sadj,* 61**,** 200-3.

Venier, M., Adami, G., Larese, F., Maina, G. & Renzi, N. (2004) Percutaneous absorption of 5 glycol ethers through human skin in vitro. *Toxicology in Vitro,* 18**,** 665-671.

Vickerman, M. B., Keith, P. A., Mckay, T. L., Gedeon, D. J., Watanabe, M., Montano, M., Karunamuni, G., Kaiser, P. K., Sears, J. E., Ebrahem, Q., Ribita, D., Hylton, A. G. & Parsons-Wingerter, P. (2009) VESGEN 2D: automated, user-interactive software for quantification and mapping of angiogenic and lymphangiogenic trees and networks. *Anat Rec (Hoboken),* 292**,** 320-32.

Vinardell, M. P. & Garcia, L. (2000) The quantitative chorioallantoic membrane test using trypan blue stain to predict the eye irritancy of liquid scintillation cocktails. *Toxicol In Vitro,* 14**,** 551-555.

Vogelaar, J. P. M. & Boogert, J. B. V. D. (1925) Development of the egg of Gallus Domesticus in vitro. *Anat Rec,* 30**,** 385 - 295.

Walgren, R. A. & Walle, T. (1999) The influence of plasma binding on absorption/exsorption in the Caco-2 model of human intestinal absorption. *Journal of Pharmacy and Pharmacology,* 51**,** 1037-1040.

Wardell, K., Braverman, I. M., Silverman, D. G. & Nilsson, G. E. (1994) Spatial heterogeneity in normal skin perfusion recorded with laser Doppler imaging and flowmetry. *Microvasc Res,* 48**,** 26-38.

Wardell, K., Jakobsson, A. & Nilsson, G. E. (1993) Laser Doppler perfusion imaging by dynamic light scattering. *IEEE Trans Biomed Eng,* 40**,** 309-16.

Wexler, E. J., Peters, E. E., Gonzales, A., Gonzales, M. L., Slee, A. M. & Kerr, J. S. (2002) An objective procedure for ischemic area evaluation of the stroke intraluminal thread model in the mouse and rat. *Journal of Neuroscience Methods,* 113**,** 51-58.

Wigger-Alberti W., Keskin M., Feistkorn G. & K.P., W. (2001) Non-invasive assessment of patch test reactions due to hair dyes with the laser doppler perfusion scanning technique. *Stratum Corneum III.* Basel.

Wright, C. I., Kroner, C. I. & Draijer, R. (2006) Non-invasive methods and stimuli for evaluating the skin's microcirculation. *J Pharmacol Toxicol Methods,* 54**,** 1-25.

Yazdanian, M. (1994) The Effect of Freezing on Cattle Skin Permeability. *International Journal of Pharmaceutics,* 103**,** 93-96.

Yogi, A., Callera, G. E., Hipolito, U. V., Silva, C. R., Touyz, R. M. & Tirapelli, C. R. (2010) Ethanol-induced vasoconstriction is mediated via redox-sensitive cyclo-oxygenase-dependent mechanisms. *Clin Sci (Lond),* 118**,** 657-68.

Yong, T., Gilmore, J. P., Joyner, W. L. & Mayhan, W. G. (1992) Invivo Responses of Allografted Cerebral Parenchymal Arterioles to Ethanol and Angiotensin-Ii - Effect of Calcium-Channel Blockade. *International Journal of Microcirculation-Clinical and Experimental,* 11**,** 417-424.

Yoshida, A., Feke, G. T., Mori, F., Nagaoka, T., Fujio, N., Ogasawara, H., Konno, S. & Mcmeel, J. W. (2003) Reproducibility and clinical application of a newly developed stabilized retinal laser Doppler instrument. *Am J Ophthalmol,* 135**,** 356-61.

Yoshiyama, Y. & Kanke, M. (2005a) Influence of hypothyroidism induced by thiamazole on the toxic interaction between propranolol and disopyramide in chick embryos. *Biol Pharm Bull,* 28**,** 1983-5.

Yoshiyama, Y. & Kanke, M. (2005b) Toxic interactions between fluconazole and disopyramide in chick embryos. *Biol Pharm Bull,* 28**,** 151-3.

Yoshiyama, Y. & Kanke, M. (2006) Influence of hypothyroidism induced by thiamazole on the toxicity of amitriptyline in chick embryos. *Biol Pharm Bull,* 29**,** 824-6.

Yoshiyama, Y., Sugiyama, T. & Kanke, M. (2003) Cardiotoxicity of trastuzumab (herceptin) in chick embryos. *Biol Pharm Bull,* 26**,** 893-5.

Yoshiyama, Y., Sugiyama, T. & Kanke, M. (2004) Influence of the light schedule on the toxicity of amitriptyline in chick embryos. *Biol Pharm Bull,* 27**,** 229-31.

Yoshiyama, Y., Sugiyama, T. & Kanke, M. (2005) Experimental diabetes model in chick embryos treated with streptozotocin. *Biol Pharm Bull,* 28**,** 1986-8.

Yu, D. Y., Su, E. N., Cringle, S. J. & Yu, P. K. (2003) Isolated preparations of ocular vasculature and their applications in ophthalmic research. *Progress in Retinal and Eye Research,* 22**,** 135-169.

Yu, G., Durduran, T., Zhou, C., Wang, H. W., Putt, M. E., Saunders, H. M., Sehgal, C. M., Glatstein, E., Yodh, A. G. & Busch, T. M. (2005) Noninvasive monitoring of murine tumor blood flow during and after photodynamic therapy provides early assessment of therapeutic efficacy. *Clin Cancer Res,* 11**,** 3543-52.

Zacharakis, N., Tone, P., Flordellis, C. S., Maragoudakis, M. E. & Tsopanoglou, N. E. (2006) Methylene blue inhibits angiogenesis in chick chorioallontoic membrane through a nitric oxide-independent mechanism. *J Cell Mol Med,* 10**,** 493-8.

Zaman, R. T., Parthasarathy, A. B., Vargas, G., Chen, B., Dunn, A. K., Rylander, H. G., 3rd & Welch, A. J. (2009) Perfusion in hamster skin treated with glycerol. *Lasers Surg Med,* 41**,** 492-503.

Zaugg, P., Djonov, V., Fuchtbauer, E. M. & Draeger, A. (1999) Sorting of murine vascular smooth muscle cells during wound healing in the chicken chorioallantoic membrane. *Exp Cell Res,* 253**,** 599-606.

Zhang, A., Altura, B. T. & Altura, B. M. (1993) Ethanol-Induced Contraction of Cerebral-Arteries in Diverse Mammals and Its Mechanism of Action. *European Journal of Pharmacology-Environmental Toxicology and Pharmacology Section,* 248**,** 229-236.

Zhang, H., Zhang, J. & Streisand, J. B. (2002) Oral mucosal drug delivery - Clinical pharmacokinetics and therapeutic applications. *Clinical Pharmacokinetics,* 41**,** 661-680.

Zhang, J. & Chen, Z. (2005) In vivo blood flow imaging by a swept laser source Fourier domain optical Doppler tomography. *Optics Express,* 13**,** 7449 - 7457.

Zhong, J., Seifalian, A. M., Salerud, G. E. & Nilsson, G. E. (1998) A mathematical analysis on the biological zero problem in laser Doppler flowmetry. *IEEE Trans Biomed Eng,* 45**,** 354-64.

Zhongping Chen, Thomas E. Milner, Shyam Srinivas, Xiaojun Wang, Arash Malekafzali, Martin J. C. Van Gemert, A. & Nelson, J. S. (1997) Noninvasive imaging of invivo blood flow velocity using optical Doppler tomography. *Opt Lett,* 22**,** 1-3.

Zorin, S., Kuylenstierna, F. & Thulin, H. (1999) In vitro test of nicotine's permeability through human skin. Risk evaluation and safety aspects. *Ann Occup Hyg,* 43**,** 405-13.

Zwadlo-Klarwasser, G., Gorlitz, K., Hafemann, B., Klee, D. & Klosterhalfen, B. (2001) The chorioallantoic membrane of the chick embryo as a simple model for the study of the angiogenic and inflammatory response to biomaterials. *J Mater Sci Mater Med,* 12**,** 195-9.

Zwilling, E. (1959) A modified chorioallantoic grafting procedure. *Transplant Bull,* 6**,** 115-6.

PART VII

LIST OF POSTER PUBLICATIONS

LIST OF POSTER PRESENTATIONS

1. S. L. M. Tay, P. W. S. Heng., L. W. Chan. *Optimising The Chick Chorioallantoic Membrane Model And Laser Doppler Perfusion Imaging For The Measurement Of Blood Flow* in *Asian Pharmaceutical Graduate Congress*. 2006. Singapore.
2. S. L. M. Tay, L.W.Chan., P. W. S. Heng. *Development Of A Chorioallantoic Membrane – Laser Doppler Perfusion Imaging Method To Assess Drug Bioavailability* in *Asian Association of Colleges of Pharmacy*. 2007. Manila, Philippines.
3. S. L. M. Tay, L. W.Chan., P. W. S. Heng. *The chorioallantoic membrane – laser doppler perfusion imaging model to assess drug absorption* In *ASEAN Scientific Conference In Pharmaceutical Technology*. 2008. Penang, Malaysia.
4. S. L. M. Tay, C. V. Liew, L. W. Chan, P. W. S. Heng, *Application of imaging technology to evaluate drug absorption through blood perfusion and dimensional changes in vessels of the CAM model* in *American Association of Pharmaceutical Scientists Annual Meeting and Exposition*, 2009, Los Angeles, United States of America
5. S. L. M. Tay, Y. X. Chua, S. M. Tan, C. V. Liew, L. W. Chan, P. W. S. Heng, *Development of the CAM as a biomembrane model to assess drug absorption* in *American Association of Pharmaceutical Scientists Annual Meeting and Exposition*, 2009, Los Angeles, United States of America